

This item was submitted to Loughborough University as a PhD thesis by the author and is made available in the Institutional Repository (<https://dspace.lboro.ac.uk/>) under the following Creative Commons Licence conditions.



For the full text of this licence, please go to:
<http://creativecommons.org/licenses/by-nc-nd/2.5/>

BLDSC no:- DX 231067



Pilkington Library

Author/Filing Title TUOR 1

Vol. No. Class Mark T

**Please note that fines are charged on ALL
overdue items.**

	LOAN COPY	
--	-----------	--

0402152905



**ENHANCING FILTRATION BY
ELECTRO-ACOUSTIC METHODS**

by

Timo Tuori

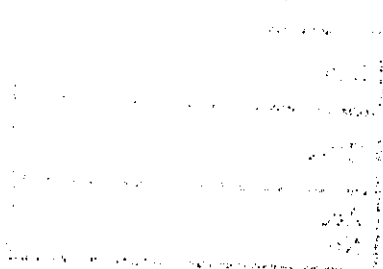
Doctoral Thesis


Submitted in partial fulfilment of the requirements
for the award of

Doctor of Philosophy of Loughborough University

3 December 1998

© by Timo Tuori 1998



 Loughborough University Pitt Rivers Library
Date Jan 00
Class
Acc No. 040215290

M0001035L8

ABSTRACT

Fouling of filter media and physico-chemical properties of suspensions decrease the efficiency of filtration devices in a wide range of process industries. Environmental protection causes increasing demand to clean effluent waters to higher standards and to recycle process waters more completely.

Conventional deliquoring processes are mainly based on a single driving force, usually gravity, underpressure or pressure. Today, multforce deliquoring processes based on a combination of ultrasonic and/or other nonmechanical forces, like an electric field, are being developed. These new technological applications, namely electro-acoustic deliquoring techniques, will most probably enable higher deliquoring rates and final solid contents than conventional methods have been able to yield.

Results from an experimental study of electric and/or ultrasonic field assisted filtrations are presented in this thesis. Both electric and ultrasonic fields can reduce fouling of the filtration medium and have a significant influence on filtration capacity. The extent of filtration improvement is affected mostly by particle size, surface charge, acoustic frequency, intensity and field strengths.

Theoretical examinations of the use of electric and/or ultrasonic fields to enhance filtration efficiency are laid out. Some aspects regarding orthokinetic interaction in acoustic agglomeration have been considered, and energy consumptions of the filtrations of different suspensions used in experiments were also determined.

Using electric field as a pre-treatment, bio/fiber suspension filtration can be enhanced 4-fold and energy consumption of electric field enhancing the filtration (kWh kg^{-1} separated water; product final dry solid content 23 % by mass) was only about 17 % of the total energy consumption of conventional vacuum filtration. Pre-treatment units can be connected to the filtration unit, for instance

before the filter drum. Possible pre-treatment apparatuses could be electroflotation equipment or a pre-treatment tube technique introduced in this Ph.D. Thesis.

The best filtration results were achieved with pyrite suspension assisted with ultrasonic field, in which cake capacity was 4-fold and the final cake moisture content decreased to 7 % from the reference value of 14 - 15 %. Energy consumption of ultrasonic assisted pyrite suspension filtration was about 23 % of the reference filtration by conventional method, calculated as ($\text{kWh kg}^{-1} \text{ D.S.}$). Also, electric field assisted filtration experiments gave good results, the filtration enhancement was over 10-fold compared to the reference filtration. Unfortunately electric pre-treatment and -filtration times added to the normal drying time (20 -30 s) made the total processing time too long, making the cake capacity increase only 3-fold.

Energy consumption calculations based on the post-feculent phosphoric acid filtration experiments, showed that using electric- and acoustic force fields together increased the filtration capacity 15-fold. Also, the energy consumption based on the separated mass of filtrate (kWh/kg filtrate) was only about 10 % of the energy consumption used in conventional filtration.

CONTENTS

ABSTRACT.....	2
CONTENTS.....	4
1 INTRODUCTION.....	6
2 LITERATURE REVIEW.....	9
2.1 BACKGROUND OF DEWATERING.....	9
2.2 PREVIOUS ELECTRODEWATERING RESEARCH.....	11
2.2.1 Electrodewatering – State-of-the-art.....	13
2.3 ELECTRO-MEMBRANE CROSSFLOW FILTRATION.....	18
2.4 PREVIOUS ACOUSTIC DEWATERING RESEARCH.....	21
2.4.1 Acoustic Dewatering – State-of-the-art.....	23
2.5 ACOUSTIC MEMBRANE FILTRATION RESEARCH.....	26
2.6 MAGNITUDE OF ULTRASONIC RADIATION FORCE.....	28
2.7 PREVIOUS ELECTRO-ACOUSTIC DEWATERING RESEARCH.....	29
2.7.1 Electro-acoustic dewatering – State – of – the art.....	30
2.8 FUNDAMENTAL ELECTRICAL PROPERTIES OF SOLID/LIQUID MIXTURES	32
2.8.1 Electrokinetic properties.....	34
2.8.1.1 Electrophoresis	34
2.8.1.2 Electro-osmosis.....	36
2.8.2 Properties which affect electrophoresis and electro-osmosis.....	36
2.8.2.1 Electric double-layer.....	37
2.8.3 Phenomenon of electroseparation.....	41
2.9 ENHANCEMENT MECHANISMS OF ULTRASOUND.....	41
2.9.1 Particle/fluid interactions in an ultrasonic field.....	44
2.9.2 Acoustic agglomeration mechanisms	45
2.9.2.1 Orthokinetic interaction	45
2.9.2.2 Hydrodynamic interaction.....	52
2.9.3 Acoustic effects in agglomeration to enhance dewatering	54
2.10 CAVITATION	55
2.10.1 Cavitation mechanism near a solid-liquid interface	58
2.11 ULTRASONIC TRANSDUCERS.....	58
2.11.1 Conversion criteria of electroacoustic transducers.....	59
2.11.1.1 Magnetostrictive transducers	59
2.11.1.2 Piezoelectric transducers.....	60
2.11.2 Physical properties of transducers	61
2.11.2.1 Focusing of sound waves.....	65
2.11.2.2 Near and far field of ultrasound.....	68

3	SUSPENSION CHARACTERISATION	72
3.1	PARTICLE DISTRIBUTIONS.....	72
3.2	SURFACE TENSION.....	77
3.3	DENSITIES AND VISCOSITIES OF SUSPENSIONS.....	79
3.4	ELECTRICAL PROPERTIES OF PARTICLES IN SUSPENSIONS....	81
3.5	MOVEMENT OF BIO/FIBER SUSPENSION PARTICLES IN ELECTRIC FIELD.....	86
3.6	CHOICE OF ACOUSTIC PROPERTIES FOR THE EXPERIMENTAL SEPARATORS	88
3.6.1	Acoustic drift.....	89
3.6.2	Basset-Boussinesq-Oseen equation	95
3.7	ACOUSTICAL PROPERTIES OF SUSPENSIONS.....	103
4	THE ELECTRO-ACOUSTIC FILTRATION EQUIPMENT.....	108
5	FILTRATION - RESULTS AND DISCUSSION.....	123
5.1	Small-scale dewatering tests enhanced by an electric and/or ultrasonic field.....	123
5.1.1	Bio/fiber suspension	125
5.1.2	Post-feculent phosphoric acid.....	129
5.1.3	Pyrite suspension	130
5.2	MINIPILOT-SCALE DEWATERING TESTS ENHANCED BY AN ELECTRIC AND/OR ULTRASONIC FIELD.....	133
5.2.1	Bio/fiber suspension	133
5.2.2	Post-feculent phosphoric acid suspension	134
5.2.3	Pyrite suspension	135
5.3	PILOT-SCALE DEWATERING TESTS ENHANCED BY AN ELECTRIC AND/OR ULTRASONIC FIELD.....	136
5.3.1	Bio/fiber suspension	137
5.3.2	Pyrite suspension	138
5.3.3	Post-feculent phosphoric acid suspension	140
5.4	ENERGY CONSUMPTIONS OF PILOT SCALE FILTRATION.....	144
5.4.1	Energy consumption comparison between small- and PILOT scale experiments.....	145
5.4.2	Connection of electro-acoustic method to filtration equipment	147
6	CONCLUSIONS.....	149
7	REFERENCES	153
8	NOMENCLATURE.....	160

1 INTRODUCTION

Nowadays solid/liquid separation processes are becoming more and more important to increase the capacity of production devices and in the treatment of waste sludges. This has led to the need to develop new kinds of separation equipment, and has enabled the tightening of environmental restrictions.

Traditionally, solid/liquid separation processes are based on a single driving force, gravity, vacuum or a positive pressure. Separation processes which are augmented by other forces such as ultrasound and/or other non-mechanical forces such as electric fields, are under development. With the electro-acoustic solid/liquid separation processes a new range of technologies is being established which will enable greater deliquoring rates and higher final solid contents of products.

Ultrasound, in the frequency range 20 kHz - 1 GHz, travels as elastic acoustic waves which propagate through gases, fluids and solid matter. High-intensity ultrasound has an effect on the medium in which the wave propagates. With a high level of ultrasound intensity it is possible to keep the filter medium open, to break the structure of the medium, or to change its properties.

The physical properties of the medium determine the mechanisms underpinning the effects of ultrasound, for example the propagation of the speed of ultrasound in the medium depends upon its temperature and consistency. So the frequency of oscillation, intensity and acoustic coupling of elastic waves to the matter, from which fluid will be separated, are important. The acoustic coupling determines the efficiency of elastic wave propagation from the ultrasound transmitter to the target material.

When a suspension to be separated is influenced by an electric field, the deliquoring process will be enhanced mainly by electrophoresis and electro-osmosis. The small negatively charged particles in suspension go to the

positively charged electrode, the so called anode, due to electrophoresis. Separation of positively charged "water droplets" on the cathode will be enhanced by electro-osmosis, sometimes referred to as a "pumping effect"/1/.

In this research project, an investigation of electro-acoustic filtration of bio/fiber-, pyrite- and post-feculent phosphoric acid suspension filtration was carried out. The theoretical part of the thesis focussed on determination of the electro-acoustic phenomenon and enhancement mechanisms connected to the filtration. Also, several properties of the suspensions connected to the electro-acoustic properties were determined. Some of these properties were also used to ensure that the suspensions were unchanged during the experimental period. Conversion criteria and physical properties of the ultrasonic transducers were explained. Also particle/fluid interactions in an ultrasonic field were investigated based on two different calculations; combined Stoke's and Newton's second law, and the Basset-Boussinesq-Oseen (BBO) equation.

In the experimental part of the thesis small- and mini-PILOT scale filtration tests enhanced using an electric and/or ultrasonic fields were carried out. On the basis of these tests enhancement values for filtration capacity were calculated. PILOT-scale filtration equipment was designed and operating parameters associated with the use of the electric and/or ultrasonic field were determined. In the filtration experiments it was detected that the best filtration results were achieved with bio/fiber suspension of 5 mass % when an electric field was used as a pre-treatment. The filtration capacity was increased 4-fold compared to the reference filtration. When a pre-treated suspension was filtered, the final dry solid content of the cake was 23 mass %, and in the reference filtration the corresponding dry solid content was 2 mass %.

When pyrite suspension filtration was enhanced by ultrasonic field, cake capacity (production capacity) was increased 4-fold and the final moisture content of the filter cake decreased to 7 %. In the reference filtration without ultrasound the

final moisture content of the filter cake was 14 - 15 %. Using an electric field to enhance the filtration, the cake capacity increased 3-fold but the final moisture content of the filter cake was the same as that in the reference filtration without an electric field.

The best result was achieved when post-feculent phosphoric acid filtration was enhanced by combined electric- and acoustic fields. The filtration capacity was increased 15-fold compared to the reference filtration capacity without a combined field. A 10-fold enhancement was achieved when only an ultrasonic field was used to enhance the filtration.

Using the optimum filtration conditions found by experiment, the specific energy consumptions associated with the enhancement techniques were calculated and compared to the energy consumptions of the conventional filtration methods.

2 LITERATURE REVIEW

2.1 Background of dewatering

Dewatering refers to removal of water from a product without producing a phase change in the associated water. Dewatering is sometimes referred to as a post-filtration process /2/ where water held between the particles or within the pores can be squeezed out by applying an external or body force.

Dewatering and filtration are hydrodynamic processes where the rate is directly dependent on the pressure drop across the filter medium and is inversely proportional to the total resistance offered by cake and the filter medium. The driving force in a conventional dewatering process is a pressure gradient across the filter cake. It is very important to minimise the filter cake resistance during the dewatering process because of the loss in the capacity of the dewatering equipment. Some of the important applications of the process are:/3/

- Separation of solid particles from a suspension
- Removal of supernatant from a solid-liquid suspension
- Removal of suspended solids by clarification.

The efficiency of the dewatering operation will have a major impact on the final stage of drying or incineration of solids.

Several types of conventional dewatering processes are used in the chemical, biological, and mineral processing industries. It has been well established that the rates of dewatering and the final solids concentration that can be obtained in a cake depend on a number of properties, such as:/4/

- Physical properties of the solids
- Physical properties of the liquid
- Electrokinetic properties of the cake or suspension.

In considering the dewatering phenomenon it is important to identify different types of water associated with a solid particle, such as:^{15/}

- Bulk or free water
- Micropore or capillary bound water
- Chemisorbed or monomolecular layer adsorbed water.

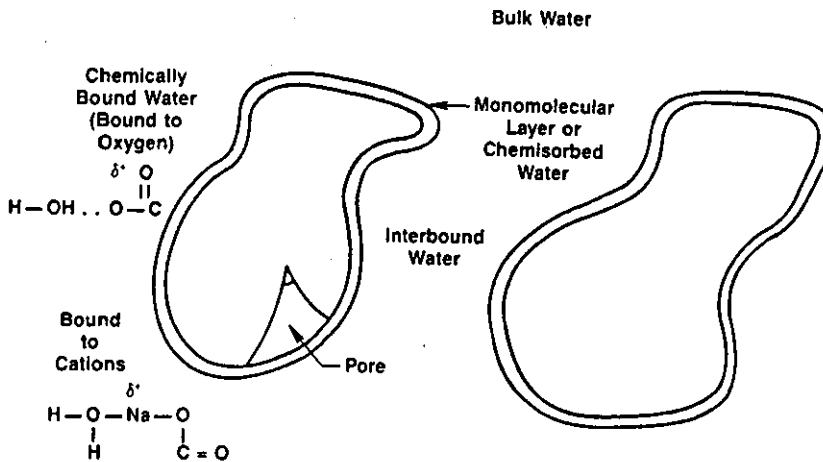


Figure 2.1. Types of water associated with a solid particle ^{13/}.

The success of the dewatering process depends on the relative amounts of the above types of water associated with the solid particle present in the suspension. For example, water in a typical colloidal suspension may be present in the following ratio: ^{13/}

- Bulk water – 40 percent
- Micropore water – 40 percent
- Colloidal water – 10 percent
- Chemisorbed water – 10 percent.

Dewatering technology in the chemical, mineral and other process industries has relied mainly on solid-liquid separation equipment that removes bulk water, such as vacuum filters, centrifuges or belt presses. Major advances in this technology in recent years have been related to the use of filter aids, surfactants or other additives in conventional systems to remove additional water. Although both

electrically and acoustically enhanced techniques are known, only limited commercial applications have been developed using these techniques.

Dewatering may be used as an intermediate process prior to some form of thermal drying. Some of the water in the capillaries or between the particles will be shaken loose or diffused out of the pores during dewatering, which is not feasible by a conventional filtration process. In many instances, if the product is the liquid dewatering can increase the recovery of the supernatant. In most cases, the energy required for dewatering is nominal; the only limitation is the level of solids concentration that can be achieved during this process. Since this intermediate step may reduce the heat load on the dryer significantly, a substantial savings on the capital and operating costs can be expected. Dewatering of fine colloidal materials is an especially difficult process. The difficulty has been attributed mainly to the fact that the particles are fine and highly hydrated. Generally, during conventional filtration, the fine particles clog the filter medium, thus reducing filtration rates significantly. In order to improve the rates of dewatering and to achieve a higher solids concentration, a number of pre-treatment steps are practiced, such as:

- Physical conditioning (heating, freezing)
- Chemical conditioning (addition of inorganic or organic polyelectrolytes) /3/.

2.2 Previous electrodeewatering research

Electrodeewatering cannot be discussed without an understanding of electrokinetics. This section therefore describes briefly the development of electrokinetic theory leading to the state-of-the-art of electrodeewatering/electrofiltration, and gives more details of the principles and underlying theory of electrokinetic phenomenon which affect movement of particles and/or fluid.

Electrokinetic phenomenon have been known for centuries. Robinson presented the earliest documented electroseparator device as attributed to the Academy del

Cimento of Tuscany. Reference is made to a report dated 1667 describing an apparatus for separating smoke into two streams using an electroacoustic field /6/.

Modern concepts of electrokinetic theory did not begin to evolve until the late eighteenth century. Coulomb first investigated the quantification of charge in 1785. Bocquet in year 1951 reported observations of electroendosmosis, today called electro-osmosis, through clay diaphragms by Reuss in Moscow in 1809. He also discovered the transport of suspended particles (clay) in water, electrophoresis, in the same year. Wiedeman took the first accurate electro-osmotic measurements in 1852.

Quincke discovered streaming currents in 1859 and went on to study the electrophoresis of starch grains in water in 1861. Quincke recognised that streaming current and electro-osmosis were correlative inverse phenomena and explained them using the double layer theory in 1861. In 1879, Helmholtz put Quincke's theory into precise mathematical form for capillaries. He referred to Wiedemann's and Quincke's experimental results for confirmation of his equations. Smoluchowski improved on Helmholtz's model, extending it to pores of random shape in 1903. There have been a number of subsequent refinements and improvements to the understanding and derivation of electrokinetic theory. The resulting mathematics are presented in Chapters 2.12.2 – 2.12.3.

Curtis (1931) described the development of industrial electrofiltration equipment applied to kaolin clays as attributed to Count von Schwerin. The equipment and process he perfected are disclosed in a series of U.S. patents issued between 1910 and 1918. They formed the basis for the Carlsbad Electro-Osmose Aktien Gesellschaft formed in 1914 near Chodau, former Czechoslovakia. The plant was originally equipped with four osmosis machines, adding two more in 1916 and two electro-osmotic filter presses in 1920 and 1926. This technology was sold to at least two other German kaolin processors before 1930 /7/.

2.2.1 Electrodeewatering – State-of-the-art

Yukawa et. al. /8/ studied electrically enhanced sedimentation, filtration and dewatering processes. Their results show: 1) batch settling curves of slurries applied with an electric field and the estimation method for the settling curves based on the gravitational batch settling curves; 2) efficiency of continuous settling and continuous thickening of slurries with an electric field; 3) electrophoretic separation of dispersed particles from an oil-in-water emulsion; 4) fundamental characteristics of electrokinetic filtration; and 5) the electro-osmotic dewatering of sludge which is difficult to dewater /8/.

The outline of the experimental apparatus was as follows. The lower electrode was set at the bottom of an acrylic resin cylinder with inner diameter of 90 mm, and was made of reticular copper or stainless steel of 20 mesh. The filter cloth was in contact with the lower electrode. The upper electrode was in contact with the surface of a sludge bed. The upper electrode was made of a perforated copper or carbon plate. In their experiments the sludge bed was not compressed by the upper electrode. The polarity of both electrodes was determined by considering of the polarity of ζ -potential of the particles. The voltage applied to the sludge bed was measured with an Automatic Recorder. The dewatered volume by electro-osmosis was obtained by subtracting the dewatered volume by gravitation from the total dewatered volume /8/.

Data for the thickening of a CaCO_3 slurry in an electric field with a continuous thickener are given by Yukawa. The data show that the mean concentration of final thickened sludge was over 65 %-wt. This final concentration of sludge was almost equal to that of a cake obtained by filter pressing. The authors mention that the settling rate and the concentration of sludge may be increased by means of electrophoresis and electro-osmosis. The batch electrokinetic dewatering experiments were performed using a slurry (calcium carbonate and white clay) concentration of 3 or 5 %-wt with the particles suspended in city water, and the filtration pressure was kept at 0.15 or 0.16 bar. The conclusion for the batch

electrokinetic dewatering experiments were that the flow rate during filtration was larger than that during conventional dewatering. Electrophoresis which occurred in the slurry reduced the rate of cake formation and at the same time the rate of permeation was increased by electro-osmosis occurring inside the filter cake /8/.

In the experiments of electro-osmotic dewatering of white clay and bentonite by gravitation at constant electric current, 1.573 mA cm^{-2} the initial water contents were adjusted to be nearly to the water content of sludge thickened by gravitational sedimentation, for white clay 55.3 and for bentonite 20.0 %-wt. According to the investigation, the authors found that electrophoresis increased the settling rate of suspended fine particles and the electro-osmosis thickened the sludge at the same time, and these electrokinetic phenomenon considerably increased the filtration rate and the dewatering rate of gelatinous sludges which are difficult to dewater /8/, /9/.

The design equations of electro-osmotic dewatering for compressible sludge under condition of constant voltage have been presented /9/. The rate of electro-osmotic dewatering and the electric power consumption were analysed theoretically by using the model of electro-osmotic flow through a compressible particle bed. The reliability of these equations was ascertained experimentally by use of compressible sludges such as white clay sludge and gelatinous bentonite sludge. Then the experimental results were compared with ones calculated from the theoretical equations. Initial concentrations of solids of white clay and bentonite sludges were respectively 55.3 and 20.0 %-wt, the same as in the previous experiments. The sludge was adequately mixed with deionized water. Both white clay and bentonite particles have negative ζ -potential. Therefore, the polarity of electrodes in the experimental apparatus was determined as in the previous experiments /8/ the upper electrode was the anode and the lower one the cathode. The electric fields under condition of constant voltage were applied to the sludge bed by a regulated D.C. power supply and current was measured. With

white clay the used constant voltages were 5, 7.5 and 10 volts and the initial height of sludge was 3.72 cm. The respective values for bentonite were 6, 9, 12 volts and 2.70 cm.

Their results showed that electro-osmotic dewatering under condition of constant voltage is very effective for gelatinous bentonite sludge which is hardly dewatered by gravitation. In the case of bentonite sludge, the dewatering efficiency (ratio of terminal to the initial water content of sludge) was 28.5 % when the voltage was 12 volts. In the experiments on vacuum dewatering of bentonite the corresponding efficiency was about 7.3 % under a vacuum of 0.8 bar. The results showed that the dewatered volume by electro-osmosis was about 4 times the dewatered volume by vacuum /9/.

The time to complete dewatering was generally reduced by electro-osmotic dewatering, but the final dewatered volume approached a nearly constant terminal value irrespective of voltage in the case of white clay sludge. The authors considered that there is a terminal water content in the case of electro-osmotic dewatering under constant voltage. Under condition of constant electric current, it was observed that the total dewatered volume by gravitation and electro-osmosis amounted to the first terminal water content and that the secondary dewatering process followed consecutively. Under condition of constant voltage, however, it was observed that electric current density passing through the cross-section of sludge bed decreased with dewatering time, because the electric resistance of the dewatered sludge bed increased with dewatering and the dewatered volume finally reached a terminal value. Consequently, the secondary dewatering process did not appear under conditions of constant voltage /9/.

Wakeman /10/ studied the effect of electric field on filtration, studying the effects of solids concentration and pH. The powders used in his work were Supreme China Clay and a china clay slurry containing an amount of extraneous fibrous

material. Size distribution of Supreme China Clay in different pH were the following: 50 % smaller than 9 μm , 2 μm and 1 μm respectively at pH 4.7, 8 and 9.

Wakeman described the nature of electrofiltration with the schematic representation in Figure 2.2. Cake formation as encountered in conventional filtration was modified in electrofiltration by the application of an electric field of suitable polarity and magnitude. If the field polarity was such that it assisted cake formation, rapid blinding of the medium would normally be experienced. In the case of a normal filtration both the liquid and suspended particles moved towards the filter medium and a cake was formed. An electric field of appropriate polarity and magnitude will initiate particle motion in the opposite direction at a rate dependent on the electrophoretic mobility of the particles and the hydraulic flow rate /10/.

In the absence of an electric field a cake grows on the filter medium. As the cake grows so the resistance to fluid flow increases and the filtrate collection rate falls off. An electric field can force the suspended particles to form a more open structured filter cake, or in the extreme will cause particle migration away from the collecting surface and prevent cake formation. In either case there is a filtrate flow rate improvement.

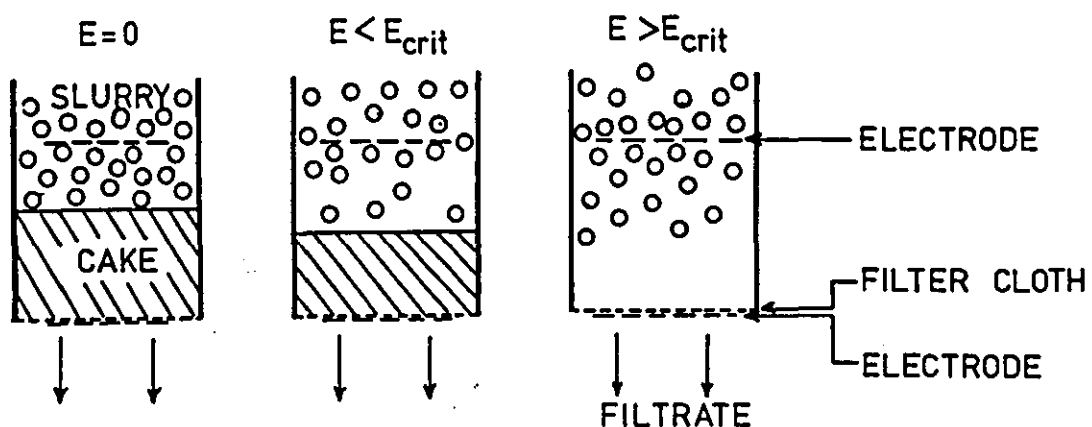


Figure 2.2. Schematic representation of electrofiltration /10/.

A critical voltage gradient was thought to exist, also referred to in other publications, at which particles will migrate counterflow to the liquid and at the same velocity as the liquid. Above this voltage gradient no cake formation was possible, but constant rate "filtration" should be obtained. This mode of operation should more correctly termed electrothickening, since no cake formation results whilst the suspension is densified /10/.

A series of experiments were conducted /10/ by filtering slurries of known concentration and pH at a constant total pressure drop at electric field strengths of 10, 20, 30, 40 and 50 V cm⁻¹. The results from these experiments showed that with no electric field the filtrate flow rate decreased rapidly, whilst at high field strengths the flow rate decreased at a lesser rate. In all cases cake resistance decreased with increasing field strength; the higher resistance noted at the greatest field strengths, 100 V cm⁻¹ at pH 4.9, and 70 V cm⁻¹ at pH 8.0, are a result of the solids concentration at the filtering medium being so low that pore blocking occurs rather than bridging filtration. The results also showed the effect of slurry concentration: as in a conventional filtration a higher resistance deposit was formed at lower solids concentrations. Also, since clay particles are poor electrical conductors, a higher electrical power consumption was experienced at the lower concentration./10/.

The effects of pH on both conventional filtration (no electric field) and electrofiltration were studied. In all cases lesser deposits are formed at higher field strengths, and more power is consumed with more conducting solutions. However, in spite of the increased solution conductivity significant cake resistance reductions were also obtained. There are two effects to consider when regarding the cake resistance data:

- ° the influence of pH on the zeta potential
- ° the effect of pH on effective particle size.

In Wakeman's experiments it can be seen that the absolute magnitude of the zeta potential (ζ) increased with pH for this type of solids. So a greater particle mobility is expected to result at higher pH values under similar electric fields. Further experiments had indicated that there was influence of solids concentration on ζ /10/.

The effect of pH to the particle size distribution was also studied /10/. It was noticed that at the natural pH of the solution the particles are aggregated, and the degree of aggregation decreased as the pH increased. This reduction of the effective particle size accounted for the underlying increase of cake resistance with increasing pH.

The results were concluded as follows: "electrofiltration may be a useful technique for the filtration of fine particles or suspensions which form a high resistance deposit. The interacting effects of solids concentration and pH on electrofilter performance are assessable and quantifiable, but the effect of pH on particle size and zeta potential should be carefully considered. The consumption of electrical power is quite low, although this will inevitably depend upon solid and liquid electrical conductivities" /10/.

2.3 Electro-membrane crossflow filtration

In normal filtration, both liquid and suspended particles move towards the filter medium and a cake is formed. As the cake grows, so resistance to fluid flow increases and the filtrate collection rate falls off. Applying an electric field modifies cake formation. If the polarity assists cake formation, the filter medium is quickly blinded. If the opposite polarity is applied, particles can be forced to form an open cake and, at the right magnitude, the electric field can cause particles to move away from the filter medium at a rate which depends on the electrophoretic mobility of the particles and the hydraulic flow rate. In either case there is an improvement in the filtrate flow rate. A critical voltage gradient is

thought to exist at which particles will migrate counterflow to, and at the same velocity as, the liquid. Above that critical voltage gradient no cake formation is possible and filtration should proceed at a constant rate.

The mode of operation above the critical voltage gradient might be more correctly termed electrothickening, because no cake is formed and the suspension gets thicker. In the crossflow mode, however, the ultimate objective of electrofiltration is the same as that of crossflow filtration: continuous production of a high purity liquid at high flux /11/.

Nowadays in industrial processes there are increasing demands with growing production capacities to separate either organic or inorganic matter (e.g. particles, variety of metabolites, microorganism, etc.) more precisely using greater separation capacities. Crossflow filtration is a promising technique for separation, concentration and fractionation of products. The modular set-up of filtration units is very suitable for scale up.

In spite of all the advantages the use of filtration in large-scale processes is still limited due to the problems arising with concentration polarisation, fouling, and flux decay. Several suspensions, e.g. biological suspensions, show a strong tendency to block membranes. Hence considerable attention has been drawn towards the development of anti-fouling strategies for crossflow filtration/12/.

Anti-fouling techniques try to remove fouling matter from the membrane, either continuously or during cleaning cycles. Examples of anti-fouling techniques that act continuously are the use of high crossflow velocities /13/, the use of baffled feed channels /14/ or the addition of bubbles to the feed solution /15/ to enhance the turbulence in the feed. The back shock technique and the back wash technique are cyclic cleaning methods for the membrane /16/. In certain time intervals the filter chamber is exposed to a short peak of overpressure which makes the fouling layer flake off or in the latter case the filtrate is washed back

through the membrane more smoothly. Both methods aim to reduce the fouling layer that is built up during the filtration cycle /12/.

Continuous or pulsating electric field is the one of the newest technologies under a development work to produce anti-fouling of filter mediums (e.g. filter cloth, woven wire, ceramic filters, different kind of membrane materials, etc.). The principle of electrofiltration is shown in Figure 2.2.

Wakeman /11/ published electrofiltration experimental results in the article Electrofiltration: Microfiltration plus Electrophoresis. The results were that normal filtration in a dead-end filter showed a flux which decreased at first and then became constant. The effect on filtration of a 1 % v/v (volume concentration) china clay suspension when the field was varied in the range 0 – 50 V cm⁻¹. Both the mass of the filter cake and its specific resistance decreased as the field increased: after an hour the volume of filtrate collected at 50 V cm⁻¹ was three folds that at zero field. These results suggest, and data from other particle systems gives further support, that if a sufficient high potential gradient were used, no deposit would collect on the surface of the filter.

Akay and Wakeman /17/ further studied electrofiltration in their article Electric Field Enhanced Crossflow Microfiltration of Hydrophobically Modified Water Soluble Polymers. The conclusion of the work was that at an electric field strength of 167 V cm⁻¹, the individual enhancements in permeate flux and pseudo-gel concentration and reduction in permeate polymer concentration can be as high as ten-fold.

Filtration flux enhanced by electric fields in crossflow microfiltration was investigated for several kind of suspensions, e.g. baker's yeast, rhodotorula glutinis by Okada and Nagase /18/. These results showed that application of the electric field in crossflow microfiltration was a useful method for improving the

filtration flux of these samples. High flux levels for the cells were achieved when an electric field above 30 V cm^{-1} was applied.

An alternating electrical field effect for the filtration was studied by Zumbusch et al /12/ using of alternating electrical fields as an anti-fouling strategy in ultrafiltration of biological suspensions. The alternating electric field diminished membrane fouling and hence yielded a higher specific filtrate flux. The effect of the electric field depended on frequency (0.5 - 50 Hz), field strength (0 - 80 V cm^{-1}), conductivity (1 - 10 mS cm^{-1}), protein concentration (0.1 - 5 w-%), and membrane material (values in brackets are the range of each parameter examined in that work). Low frequency and high field strength yielded the best result for electro-ultrafiltration with alternating fields. The effectiveness of the electric field increased with rising conductivity up to the point where a limiting electrolytic current was reached. Increasing protein concentration diminished the effect of the electric field /12/.

The theory of electric field enhancement of filtration such as electrokinetic properties and properties which affect electrophoresis and electro-osmosis are presented in this thesis more thoroughly in Chapter 2.8 .

2.4 Previous Acoustic Dewatering Research

Difficulties in the separation of finely dispersed solids in solid-liquid suspensions by conventional techniques, as well as interest in energy conservation, have spurred a research for more efficient and effective methods of filtration.

Ultrasound and electric field can provide the driving force for a wide range of chemical and industrial processing. While the major exploitation of ultrasound still remains in cleaning and welding a range of other applications are emerging. These include the cutting of brittle materials, atomisation, crystallisation and separation technologies while other developments are in the fields of mixing and environmental remediation.

In separation technology the applications of ultrasound are filtration and manipulation of particles in an acoustic field. Ultrasonic energy has been suggested many years ago to enhance dewatering efficiency. It is specially appealing as a means of dewatering heat sensitive materials such as food additives and pharmaceuticals where fast dewatering could prevent deterioration of the products if damaging heat levels can be avoided /19/.

Very little work has been done specifically on acoustic dewatering. However, the work that has been reported in literature illustrates to an extent the variety of ways in which dewatering may be enhanced acoustically.

Ensminger /20/ has described the history of acoustic dewatering in his article. As early as in 1936, Burger and Sollner suggested that sonic energy could be used for drying. In later years, 1957 Brun and Boucher suggested acoustic dewatering as an application for acoustic air-jet generators. In Brun's and Boucher's writings and in those of their contemporaries, acoustic energy was proposed for drying heat-sensitive materials, especially those that degrade in a moist environment, for example pharmaceuticals.

In year 1976, Bongert described a method of separating liquids from a mixture of solid matter and liquids by applying vibrations and vacuum simultaneously in a filtration process. The vibrational energy causes the solid particles to move constantly on the filter, thus maintaining a free flow of liquid through the filter. The result was improved filtration rate under vacuum. In 1983, Puskar also claimed improved filtration rate by the use of acoustic energy, which keeps the filter surfaces free of particles. Furedi used an acoustic interferometer technique to remove fine particles from a liquid medium in 1977. His method utilises the radiation pressure of a standing acoustic wave at approximately 1.0 MHz to cause small particles to migrate toward velocity nodal regions. The ultrasound was applied periodically, during which time the particles flocculate at the nodes. Flocculation increases the concentration and size of particles, and thus will

facilitate filtration. During the off periods, the particles settle through baffle plates. Among other applications, Furedi's technique has been used to separate algae from a solar or refuse pond, and blood cells from blood.

In 1978, Kowalska et al. used ultrasonic energy at 20 kHz with flocculants to reduce the water content of municipal sludges and mineral sludges. The sludges contained initially 2 to 3 percent solids. The water content was lowered by as much as 75 percent within 2 minutes. Again, the dewatering was a filtration process in which the ultrasonic energy enhanced the action of the flocculants and improved the filtering properties of the sludges. White was able to reduce the moisture content in wet sheets of paper in his experiments in 1964 by applying intense ultrasound at 20 kHz. The water in paper is held predominantly in pores. The ultrasonic energy was credited with overcoming the interfacial forces that held the water in the pores of the paper. Swamy et al. studied in 1983 the effects of soundwaves on the dewatering of granular materials including calcium carbonate, magnesite, sand, and sawdust, prior to drying. Acoustic energy was applied in combination with a centrifuge. Dewatering effectiveness was related to the variations in particle size.

2.4.1 Acoustic Dewatering – State-of-the-art

Beard and Muralidhara investigated coal/water slurry dewatering by ultrasonic and vacuum filtration, individually, and in combination /21/. The experimental apparatus was for high moisture suspensions. A cylinder 5 cm in diameter and 130 cm long was connected through a stainless steel grid which acted as a filter disc to a Buchner funnel where suction was applied. Ultrasonic energy was applied by a transducer and a wave guide or horn designed for these experiments. The stainless steel cylinder horn was immersed in the slurry to couple the ultrasonic energy for dewatering. The ultrasonic power generator produced a nominal 20 kHz electrical signal. The power level could be externally controlled. The converter, booster and horn were the three functional parts of the transducer. The piezoelectric converter converted the electrical power signal to mechanical

vibration in the booster. The booster and horn were mechanical wave guides and amplifiers. The horn transmits the ultrasonic vibration energy from the horn to the suspension being dewatered.

Each of the dewatering experiments was performed on a 50 g suspension. Coal/water slurries were prepared on a 1:1 basis using the following coal particle size distribution:

- ° 200 x 270 mesh – 25 percent by weight
- ° 270 x 325 mesh – 25 percent by weight
- ° 325 x 0 mesh – 50 percent by weight.

The prepared sample was transferred into the cylindrical portion of the apparatus, at the bottom of which a filter paper (Whatman 41) was placed on the top of the stainless steel grid. The sample was subjected to vacuum or ultrasound, or a combination, for different intervals of time. After the experiment the moisture in the cake was determined by moisture balance. The accuracy of the moisture balance was in the range of ± 3 percent. In order to check the results, the volume of water removed was also collected and weighed /21/.

Initial experiments were run with coal slurry of 50 percent moisture content. In their experiments it was observed that the moisture remaining in the cake decreased with time. At 50 watts input electrical power for 12 minutes, the final moisture content present in the cake was 15 %. As a base case, the experiment was repeated with vacuum only for comparison. Solids concentration achieved with vacuum gave a 30 % moisture content /21/.

The authors concluded from their results that ultrasound could significantly increase dewatering rate and decrease the final moisture content of high moisture suspensions when used in combination with conventional dewatering techniques /21/.

Fairbanks studied the filtration of coal slurry using ultrasound to increase filtration rate /22/. The liquids used included West Virginia crude oil and 30 % by weight motor oil. The solids which were added to the hydrocarbon liquids to make a slurry were made from coal washer waste materials. The coal wastes were crushed, pulverised, and then air classified. Only the particles having a size range between 1 and 40 microns were used. 5 % by weight of this solid material was added to the crude oil and 7.5 % by weight was added to the motor oil to make up the slurries.

The experimental equipment used included an open filtration unit, a closed filtration unit, and two different ultrasonic units, one for each filtration unit. The initial experiments used an open filtration unit which consisted of a clear plastic tube with about a 1 cm thickness of porous sandstone at one end. The tube was 25 cm in length and had a 7.5 cm inside diameter. The ultrasound radiation was introduced into the filtration system through the open end of the tube, radiation countercurrent to the liquid flow /22/.

The open filtration unit used an ultrasonic horn having a flat radiating end of 1.25 cm diameter. This unit was capable of producing 150 W of power and operated at a frequency of 20 kHz /22/.

In order to better study the effect of the pressure on the filtration system along with ultrasonic radiation, a closed filtration system made up of steel pipe was used. The slurry inlet section was located at the base of the unit and was made up of a 15 cm length of 7.5 diameter steel pipe with flanges welded on at each end. In the side of pipe was roughly a 0.6 cm inlet for running the slurry into the filtering system. The filter media section consisted of a 7.5 cm section of steel pipe also fitted with flanges at each end for assembling between the slurry inlet section and the filtrate outlet section. The filtrate section was of the same size and construction as the slurry input section except that a 0.6 cm diameter discharge outlet was located near the upper flange in the pipe. The cover plate for

the top of the filtrate section was specially designed for insertion of the ultrasonic horn through the plate and into the liquid filtrate. Both the slurry inlet section and the filtrate section could be pressurised independently between 0 – 0.9 bars /22/.

The closed filtration unit used an ultrasonic power source capable of producing up to 500 W of power. The frequency was also 20 kHz. The horn end was about 0.9 cm in diameter and had a flat radiating surface /22/. Ultrasonic energy between 0.6 – 6.0 W cm⁻² of filter area was applied to the system. A substantial increase in the filtration rate, up to 12 fold, could be obtained by the introduction of ultrasonic energy into the filtration system /22/.

2.5 Acoustic membrane filtration research

There has been little investigation using ultrasound to enhance cake dewatering. This is perhaps mainly due to the difficulties met on earlier research. In cake dewatering the solid concentrations are higher than in membrane filtration. This leads to the situation that commercial ultrasonic transducers with high enough output intensities are not available. So in cake dewatering enhanced by ultrasound, in many cases there is also a need for transducer development work to achieve positive results in experiments. The transducer development work is time consuming and expensive. There is a greater possibility of finding commercial transducers for experiments in membrane filter systems where much lower solids concentrations are encountered, because normally the needed output powers are lower than in cake dewatering. Cavitation levels to clean the membrane (if this is the aim) are lower in membrane filtration than in the cake dewatering due to the lower solid concentrations. Also, one of the driving forces towards membrane filtration during the 1990s is the need of industries to filter their process streams and effluent waters to higher purities. New industrial applications, especially in the areas of biotechnology and the pharmaceutical industry, have set greater demand for the development of new kinds of anti-fouling membrane technologies for their purposes.

The capabilities of ultrasonic radiation forces for manipulating suspended particles have engendered a broad spectrum of experimental investigations. Ultrasonic aggregation has been exploited to improve the sensitivity of medical latex agglutination tests for detecting immunogenic agents /23/ to enhance the recovery of two cell populations by phase partitioning /24/. Continuous cell separation has been achieved for mammalian cells /25/, continuous fractionation of mixed-particulate suspensions based on the compressibility of the solid phase /26/ and the selective retention of generally larger viable mammalian cells over nonviable cells and cell debris /27/ have been reported among several others in these new areas. The advantages in the membrane filtration reported by the latest articles are as follows: particle separation by ultrasonic forces exhibits innate advantages relative to conventional methods, particularly in the area of biotechnology. Cross-flow membrane filtration and spin-filter separators suffer from fouling, continuous centrifuges are susceptible to mechanical failure, conventional systems require long hold-up times. For ultrasonic separation, no physical barrier is required, hold-up times are low, and chemical flocculants are not necessary /28/.

The phenomenon of acoustic dewatering is described more thoroughly in the sub-chapters 2.9 (Enhancement mechanisms of ultrasound) and 2.10 (Cavitation).

A few patents have been granted that describe various mechanisms associated with ultrasonic dewatering /29/.

Bongert /30/ developed a method to separate liquids from a mixture of solids matter and liquids by applying vibrations and vacuum simultaneously. The solid particles were allowed to move constantly on a permeable medium (filter), thus allowing good drainage of the liquid through a filter. However, according to Bongert, the rates of filtration improved only with the continuous withdrawal of the liquid by vacuum.

Furedi /31/ developed an apparatus for removing fine particles from liquid medium in the presence of sonic waves. This technique has been applied to materials such as algae from a solar or refuse pond, blood cells from blood, etc. The frequency of the generator was about 1.0 MHz. This is an interferometer technique of low intensity which utilises the radiation pressure of a standing acoustic wave to cause small particles to migrate toward velocity nodal regions. The sound is applied periodically, during which time the particles flocculate at the nodes. During the off periods, the particles are allowed to settle through baffle plates.

Kowalski et al. /32/ performed experiments using ultrasonic energy and flocculants to treat municipal sludges and mineral sludges. The ultrasonic frequency was 20 kHz and the power into the transducer was 800 W. The initial solids concentration of the sludges was 2 to 3 percent. Under the influence of the ultrasound with an exposure of 2 minutes and suitable use of flocculants, the moisture content of the sludges was reduced by as much as 75 percent.

2.6 Magnitude of ultrasonic radiation force

Woodside et al. /33/ determined the magnitude and direction of the ultrasonic radiation forces that act on individual particles in a standing-wave field by a microscope-based imaging system. The relevant ultrasonic forces are the axial and transverse components of the primary radiation force (PRF), and the secondary radiation force (SRF). In their experiments to measure the axial PRF, they used the frequency range between 2.1 and 2.4 MHz, input power of 26 W l⁻¹. In these conditions the particle reached a maximum velocity of 750 $\mu\text{m s}^{-1}$. The wavelength calculated from the sound speed and frequency was 671 μm /33/.

Despite the nonuniform energy density of the field, the relationship between the power and the axial PRF was expected to be linear at any given resonance frequency and location in the field due to the linear dependence of the axial PRF

on acoustic energy density. By experiments they pointed out that the discrepancy between fitted and calculated values for the above mentioned presumption was only 10 % /33/.

Direct measurements of the transverse PRF were performed in the conditions of input power 59 W l^{-1} and the measured particle velocities were about $10 \mu\text{m s}^{-1}$ /33/.

The results showed that the estimated transverse PRF was two orders of magnitude less than the axial PRF. Their assumption of constant acoustic energy density in the axial direction was also supported by these results. The transverse PRF would be approximately $6 \times 10^{-12} \text{ N}$, 20 times greater than gravitational force on a single particle ($3 \times 10^{-13} \text{ N}$). The approximate flow rate against which a single particle of diameter $10.2 \mu\text{m}$ could be held by the transverse PRF at these power levels is $60 \mu\text{m s}^{-1}$. Under similar operating conditions single particles could be retained by the axial PRF against flow velocities of the order of 1 cm s^{-1} /33/.

Taking these observations in isolation, it would appear that exploitation of the axial PRF is the logical choice for particle – liquid separation /33/.

2.7 Previous electro-acoustic dewatering research

The electro-acoustic dewatering technique uses conventional mechanical processes in combination with electroseparation and acoustic dewatering technology. The principles behind the both techniques are described above and explained in more detailed in later chapters .

A synergistic effect of electroseparation when combined with acoustics was discovered by the Battelle-Columbus Division in the USA. In the late 1980s Battelle had tested over 30 suspensions and established a wide applicability of

the electro-acoustic dewatering process. Based on the work done, they have found many applications in industries such as coal/lignite, food, pulp/paper, biomass/peat, ceramics/clays, minerals, and wastewater treatment.

For some applications, such as food processing, municipal wastewater treatment sludge dewatering, and mineral sludge dewatering the process has been tested in a continuous bench-scale (about 3 or 7 kg h⁻¹ feed rate). For others, the data were essentially limited to batch scale dewatering /34/.

2.7.1 Electro-acoustic dewatering – State – of – the art

Combined field, electro-acoustic, dewatering research has been studied by few scientists. This kind of research has been carried out mainly by Battelle-Columbus Division in the USA and by Technical Research Centre of Finland in the Energy Research Division (VTT/ENE).

Senapati /35/ carried out research using an electric field to enhance dewatering and then continued dewatering using acoustic field to enhance the final part of dewatering. With Hertogenbosch sludge at a batch-scale the initial solid concentration were about 16.4 % w/w. This sludge was subjected to an electric voltage of 35 V, and the ultrasonic power was varied from 0 to 20 W. The total dewatering time was 2 minutes. The electric field alone was effective in increasing the solids from 16.4 to 24.2 percent. The final solids percent appeared to increase monotonically from 24.2 to 30.2 percent with the increase in ultrasonic power from 0 to 20 W. The rate of increase appeared to be almost constant with increase in ultrasonic power.

Similar batch test on Ridderkerk sludge were also carried out. The initial solids concentration was 16 %, and the electro-acoustic dewatering (EAD) residence time was 3 minutes. When a 60 V field was applied, the solids increased from 16 to 24 % with no ultrasonic power. Similar to the previous example, the final solids appeared to increase from 24 to 26 % with increase in ultrasonic power

from 0 to 20 W. Senapati concluded that not only was the change in percent solids significantly lower than the previous example, but also that the rate of increase appeared to be decreasing with ultrasonic power /35/.

A further batch test on Columbus Southerly waste activated sludge was done. For this sludge the final solids content was not affected by ultrasonic power up to 10 W. Between 10 and 20 W, the final solids concentration appeared to assume a bell-shaped curve with the highest value for an ultrasonic power of 15 W. Senapati concluded that these three examples illustrate that the effect of ultrasonic power on the rate and the degree of dewatering is a strong function of the type of sludge /35/.

Muralidhara et al. /36/ presented results on the simultaneous use of electric and acoustic fields during dewatering. Corn gluten slurry experiments was carried out at the bench-scale. Corn gluten slurry is one of the products of corn wet milling. A sample of the corn gluten slurry had an initial solid concentration of 13.01 %. The corn gluten slurry is a colloidal, low conductivity slurry with high zeta potential values. The synergistic effect of combined electric and ultrasonic fields showed the variation of solid content as a function of dewatering time in minutes. The results confirmed that the rate of dewatering and solid content increased with simultaneous application of electric and ultrasonic field. For example, at 6 minutes with a vacuum field, a cake with about 34 percent solids was achieved. However, in the presence of electric and ultrasonic fields and vacuum, the solid content increased to 46 % and, simultaneously, rate of dewatering increased by about 2.4 fold /36/.

In the same article the authors also presented results with corn fiber slurry. At the present time, screw presses are utilised in the industry to dewater this slurry. Typically a solid concentration of about 38 % is achieved. Hence, experiments were performed in pressurised dewatering equipment, the results clearly indicated that a combination of electric and ultrasonic fields in the presence of pressure

was always better than either electric or ultrasonic field when used separately in the presence of pressure. For example, at 60 seconds with 2.7 bars pressure alone, the solids content achieved was 27.5 %. However, under the same condition, in the presence of ultrasonic and electric fields the solids content achieved was 32 %.

The authors concluded that the above results indicates that the electro-acoustic dewatering process could be successfully applied to different types of suspensions having varying properties including physical, chemical and electrokinetic /36/.

This Ph.D Thesis consists of those electro-acoustic dewatering studies done at VTT/ENE during the period of 1991-1995. Experiments were done in the batch-, miniPILOT- and PILOT scale using electric and ultrasonic field either separately or simultaneously depending on the nature of the suspension and/or dewatering method. The results describe the best electric and/or acoustic conditions and dewatering methods for the suspensions used in the experiments.

2.8 Fundamental electrical properties of solid/liquid mixtures

The enhancement of filtration by electric fields is determined by several factors including the surface charge of small particles which are suspended in the fluid. Particle surface charge is due to the interaction between the particles and the fluid. In fluids the surface charge of small particles is normally negative. The electric repulsion between small particles keeps them well dispersed in the suspension, preventing settling, so the suspension is stable and deliquoring is difficult. When an electric field is applied to this kind of suspension, small negatively charged particles drift to the anode by electrophoresis where the surface charge of the particles is neutralized and the particles agglomerate. The separation of positively charged fluid droplets will be enhanced at the cathode filter by the effect of electro-osmosis. In Figure 2.3 are shown electrical forces and the different effects which occur /3/.

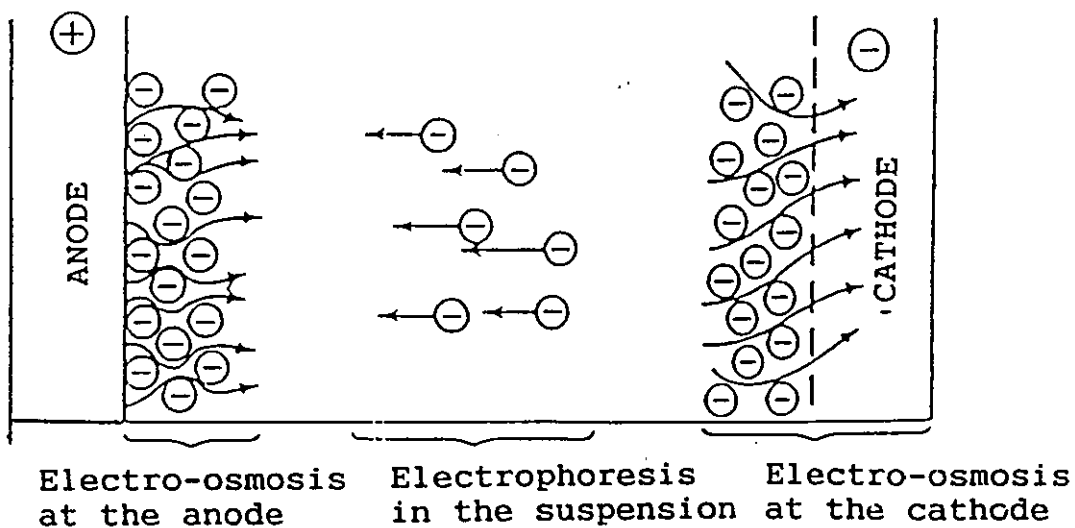


Figure 2.3. Electric forces and the different effects which occur /38/.

Furthermore, small particles can agglomerate due to the electric field. Also the field moves particles away from the filter medium (cathode), when the flow resistance and the fouling of the filter medium decreases. In the Figure 2.4 is shown a solid/liquid separation process enhanced by an electric field. The enhanced deliquoring due to electro-osmotic forces causes a decrease in the fluid content of the cake; the electric field dries the wet cake by moving the fluid from the pores to the cathode /37, 38, 39 /.

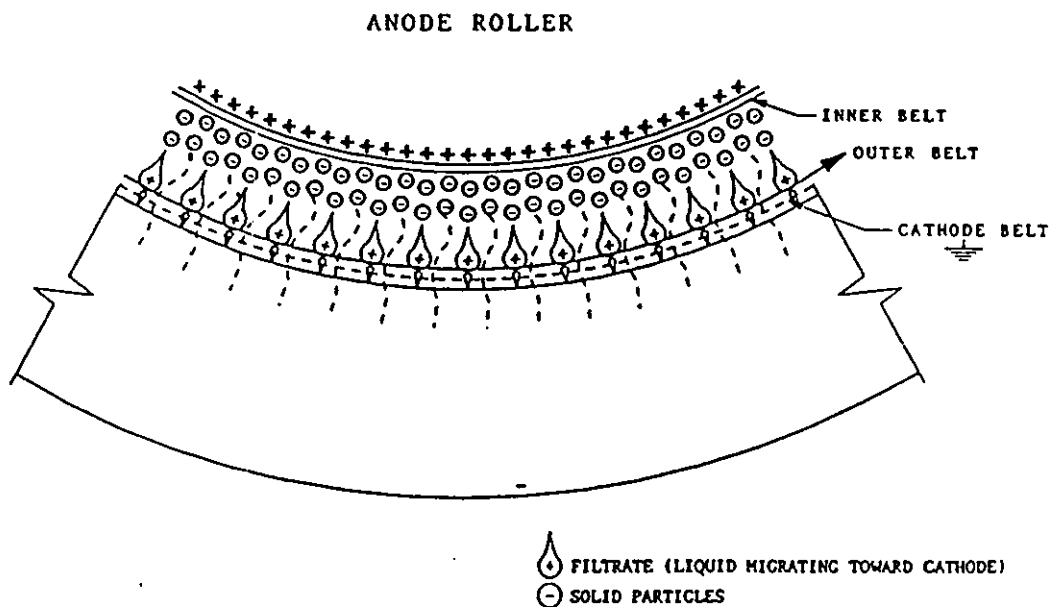


Figure 2.4. Solid/liquid separation process enhanced by electric field /38/.

2.8.1 Electrokinetic properties

The enhancement of filtration depends on the electrokinetic properties - electrophoresis, electro-osmosis, streaming potential and sedimentation potential. Electrophoresis has the greatest effect in filtration. In electrophoresis a charged particle moves relative to the fluid in the electric field. In electro-osmosis, due to the electric field the fluid moves compared to a stationary charged particle. The opposite phenomenon to electro-osmosis is the streaming potential, in which an electric field is created when the fluid moves along the charged surface. The sedimentation potential, the opposite phenomenon to electrophoresis, is an electric field caused by the charged particles when they move relative to the fluid /40/.

The size and surface charge of the particles, and the strength of the electric field have an effect on the deliquoring rate. In the enhancement of solid/liquid separation by an electric field, the process is dependent on the electric field strength, which in turn depends on the distance between the electrodes, the voltage which is applied and the conductivity of the suspension. The filtration can be made faster by increasing the strength of the electric field and the surface charge of the particles /41/.

2.8.1.1 Electrophoresis

Equations 2.1 and 2.2 describe the rate of electrophoresis and the mobility in the DC field compared to a stationary fluid /40/.

$$u_E = v_E/E = \zeta\epsilon/\mu \quad (2.1)$$

$$\text{i.e.} \quad v_E = E\epsilon\zeta/\mu \quad (2.2)$$

where: E = electric field strength, (Vm^{-1})
 ϵ = permittivity of electrolyte solution, ($\text{C}^2\text{N}^{-1}\text{m}^{-2}$)
 ζ = zeta potential, (V)

μ = viscosity of fluid, (Nsm^{-2})

u_E = mobility of particle due to electrophoresis, ($\text{m}^2\text{s}^{-1}\text{V}^{-1}$)

v_E = rate of electrophoresis, (ms^{-1}).

The rate of electrophoresis for spherical particles, both conductive and non-conductive, can be described by Henry's electrophoresis equation (2.3). The conductivity is not significant in the case of charged dots but the conductivity can be significant in the case of particles which are acting as a surface (large values of (κa)). κa is the ratio of the radius of the particle to the thickness of the electric double layer, and $1/\kappa$ is the thickness of the diffuse part of the electric double layer. When κa is small, the charged particle can be handled like a dot charge, and when κa is larger a surface describes the double layer in the best way. Often conducting particles, although they polarize in the electric field, act like non-conducting particles. Henry's equation in the DC field can be written as /40/

$$v_E = (\zeta \epsilon / 1.5 \mu) f(\kappa a) \quad (2.3)$$

The value of the function $f(\kappa a)$ is about 1 with small values of κa (charges like a dot), and about 1.5 with large values of κa (charges like a surface) /40/.

Another equation, similar to Henry's equation, takes account of the particle's size, shape and surface charge and is known as Kirshnaswamy's electrophoretic equation for the DC field (2.4) /37/.

$$v_E = (\zeta E \epsilon / \pi \mu) f \quad (2.4)$$

where: $f = 1/8 - 1/4$, depending on the particle's size, shape and electrical properties

2.8.1.2 Electro-osmosis

When the electric field causes the fluid to move relative to a stationary charged particle, the phenomenon is called electro-osmosis. When ka is large, the electro-osmotic flow rate in the DC field can be calculated from equation (2.5) /40/.

$$dV/dt = Av_E = AE\varepsilon\zeta/\mu = \varepsilon I\zeta/(\mu k_0) \quad (2.5)$$

where: V = volume, (m^3)
 t = time, (s)
 A = area, (m^2)
 μ = viscosity of fluid, (Nsm^{-2})
 I = current, (A)
 k_0 = conductivity of fluid, ($\Omega^{-1}m^{-1}$).

The Kirshnaswamy's electro-osmotic equation (2.6) in the DC field is once again similar /37/.

$$dV/dt = \varepsilon I\zeta/(4\pi\mu k_0) \quad (2.6)$$

2.8.2 Properties which affect electrophoresis and electro-osmosis

The strength of the electric field, conductivity of the fluid, permittivity and viscosity all have an effect on electrophoresis and electro-osmosis, according to equations (2.1) - (2.6.) Zeta potential, particle size and shape, and electrical properties of the particles also have an effect.

From equation (2.7), the parameters that affect the permittivity of the fluid can be seen /40/

$$\varepsilon = 1/F(q_1q_2/(4\pi r^2)) \quad (2.7)$$

In equation (2.7), F is the force with which the charges q_1 and q_2 repel or attract each other over the distance r . The dielectric constant of material (ϵ_r) is proportional to its permittivity ($\epsilon = \epsilon_r \epsilon_0$). The permittivity of vacuum is $\epsilon_0 = 8.854 \times 10^{-12} \text{ J}^{-1} \text{ C}^2 \text{ m}^{-1}$. (This is the reason why water is a good solvent because water decreases strongly the Coulombic attractive forces between ions. Interactions between ions then decrease and crystallization is prevented) /42/.

2.8.2.1 Electric double-layer

Around the surface of most dispersed materials there is an electric double-layer when it is in contact with polar matter, for example water. A particle's surface charge is due to the interaction between the particle and the fluid. The zeta potential is the potential difference between the electrolyte bulk solution and the fluid near the particle surface. If the fluid in the suspension is water, the surface charge is normally negative because the cations normally hydrate more easily than the anions. This is also why cations sediment more easily than anions in aqueous suspensions /40/.

Charging of the surface can be due to ionization, ion adsorption (complete adsorption of oppositely charged ions) and dissolution of ions (incomplete dissolution) /43/. The electric double layer can be regarded generally as consisting of two regions: an inner region which may include adsorbed ions, and a diffuse region in which ions are distributed according to the influence of electrical forces and random thermal motion. The diffuse part of the double layer will be considered here /40/.

Specifically adsorbed ions are those which are attached to the surface by electrostatic and/or van der Waals forces strongly enough to overcome thermal agitation. They may be dehydrated in the direction of the surface. The centres of any specifically adsorbed ions are located in the Stern layer, i.e. between the surface and the Stern plane. The electric potential from the surface in the distance x can be calculated by equation (2.8) /40/

$$\Psi = \Psi_0 \exp[-\kappa x] \quad (2.8)$$

where: Ψ = electric potential from surface at distance x , (V)
 Ψ_0 = potential of surface, (V)
 x = distance from surface, (m)
 $\kappa = (2e^2 n_0 z^2 / (\epsilon k T))^{1/2} = (2e^2 N_A C z^2 / (\epsilon k T))^{1/2}$
 N_A = Avogadro's constant = $6.022 \times 10^{23} \text{ mol}^{-1}$
 C = concentration of electrolyte solution, (kgm^{-3})
 z = charge of ion, (C)
 e = charge of electron = 1.60219×10^{-19} , (C)
 n_0 = ionic concentration, (m^{-3})
 k = Boltzmann's constant = 1.38066×10^{-23} (J K⁻¹)
 T = temperature, (K)
 ϵ = permittivity, ($\text{C}^2 \text{N}^{-1} \text{m}^{-2}$).

Many of the properties of fine particle systems can be predicted or explained by reference to the zeta potential, but it is important first to understand that zeta is not a uniquely definable parameter of the particle alone as the particle size may be, for instance. Rather, it is dependent not only upon the nature of the particle, but also upon that of the medium in which it is dispersed. Thus, it will not normally be meaningful to talk of zeta potential without first fully describing the conditions under which it is measured. Indeed, the majority of experiments will be aimed at studying the way in which zeta potential changes as pH, electrolyte concentration or, perhaps, the nature of a polymeric flocculant, is altered /44/.

Many examples are concerned with coagulation or flocculation and colloidal stability. In the pharmaceutical industry, for instance, effective methods of producing physically stable dispersions of drugs in suitable suspension media can be devised after thoroughly studying the conditions for maximum deflocculation by means of electrophoretic mobility measurements. The stability of drug suspensions can affect dosage requirements as well as shelf life. In paints, the

degree of dispersion of a pigment can affect the colour quality, gloss, texture, and flow properties. Optimum dispersion conditions in relation to particle size, composition, and additive usage can be established with the aid of zeta potential analyses /44/.

As an example of how zeta potential is affected by small changes in electrolyte concentration, Figure 2.5 shows results for a silver iodide sol that is used in many investigations as a model not only for photographic materials but also for colloidal systems in general. Measurements were made at a constant iodide ion concentration, pH 3, and the sensitivity is apparent even over the small range of concentration of indifferent electrolyte studied, zero to 8.5 mM /44/.

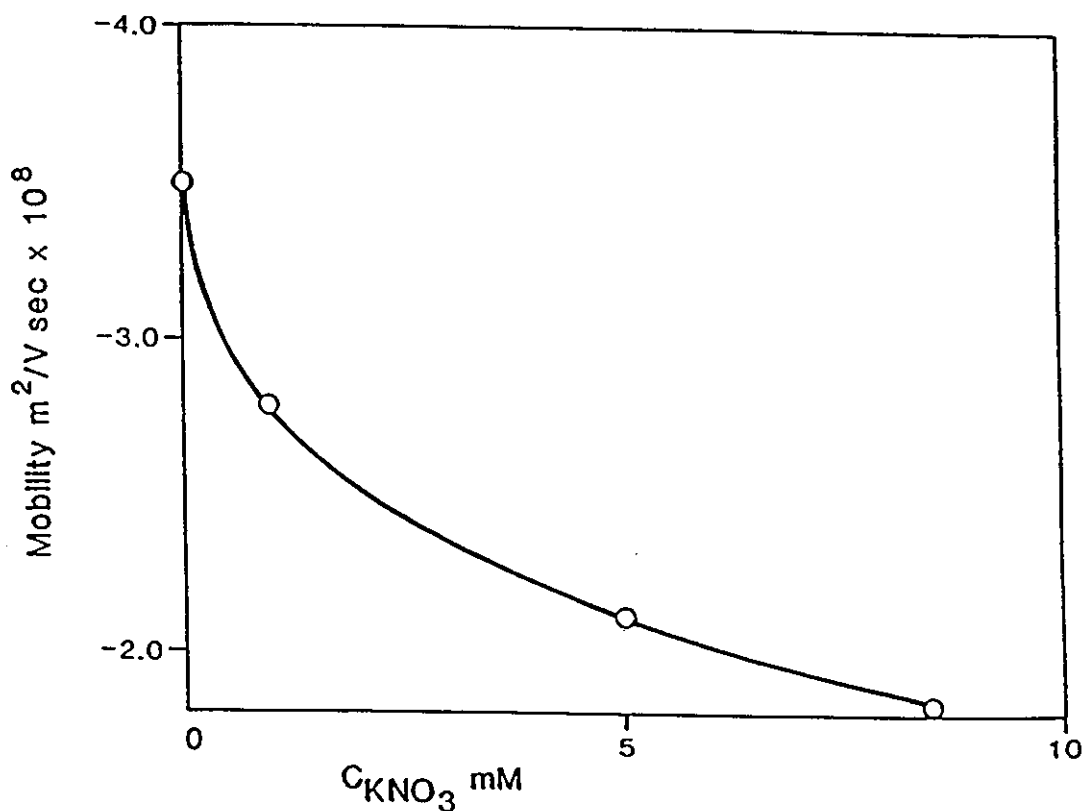


Figure 2.5. Effect of electrolyte concentration on electrophoretic mobility of a silver iodide sol at constant iodide concentration /44/.

In mineral refining, enrichment of metal ores is frequently achieved by a process of differential flotation in which collector oils are added to a suspension of the

ground ore. The efficiency of adsorption of these oils and the subsequent recovery process depends heavily on the size and magnitude of the charge on the ore particle, anionic oils adsorbing efficiently on positively charged ore surfaces and vice versa. At low zeta potentials, little oil is adsorbed. Another consequence of low zeta potential is the loss of dispersion stability resulting in coagulation and increased particle size. Oxides and hydrated oxides are particularly sensitive to pH as H^+ and OH^- ions act as potential determining ions, for instance with a ferric oxide sol as the pH is varied. In this case, Figure 2.6, the stabilizing effect of a moderate to high zeta potential is clearly reflected in the lower average particle size seen both at low pH, where the potential is positive, and at high pH, where the excess of OH^- has led to charge reversal /44/.

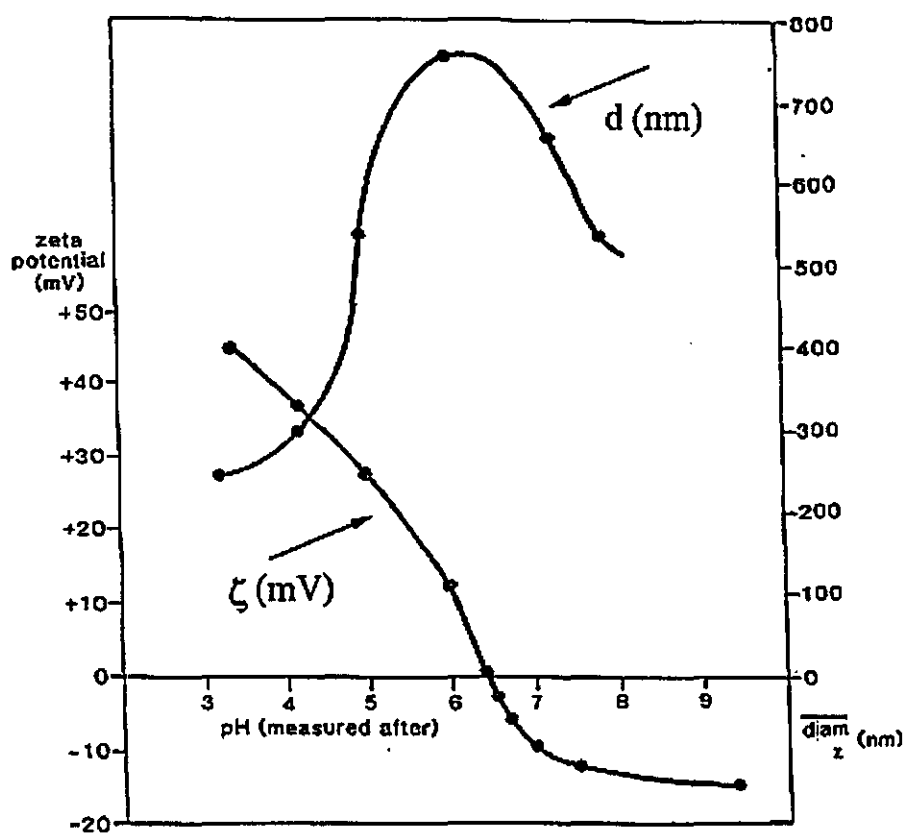


Figure 2.6. Changes in particle size reflect the changes in zeta potential of a ferric oxide dispersion as the pH varies; at low potentials, the system is unstable and flocculates /44/.

In the intervening region, where the zeta potential is low and passes through zero, the freedom of the particles to collide and form aggregates, i.e., flocculate, results in a substantially larger average particle size /44/.

2.8.3 Phenomenon of electroseparation

Electroresparation takes place due to the fact that most fine particles suspended in water tend to be negatively charged. Often the mutually repelling effect of these small charged particles keeps them well dispersed, making the suspension very stable, hence difficult to dewater. When the slurry is subjected to an electric field of appropriate strengths, the charged particles migrate toward an oppositely charged electrode. This phenomenon is described in Fig. 2.3. Using an electric field to enhance dewatering, one or more of the following effects can be achieved:

1. The electric field neutralizes charges on the particles, causing them to agglomerate and accelerate dewatering rates.
2. The electric field causes particles to move away from the permeable electrode (filter medium) so more rapid dewatering can occur without blocking the filter medium.
3. The electric field moves the water due to the electro-osmotic forces. This is the primary mechanism involved in dewatering of a wet cake. The same phenomenon will occur in the presence of an electrical double layer at the capillary walls of a pore. In many colloidal materials, bound water and a water film are trapped by counter ions to the capillary walls of a pore. If an electric field is applied to the ends of the capillary containing water, a mobile layer containing water moves towards the cathode. The flow of water stops in the absence of an electric field /3/.

2.9 Enhancement mechanisms of ultrasound

It has been observed that ultrasound enhances solid/liquid separation processes. Ultrasound has been incorporated with mechanical processes, e.g. vacuum

filtration, compressive pressure filtration, membrane filtration or connected to electro-mechanical separation process /37, 38, 39, 41, 45, 46, 65/.

The enhancement mechanisms of ultrasound in solid/liquid separation are still unclear. In dewatering processes based on electro-osmosis, ultrasound has been used to enhance the process and it is thought that the enhancement mechanisms are due mainly to: 1) an increase of contact between the electrodes and the water, 2) easier penetration of water through the filtration surface, 3) enabling detachment of the expelled water from the filtration surface, and 4) an increase of the packing density and the conductivity of the filter cake /37/. It must be said that these mechanisms are largely conjectural.

The enhancement in the dewatering rate and in the final dry solid content of the product are based on mechanical dewatering processes, and the properties of the suspension. In particular, these properties are: 1) physical properties (density of solid phase, particle size distribution, porosity, shape of particle, compressibility of particle, density of fluid phase, temperature and viscosity), 2) electrokinetic properties (zeta potential, pH of suspension and conductivity) and 3) operating conditions (feed and final concentrations, rate of process) /37/.

The so called internal water, water in micropores, water inside colloids and chemically bound water, is very difficult to remove mechanically. Ultrasound affects the internal water, it also increases the rate of dewatering and the final dry solid content of the product /37, 38, 41, 45, 46, 65/.

There are many fundamental mechanisms by which ultrasound can enhance solid/liquid separation. The importance of different mechanisms is difficult to estimate, and the mechanisms are related to each other. Below is a list of the main mechanisms connected to ultrasound:

1. Mechanical

- a) wave propagation effects: - radiation force, standing wave.
- b) inertia effects: - high relative acceleration, high relative inertia forces.
- c) bubble oscillation effects: - streaming, Bernoulli forces, Oseen forces, Stokes forces.
- d) bulk effects: - decrease in effective viscosity.

2. Chemical

- a) transient cavitation: - high localized pressures and temperatures, free radical formation.
- b) mass, momentum and heat transfer: - synergistic effects of bubble oscillation on wave effects.

3. Thermal

- a) internal heating: - internal heating, molecular adsorption, internal reactions.
- b) surface heating: - surface friction, higher harmonic oscillations of bubbles /37/.

The drag force connected to the motion of a particle can be described by Stoke's law ($Re < 0.1$)

$$F = 6\pi r \mu \Delta u \quad (2.1)$$

where: r = radius of particle, (m)
 Δu = velocity difference between particle and fluid (ms^{-1}).

The product $(\mu \Delta u)$ during one cycle will have an average value. This causes F to have an average value, which can cause the particle to drift toward the sound source /37/.

The Oseen force arises from wave shape distortion associated with large amplitudes. If the particle is much smaller than the wavelength, the momentum transfer rate is greater during the descending portion of a saw tooth shaped wave than during the slowly rising part. This produces a small net pressure which is proportional to the degree of wave distortion. For low distortion in the sound field, this force is negligible /37/.

2.9.1 Particle/fluid interactions in an ultrasonic field

In general, power ultrasound is characterized by an ability to transmit substantial amounts of mechanical power at small mechanical movements. Ultrasonic motional amplitude is limited by the allowable stress in the ultrasonic transducer material and is frequency dependent. To illustrate typical values, a 20 kHz transducer operating at a peak displacement amplitude of 50 μm has a peak velocity of 6.28 ms^{-1} and a peak acceleration of $8 \times 10^4 \text{ g}$. More completely then, power ultrasound is characterized by high vibrational frequencies (for reciprocating mechanical movement), small displacements, moderate point velocities, and extremely high accelerations /47/.

Most macrosonic applications depend on compound acoustic phenomena occurring in matter, which, in turn, are caused by primary vibratory inputs. Thus acoustic pressure causes, for example, cavitation and microstreaming in liquids, vibratory stress causes heating and fatigue in solids, and ultrasonic acceleration is responsible for surface instability occurring at liquid-liquid and liquid-gas interfaces /47/.

Bell and Dunnill /48/ have studied low frequency acoustic conditioning of protein precipitates. They also consider 3 major factors to be important using ultrasound. They are:

1. Orthokinetic aggregation due to covibration of the particles.
2. Attractive and repulsive hydrodynamic forces between neighbouring particles.
3. Radiation pressure due to particles scattering the incident wave /48/.

In general however, the application of ultrasonics to dewatering, aggregation etc. is not well understood. In many cases the enhanced effect of ultrasound is due to a combination of many effects acting synergistically.

2.9.2 Acoustic agglomeration mechanisms

Under ultrasonic irradiation at low power, standing waves can be set up in a liquid. It has been shown that small particles suspended in a liquid migrate to the nodes of these standing waves /49, 50, 51/. The most important mechanisms for particle agglomeration in a sound field are the orthokinetic and hydrodynamic interactions. There are also other mechanisms which have an effect on acoustic agglomeration, such as acoustic turbulence, acoustic streaming and acoustic drifting. But these do not have so great an effect on particle agglomeration as the orthokinetic and hydrodynamic interactions /52/.

2.9.2.1 Orthokinetic interaction

According to the orthokinetic interaction mechanism, small particles are collected by larger ones because of the relative oscillatory motion caused by the sound field. An important concept involved in the process is the acoustic entrainment of particles. Particles exposed to the sound field attempt to move back and forth with the oscillatory motion of the medium. Smaller particles move more easily with the medium than larger ones. As a result, different sized particles move relative to each other. Each large particle, acting as a collector, will sweep a certain volume by its relative motion to small particles in one acoustic cycle. If any small particles are present in the volume, they may collide and stick with the large one. This volume, shown in Figure 2.7 is often called the acoustic agglomeration volume. The larger the agglomeration volume, the more small particles are likely to be collected in an unit time. Thus the rate of agglomeration is directly proportional to the dimension of the agglomeration volume.

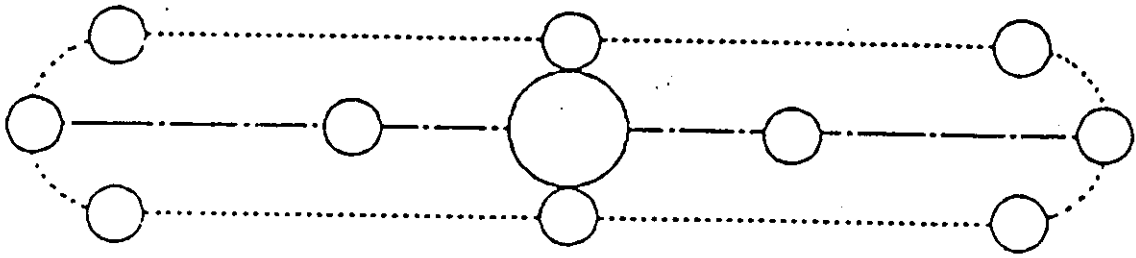


Figure 2.7. Diagram of acoustic agglomeration volume /52/.

The dimension of the agglomeration volume depends on the amplitude of the relative oscillation between small and large particles and their sizes. Consider the motion of a single spherical particle in a plane wave field in which the acoustic wave travels in one direction and varies with time harmonically. The velocity of the particle subject to this acoustic field can be given by

$$u_p = \eta_p \cos(\omega t - \Phi) U_f \quad (2.10)$$

where U_f = amplitude of the acoustic velocity (i.e. the fluid velocity), (ms^{-1})

ω = acoustic angular frequency, (rad s^{-1})

t = time, (s)

η_p = ratio of the velocity amplitude of the particle to that of the medium (particle entrainment factor)

Φ = phase delay of the motion of the particle relative to that of the medium (phase factor).

When η is unity and Φ is zero, the particle is said to be fully entrained by the acoustic wave, which is only true for small particles ($< 10 \mu\text{m}$, also depending heavily on the particle's density) and/or low frequencies ($< 10 \text{kHz}$). Generally, a particle will be partially entrained. Using Newton's second law and Stokes' drag law (2.9) leads to the following relations:

$$\eta_p = 1 / \sqrt{[1 + (\omega \tau_p)^2]} \quad (2.11)$$

and

$$\Phi = \tan^{-1}(\omega\tau_p) \quad (2.12)$$

where: τ_p = relaxation time of the particle, (s).

This relaxation time is related with the particle density ρ_p the particle diameter d and the medium viscosity μ by

$$\tau_p = \rho_p d / (18\mu) \quad (2.13)$$

It should be noted that the above expressions are only valid when the acoustic wave is sinusoidal and spatial effects of the acoustic wave are negligible /52/.

Now consider two particles with diameters of d_1 and d_2 , respectively. The oscillation of particle 1 relative to particle 2 can be described by

$$u_{p12} = [\eta_1 \cos(\omega t - \Phi_1) - \eta_2 \cos(\omega t - \Phi_2)] U_f \quad (2.14)$$

With this relative velocity particle 1 sweeps over an agglomeration volume in one acoustic cycle with respect to particle 2. The volume is simply given by

$$V_{12} = [\pi(d_{p1}^2 + d_{p2}^2)/4] L_{12} + \pi/6(d_{p1} + d_{p2})^3 \quad (2.15)$$

as deduced from Figure 2.7., where the first term on the right-hand side of Eqn. (2.15) is the volume of the cylinder section and the second term is the volume of two spherical endcaps. The length of the cylinder is equal to twice of the amplitude of the displacement of particle 1 relative to particle 2, which is found to be

$$l_{12} = 2 |\tau_{p1} - \tau_{p2}| \eta_1 \eta_2 U_f \quad (2.16)$$

after integration of $|u_{p12}|$ over half of one acoustic period.

In deriving Eqn. (2.15), particles are assumed to move independently. In reality, this is not true. When two particles approach each other, particularly when they become very close, the motion of one particle will be strongly affected by the other. If the mutual interactions between particles are included, not all particles 2 in the volume V_{12} defined by Eqn. (2.15) will collide with particle 1. For this reason, V_{12} may be considered an ideal agglomeration volume [52].

A more realistic collision process is illustrated by Figure 2.8 where the dotted lines are the ideal location lines on or within which particle 2 would collide with particle 1 if particle-particle interactions were absent, the solid lines are the actual location lines on or within which particle 2 will make contact with particle 1.

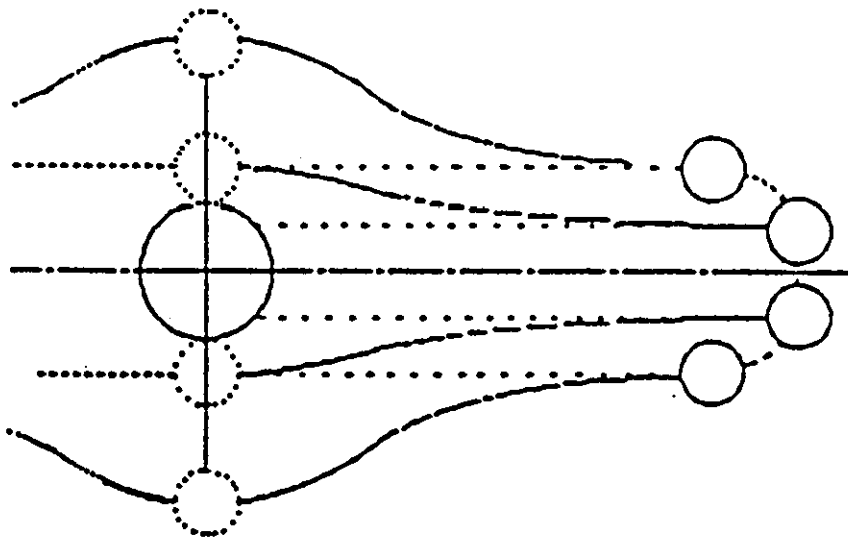


Figure 2.8. Diagram of actual agglomeration volume [52].

The volume enclosed by those solid lines is the actual agglomeration volume which can be related with the ideal agglomeration volume by

$$V_{a12} = \epsilon_c V_{12} \quad (2.17)$$

where ϵ_c is often called the collision efficiency measuring the portion of the small particles in an ideal agglomeration volume which collide with the large particle.

The determination of ϵ_c is one of the major challenges of using Mednikov's orthokinetic theory to calculate the agglomeration rate. At present, there are neither experimental correlations nor solid theoretical relations available for ϵ_c . This is due to the difficulty in analyzing particle-particle interactions and finding the actual trajectories of particles.

In current simulation models, the collision efficiency is estimated roughly by the following two approaches. By the first approach, the mutual interactions between particles are simply neglected and the collision efficiency is assumed to be unity for all paired particles. The unit collision efficiency, used by Miao /53/ and Tiwary /54/ in their models, obviously overestimates the agglomeration rate. The second approach draws an analogy of acoustic agglomeration to the cleaning process of small particles by large spherical collectors in a steady flow and uses the well-known relations for the latter process such as the Langmuir formula /55/ directly for ϵ_c . However, this type of analogy is not justified because the two processes differ from each other in many fundamental aspects. In the latter process, the flow of the aerosol stream relative to the collectors is uniform, unidirectional and steady. The dimensions of the collectors are much larger than those of the particles to be collected so that the effects of particles on flow are negligible. Furthermore, the thickness of the viscous boundary layer on the surfaces of the collectors is much smaller than their sizes so that potential flow is dominant. Thus the collision efficiency in this case can be characterized by a single dimensionless Stokes number, as the ratio of the stopping distance of a particle to the diameter of the collector /55/. In the acoustic agglomeration process, however, none of the above conditions are satisfied. Firstly, the motion of particles is inherently unsteady due to the oscillatory motion and entrainment by acoustic waves is nonuniform due to different sizes of particles. Secondly, the sizes of both small particles and large particles in collision are comparable so that their effects on each other are mutual and equally important. And lastly, the thickness of the boundary layer on the surface of even a large particle is considerably greater than its size so that viscous effects on flow become very important. Therefore similarities (gas flow similarity

based on Reynolds number and particle motion similarity based on Stokes number) between two processes do not exist and use of the Langmuir formula to calculate the collisions efficiency in acoustic agglomeration is indeed questionable /52/.

The orthokinetic interaction mechanism leaves another question unanswered. That is, since all small particles in the agglomeration volume are cleaned up in the first cycle, how additional small particles from outside the agglomeration volume fill up the volume to continue the agglomeration process.

Mednikov and others proposed two major refill mechanisms - parakinetic (flow line distortion) and attractive (hydrodynamic) interactions - as the processes primarily responsible for rapid refill of the agglomeration volume after every acoustic cycle /56/. They also proposed several secondary refill mechanisms such as acoustic streaming, acoustic turbulence, thermal diffusion and gravity settlement. Those secondary refill processes push small particles a large distance from the agglomeration volume to the immediate neighbourhood of the volume. From there the primary refill processes take over and send the particles into the volume. The degree of fill-up of the agglomeration volume can be expressed by the fill-up efficiency:

$$\epsilon_f = n_v / n \quad (2.18)$$

where n_v = the number concentration of small particles in the agglomeration volume after fill-up
 n = the number concentration of small particles outside of the volume
and $\epsilon_f \leq 1$.

Like ϵ_c , ϵ_f is also very difficult to estimate. Tiwary /54/ performed a numerical analysis on the fill-up problem. His results indicate that hydrodynamic interactions between particles push small particles away from the larger particle in an agglomeration volume. Then he proposed the following hypothesis: the

agglomeration volume may get filled up by small particles which are pushed in by larger particles in nearby agglomeration volumes. The effect of a larger particle on the motion of a smaller particle decreases with the distance between them. Therefore the small particles should be always pushed away from their agglomeration volumes, according to Tiwary's numerical results. Further research on the fill-up problem is needed /52/.

Using the assumption that every collision results in an agglomeration, Mednikov derived a well-known formula for the rate of acoustic agglomeration:

$$dn_{12}/dt = \beta_{12} n_1 n_2 \quad (2.19)$$

where n_1 and n_2 = the number concentration of particles 1 and 2

dn_{12} = the number of collisions between particles 1 and 2 in a time interval dt

β = agglomeration frequency function or agglomeration coefficient.

The agglomeration frequency function is defined as

$$\beta_{12} = (\omega/\pi)\epsilon_{c12}\epsilon_{f12}V_{12} \quad (2.20)$$

The optimal frequency at which the acoustic agglomeration rate is a maximum can be determined by taking the derivative of β with respect to ω and setting it equal to zero, provided that both collision and fill-up efficiencies are independent of frequency. This optimal frequency can be written as

$$\omega_{opt} = 1/\sqrt{(\tau_{p1} \tau_{p2})} \quad (2.21)$$

Because most suspensions consist of more than two groups of particles in terms of size, and each pair of particles has their frequency, Eqn. (2.21) is difficult to use in applications /52/.

2.9.2.2 Hydrodynamic interaction

If the orthokinetic interaction is the only mechanism responsible for acoustic agglomeration, application of acoustic waves to a monodisperse suspension (a suspension in which all particles are the same size) should not lead to any measurable agglomeration because the relative velocity between any two particles is zero. But this is not the case. Experiments show that relatively monodisperse particles agglomerate very rapidly under either standing wave /57/ or travelling wave conditions /58/. Therefore, a hydrodynamic interaction has been proposed and studied.

In contrast to the orthokinetic interaction, the hydrodynamic interaction does not require interacting particles to be different in size; therefore, it is considered to be the principal mechanism for the acoustic agglomeration of monodisperse particles. Two types of hydrodynamic interaction have been studied in the past.

The first type of hydrodynamic interaction most likely occurs when the line joining the centers of two particles is perpendicular to the direction of acoustic velocity. In this case, two interacting particles form an effective jet and the gas velocity relative to the particles would be higher between the particles than that outside. From Bernoulli's hydrodynamic principle, this velocity difference results in a net pressure force which drags two particles toward each other. Thus this phenomenon increases the probabilities of collisions and agglomerations among particles. Bjerknes /59/ investigated the interaction force between two spheres under ideal flow. His results showed that the force is inversely proportional to the fourth power of the particle separation, so that it is not important unless the particles are very close together. Using this force, Shaw /60/ calculated its contribution to acoustic agglomeration and concluded that its effect is almost negligible. However, a more recent study made by Danilov and Mironov /61/ indicated that the viscosity of a gas could increase the interaction force by several orders. If the hydrodynamic interaction force depends on the viscosity of the medium, then in the case of suspensions its effect should be markedly greater than in the case of gases. Limin /52/ extended

their theory to the case of two entrained particles. The results show that the convergent velocity between particles caused by the hydrodynamic interaction can be comparable to that caused by the orthokinetic interaction, particularly when the sizes of particles are relatively large and the sound frequency is high.

Another type of hydrodynamic interaction is caused by the asymmetry of the flow field around each particle. When a particle moves relative to a fluid, the perturbation velocity of the fluid in front of the particle decreases more quickly with the distance from the surface of the particle than that behind the particle. Thus if two particles are spaced relatively close to each other along the direction of the acoustic velocity, each perturbs the flow field around the other. Due to the asymmetry of the flow field, the drag reduction will be less significant for the "head" particle than for the "tail" particle /54/.

This difference in the drag reduction is equivalent to the action of a certain force of attraction between two particles. Many researchers, e.g. Tiwary /54/ and Shirokova /62/ claim that this type of interaction can enhance acoustic agglomeration significantly. The asymmetric pattern of the flow field around a particle is caused by the nonlinear convection term in the momentum equation of the fluid. A complete solution of the flow field is extremely difficult even with the help of a numerical method. In order to analyze the interaction between particles, Pshenai-Severin /63/ and Timoshenko /64/ used the Oseen's solution and Tiwary /54/ solved the steady Navier-Stokes equations numerically. These analyses regard the process as quasi-stationary, i.e., the flow is incompressible and the medium velocity is in phase everywhere over the whole domain. Their results show that the hydrodynamic interaction is very large even at small Reynold's numbers. However, in reality, the flow takes an incompressible form only near the particle where the nonlinear convection is smallest, and takes a compressible form away from the particle where the nonlinear convection effect becomes larger. The most important factor is that the wavelength of the viscous wave caused by the viscosity is comparable to the size of the particle. As a result, there is significant phase delay

between the medium velocity inside and outside the acoustic boundary layer around the particle. Thus, the quasi-stationary state of the fluid flow is not an appropriate assumption.

2.9.3 Acoustic effects in agglomeration to enhance dewatering

In an acoustic field any point in a sound conducting medium is alternately subjected to compression and rarefaction. At a point in the area of a compression, the pressure in the medium is positive, at a point in the area of a rarefaction, the pressure in the medium is negative. The PRF (Primary Radiation Force) can be approximately 6×10^{-12} N, 20 times greater than gravitational force on a single particle /33/ Figure 2.9.

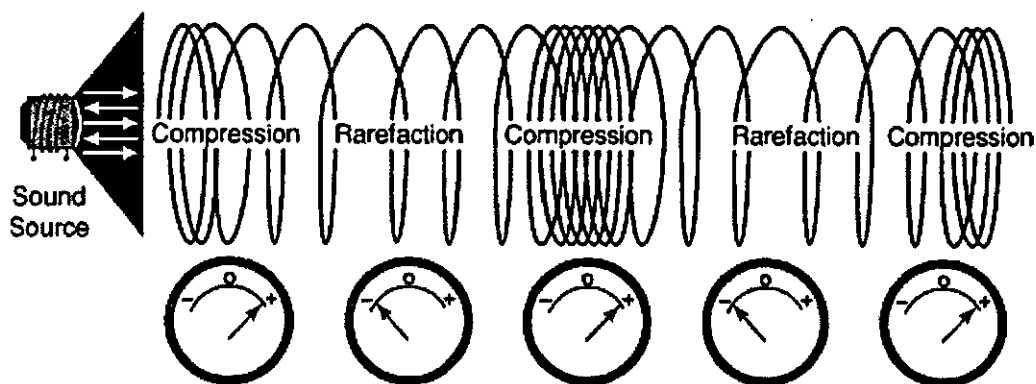


Figure 2.9. Compression and rarefaction areas in a standing acoustic wave.
Source: <http://www.caebblackstone.com/page3.html>.

A nonlinear effect of the interaction of a sound field with an object within an acoustic field provides the possibility of manipulating an object in a host medium using only the acoustic field. This is a very special application of radiation force. The radiation force generated by the sound field pushes the particles of density higher than that of the liquid away from the source of sound.

In the case of a standing wave, particles can be drawn to the wave's pressure maxima and thus put the suspension into a state in which the particles are located in

a controlled fashion at intervals of half the wavelength. In these positions the particles collide with each other in favourable chemical and physical conditions, creating acoustic agglomeration.

By agglomeration it is possible to decrease the number of small particles, which normally block the filter media very rapidly, in the suspension during dewatering. At the same time when increasing the average particle diameter by agglomeration a more porous filter cake with bigger pores will also be created and thus the filtration resistance through the cake during dewatering decreased.

2.10 Cavitation

Most of the energy supplied by an ultrasound source to liquids is dissipated as cavitation. Practically, all high power uses of ultrasound in liquids depends upon cavitation and its secondary effects.

First of all, what are the physical phenomena behind cavitation? Sound energy is carried through the liquid by the back-and-forth motion of the molecules along the direction of propagation. This produces alternate adiabatic compressions and rarefactions, together with corresponding changes in density and temperature. Consider the case of a 1 MHz sound wave of high intensity (10 W cm^{-2}) travelling through water. The amplitude of motion of the molecules turns out to be small, less than 10^{-5} cm. But their acceleration attains values about 250,000 times greater than the acceleration due to gravity. The maximum instantaneous velocity is 40 cm s^{-1} . The pressure at a given point in the water changes from +5 atm to -5 atm one million times each second. Obstacles in the path of the wave experience a repulsive force along the direction of propagation, due to the radiation pressure of roughly 100 N.

One effect of the great changes in pressure (between +5 and -5 atm) is cavitation. In the case of water saturated with air, the negative pressure portion of the sound wave (a fraction of an atmosphere is sufficient) causes some of the air to come out of

solution as minute bubbles, which act as weak spots for the further tearing apart of the liquid to form larger cavities. Then, when the pressure increases (as in the other half of the sound-wave cycle) the cavities collapse with a violent hammering action which generates local pressures up to thousands of atmospheres and local temperatures up to several hundreds or thousands of degrees. Electrical discharges are also believed to occur during the collapse. If the water is free from dissolved gases and suspended particles, its apparent cohesive strength is much greater and no cavitation occurs unless negative pressures of the order of 100 atm. are applied /67/.

Gaseous or vapour bubbles expand and contract in response to high frequency alternating pressure of the sound field. Cavitation bubbles can be of two types, stable or transient. Transient cavitation involves large-scale variations in the bubble's size (relative to its equilibrium size) over a time scale of a few acoustic cycles, and this rapid growth usually terminates in a collapse of varying degrees of violence. Stable cavitation, on the other hand, usually involves small-amplitude (compared to the bubble radius) oscillations about an equilibrium radius. Stable cavitation in most instances results in little appreciable bubble growth over a time scale of thousands of acoustic cycles. This classification of cavitation is not strict, however. Stable cavitation can lead to transient cavitation, and the collapse of a transient cavity can produce smaller bubbles that undergo stable cavitation /68/.

Cavitation is more intense at lower frequencies and ceases in the high frequency range. Cavitation intensity is markedly different for different liquids at equal acoustic pressure. It is also dependent upon temperature where typically there is an optimum value. Other factors affecting cavitation are vapour pressure, dissolved gases, and the presence of nuclei /72/.

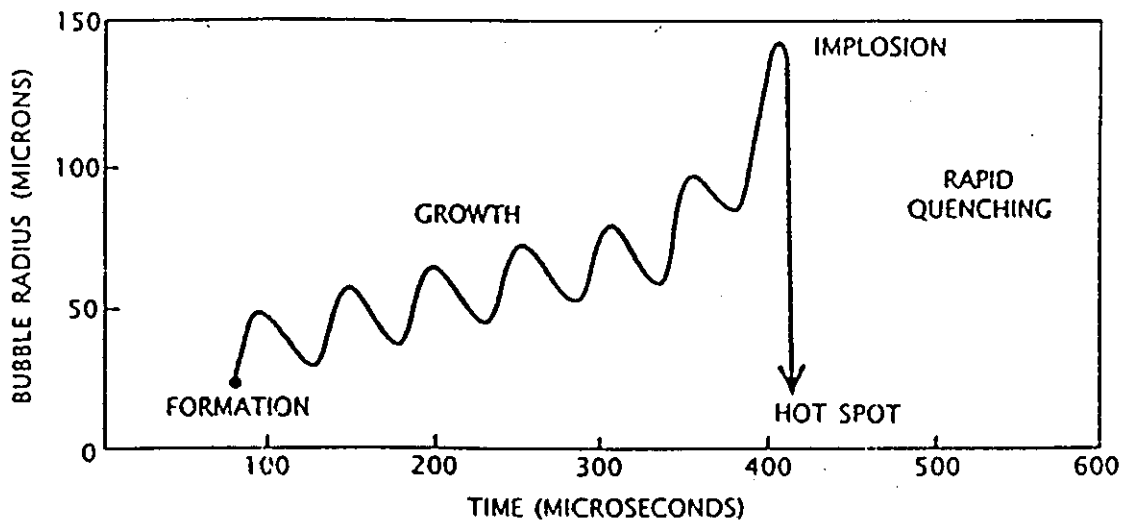


Figure 2.10. Bubble growth and implosion in a liquid irradiated with ultrasound is the physical phenomenon. Intense ultrasound waves generate large alternating stresses within a liquid by creating regions of positive pressure and negative pressure. A cavity can form and grow during the episodes of negative pressure. When the cavity attains a critical size, the cavity implodes, generating intense heat and tremendous pressure [69].

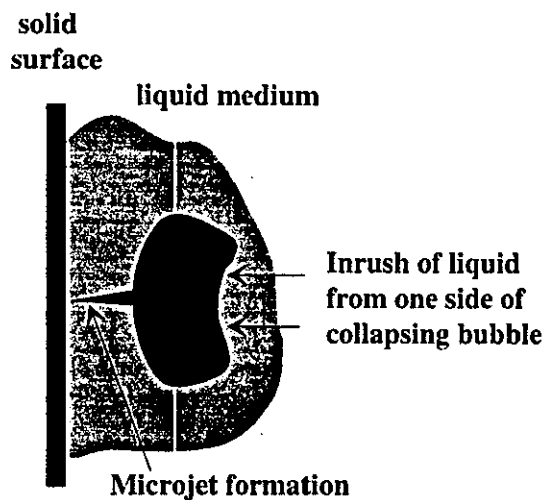
Parameters affecting the cavitation threshold can be summarised as in Table 2.1 [70].

Table 2.1. Parameters affecting the cavitation threshold [70].

An increase of	Causes a.... in cavitation threshold
Dissolved gas saturation	Decrease
Hydrostatic pressure	Increase
Surface tension	Decrease (in spite of the Laplace equation)
Temperature	Decrease
Solids concentration	Decrease
Particle size	Decrease
Dissolved ion concentration	Increase (at low concentrations)

2.10.1 Cavitation mechanism near a solid-liquid interface

Cavitation level depends on the suspension's properties, described in Table 2.1. In very many cases an overall cavitation level for suspensions (solid concentration over few percent by weight) is approximately $3 - 4 \text{ W cm}^{-2}$. In the case of solid-liquid mixtures the collapse of the cavitation bubble will have significant mechanical effects. Collapse near a surface produces an asymmetrical inrush of fluid to fill the void with the results that a liquid jet is formed, targeted at the surface, Figure 2.11.



Cavitation near a solid-liquid interface.

Figure 2.11. Cavitation near a solid-liquid interface.

The effect is equivalent to high pressure jetting and is the reason that an acoustic field is used for cleaning, e.g. a filter medium. Using cavitation it is possible to regenerate already blocked filter media and continue filtration at a higher filtrate flow level. The effect can also increase the mass and heat transfer by disruption of the interfacial boundary layers.

2.11 Ultrasonic transducers

The production of a high-intensity ultrasonic wave can be accomplished by one of three classes of generators; mechanical, magnetostrictive, and piezoelectric. Sonic

energy is produced by converting from one form of energy into another via a transducer.

Mechanical transducers produce comparatively low-power ultrasonic waves but have a high efficiency for transfer of power to the medium. For high intensity ultrasonic waves in liquids, magnetostrictive transducers are often used at low frequencies. Piezoelectric transducers are also used over a range of frequencies. Magnetostrictive and piezoelectric transducers convert electricity into ultrasonic energy.

2.11.1 Conversion criteria of electroacoustic transducers

For most applications of electroacoustic transducers there are general performance criteria. Among these are:

- a. **Linearity.** This implies that the output of the transducer is substantially a linear function of the input.
- b. **Passivity.** This implies that all of the output energy delivered by the device, electrical or acoustical, is obtained from the input energy, acoustical or electrical.
- c. **Reversibility.** This indicates the ability of the device to convert energy in either direction [72].

2.11.1.1 Magnetostrictive transducers

Magnetostrictive transducers use solid materials which change dimensions when subjected to a magnetic field. To produce ultrasonic waves, a variable magnetic field at the ultrasonic frequency is applied across the material causing mechanical vibrations to be produced at the same frequency. The external magnetic field is normally produced by passing a high-frequency oscillating current through a coil surrounding the transducer material using an arrangement shown by Figure 2.12.

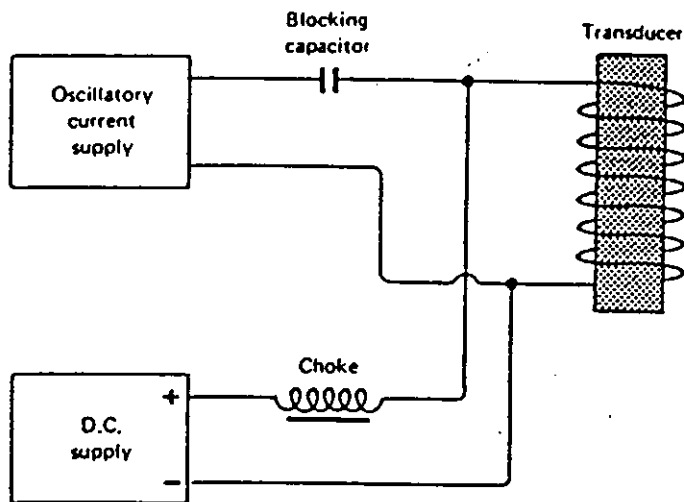


Figure 2.12. Magnetostrictive transducer, ultrasonic generator /73/.

Various shapes of transducers have been studied. Typical transducer materials are Nickel (annealed), Cobalt-Nickel alloys, Permalloy (45% Ni in Fe), Alfenol (13% Al in Fe) and Ferrite (Ni, Cu, Co ferrite).

Magnetostrictive transducers possess many suitable properties for industrial use.

Their advantages include:

- 1) Rugged construction
- 2) High power output
- 3) Efficient output range 5 to 40 kHz
- 4) Simple mounting techniques
- 5) Can drive high resistance loads such as liquids and solids
- 6) Large size installations are possible by using several transducers /73/.

2.11.1.2 Piezoelectric transducers

Piezoelectric transducer (Fig. 2.13.) materials change shape when in contact with an electric field and are analogous in principle to magnetostrictive materials. Typically, they consist of slabs made of crystals having piezoelectric properties. Suitable electrodes are usually placed on the opposite surfaces and the crystals vibrate at the same frequency as the frequency of the applied voltage. The

amplitude is at a maximum if the mechanical resonant frequency matches that of the applied frequency.

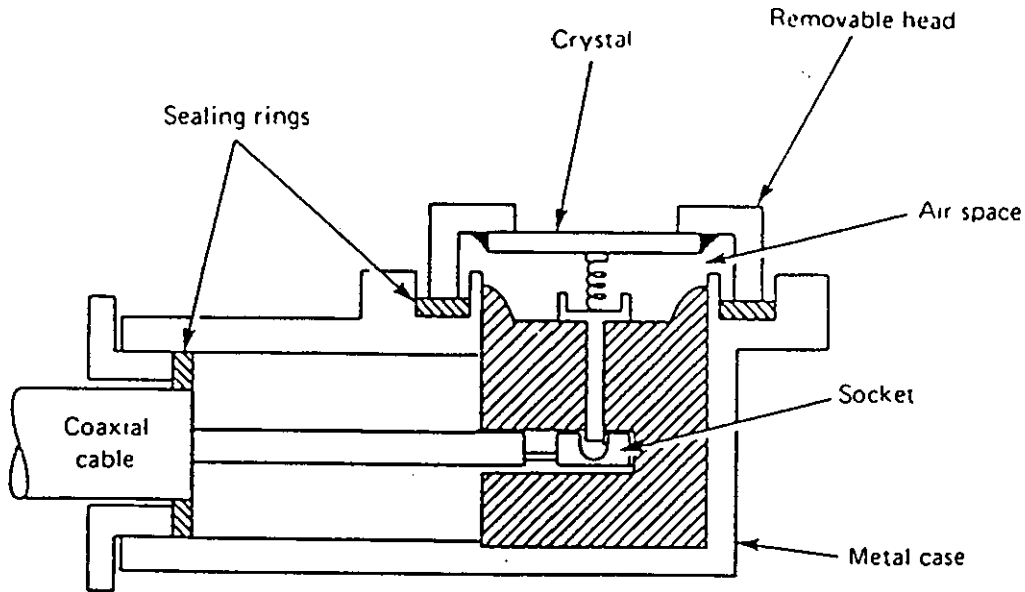


Figure 2.13. Quartz crystal piezoelectric transducer /73/.

Single crystals of quartz are commonly used for piezoelectric transducers. Barium titanate is a cheaper alternative material and can be shaped into many forms. This is advantageous if it is required to focus sonic beams. The disadvantage is that it is less efficient than quartz crystals /74/. Other materials include lithium sulphate and lead zirconate. For high power outputs, at low frequencies, it is necessary to apply several kilovolts across the plate. In many industrial processes, it is necessary to have the crystal in direct contact with the processing liquid. Figure 2.13 shows a water tight design for such an application /73/.

The advantages of piezoelectric transducers are same than the advantages of magnetostrictive transducers. Piezoelectric transducers can reach higher power output and have a wider efficiency over the output range (even at 100 MHz).

2.11.2 Physical properties of transducers

The distinction between the various regions is also important because the generators required are so widely divergent. At low power levels almost any

transducer type can be used, but at high power levels of interest in industrial processing the choice is severely limited by the requirements of high power handling capability. Figure 2.14 illustrates the available transducer types for use at high power levels for the various regions. While these transducers can be used generally in the regions illustrated, the maximum sound intensity levels can produce depend on the frequency [75].

Sound is usually produced either by the vibration of a solid object, such as a piston, or by the modulation of a stream of gas, as in a whistle or a siren. Sound can also be produced by a variety of other means, as by the modulation of a liquid stream or by modulating the flow of heat from a heat source (as in the singing flame or in the use of a spark as a sound source). When sound is produced by moving a piston back and forth in the medium, the size of the piston is important. If the piston is large compared with the wave length of the sound corresponding to the frequency with which the piston is moved, the medium is compressed periodically by the piston.

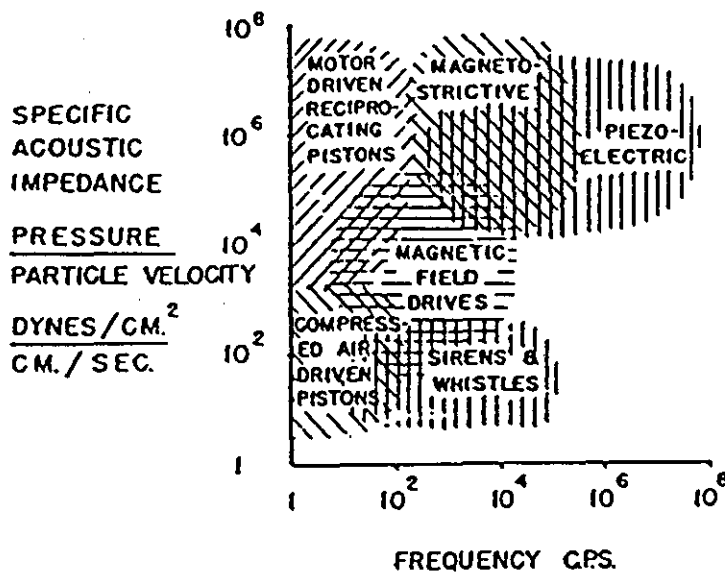


Fig. 2.14. Available transducer types useable at high power levels for various regions of specific acoustic impedance vs. frequency [75].

The energy stored elastically in this way travels away from the piston in the form of a sound wave. When the piston is small compared with the wave length, something quite different happens. As the piston moves forward the fluid medium simply slips off to one side without being appreciably compressed. Consequently, only a small amount of sound energy is transferred to the medium. Figure 2.15 shows how the large piston compresses the fluid while the small piston merely pushes it aside [75].

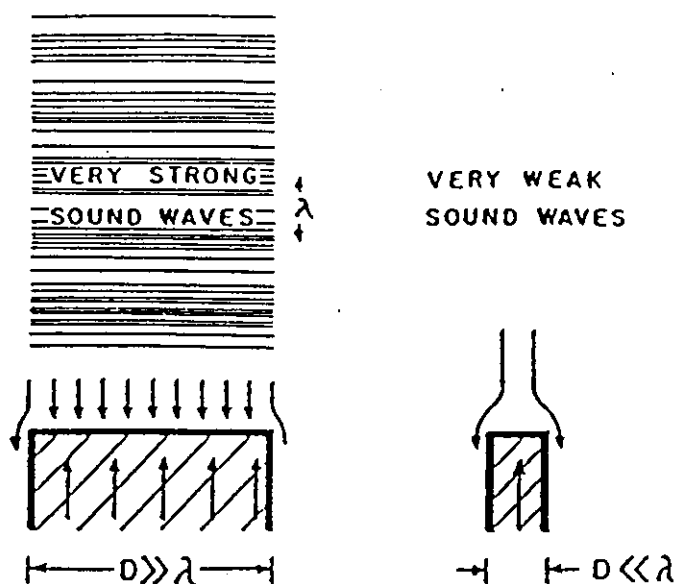


Figure 2.15. Sketch showing how a large piston compresses an unconfined fluid while a small piston merely pushes it aside [75].

Of course, if the small piston acts on a fluid which is confined, as by a cylinder, it, too, will be able to produce compression. This effect is important because it sets a lower limit to the size of a piston which will serve to generate sound in an unconfined medium. This lower limit to the piston size is shown as a function of the frequency in Figure 2.16. Roughly speaking, the piston diameter must be at least a wave length [75].

It is immediately apparent that the large pistons required at low frequencies are unattainable practically and, therefore, some alternative must be sought if low frequencies are to be employed. One such alternative is to accept the considerable

reduction in sound intensity resulting from the use of a small piston. Another alternative is to confine the fluid, as by means of a cylinder, so that the fluid medium cannot slip around to the side.

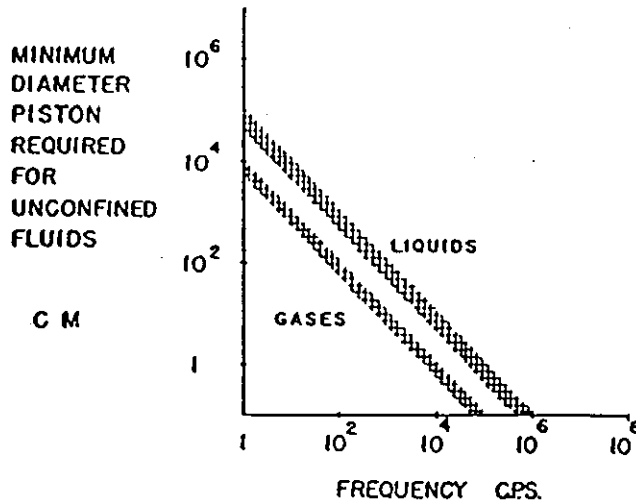


Figure 2.16. Piston size required to effectively generate sound pressures in an unconfined fluid as a function of frequency [75].

Generators for use in liquids are usually magnetostrictive or piezoelectric. Figure 2.17 is a spectrum illustrating the sounds which can be produced by means of piezoelectric generators [75].

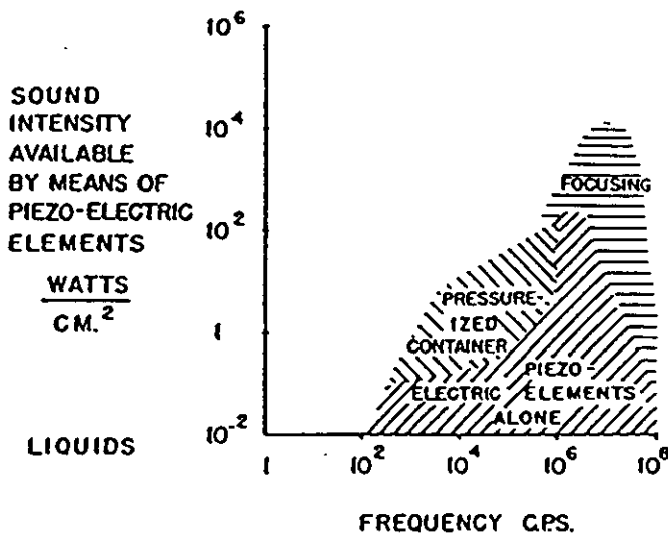


Figure 2.17. Spectrum (sound intensity vs. frequency) of the sounds that can be produced by means of piezoelectric generators [75].

Figure 2.18. is a spectrum showing the sounds which can be produced by magnetostrictive generators [75].

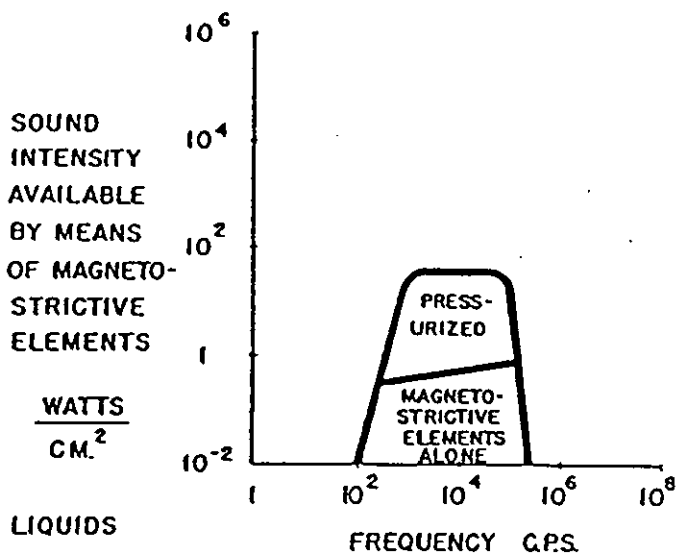


Fig. 2.18. Spectrum (sound intensity vs. frequency) of the sounds which can be produced by magnetostrictive transducers [75].

Both of these generators are capable of producing intensities in excess of the cavitation level. The phenomenon of cavitation itself produces an erosion of the generator parts; this can be prevented by separating the generator from the cavitating medium by pressurization or by focusing.

2.11.2.1 Focusing of sound waves

At first thought it might seem that the use of focusing could produce any desired amount of sound intensity (see Figure 2.17). This, however, is not the case. Because of the diffraction of sound, the area into which the sound may be focused is definitely limited. This limitation is illustrated in Figure 2.19.

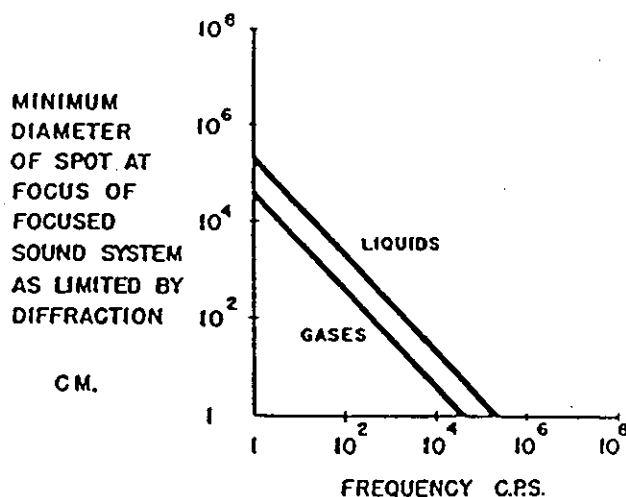


Figure 2.19. Diameter of the smallest spot which can be produced at the focus of a focused sound system as limited by the diffraction of sound vs. the frequency of the sound (75).

This is essentially the same kind of problem as that mentioned earlier regarding the minimum size of piston required for various frequencies. Since the peak sound intensity which can be produced at the face of a transducer is limited, the maximum power output is determined by the area of the transducer. Focusing can concentrate this sound power into an area no smaller than that dictated by the diffraction limit. The peak sound intensity obtainable at a focal point is then the ratio of this maximum power output to the minimum area. This limitation is shown graphically in Figure 2.20.

By focusing an ultrasound transducer it is possible to move the far field (Frauenhofer zone) nearer to a transducer. In Figure 2.21 the effect of the degree of focusing on the relative sound pressure is shown.

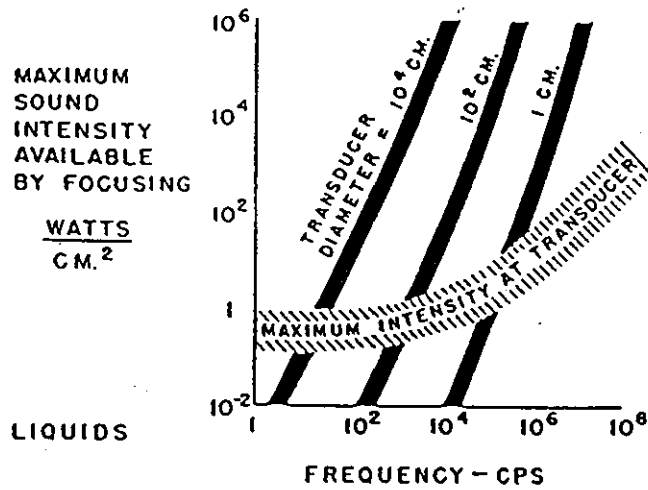


Figure 2.20. The peak sound intensity obtainable at the focus of a sound system as a function of the frequency of the sound and the diameter of the transducer used to produce the sound [75].

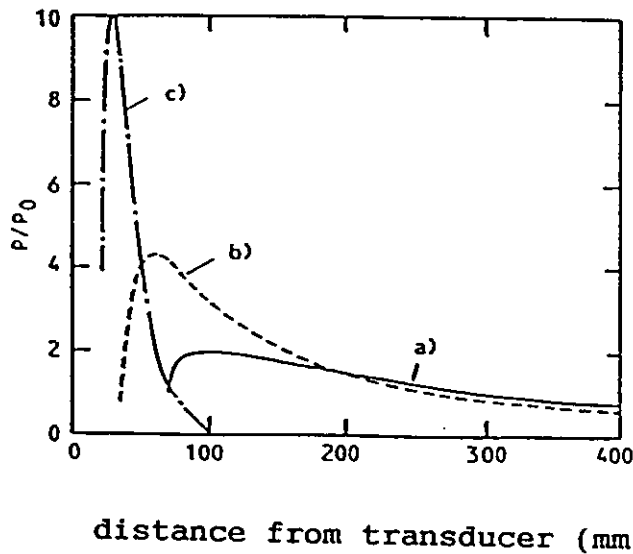


Figure 2.21. The effect of the degree of focusing to the relative sound pressure. a) no focused, b) focused to 67 mm, c) focused to 33.3 mm [76].

It should not be concluded, however, that pressurizing is the solution to all problems because in many cases it is the cavitation itself which is needed to produce the desired effects. Its elimination by pressurizing would then not be

desirable. Neither should it be concluded that focusing itself is always desirable. For example, at low frequencies extremely large transducers must be used which demand unreasonably high power inputs to produce the intensity levels of interest.

When the desired sound intensity lies in a region in which cavitation occurs, it is not necessarily possible to produce that intensity, even though diffraction offers no obstacle. This is because the cavitation process produces bubbles which in turn obstruct the passage of sound. This prevents any further increase in sound intensity by focusing.

Pressurizing the vessel containing the medium raises the intensity at which cavitation occurs and hence makes possible greater intensities by focusing /75/.

2.11.2.2 Near and far field of ultrasound

In commercially available ultrasonic transducers, for example a lead-zirconate-titanate (PZT) ceramic, a disk is generally used. This is arranged to radiate or receive energy at its front flat surface, the rear being highly damped to avoid rear face reflection and hence interference. Such a disk can be theoretically treated as a cophasally vibrating piston, producing a picture of the ultrasonic field normal to the plane of the disc which agrees remarkably well with experimental data /77/. Using this analysis, it has been shown /78, 79/ that for steady state conditions (continuous wave, constant amplitude drive) the intensity distribution along the beam's central axis is given by:

$$I_x = I_0 \sin^2 [\pi/\lambda (\sqrt{(r_p^2 + x^2)} - x)] \quad (2.22)$$

where I_0 = the principal intensity maximum, ultrasonic intensity I being defined as the power transmitted normally through unit area, (W m^{-2})

I_x = intensity at distance x from piston, ($W m^{-2}$)

r_p = radius of piston, (m)

λ = wavelength of propagated ultrasound, (m).

C = concentration of solution, ($kg m^{-3}$)

Equation (2.22) can be solved to give the position of the axial maxima and minima as:

$$x_{\max} = [4 r_p^2 - \lambda^2 (2m + 1)^2] / [4\lambda (2m + 1)] \quad (2.23)$$

where x_{\max} = position of max. intensity along axis normal to transducer,
and $m=0,1,2,\dots$

and

$$x_{\min} = (r_p^2 - \lambda^2 m^2) / 2(m\lambda) \quad (2.24)$$

where x_{\min} = position of min. intensity along axis normal to transducer,
and $m=1,2,3,\dots$

Putting $m = 0$ into Eqn. (2.23) gives the distance of the last axial maximum from the transducer as:

$$x'_{\max} = (4r_p^2 - \lambda^2) / 4\lambda \quad (2.25)$$

Now if the radius of the transducer is much greater than the ultrasonic wavelength i.e. $r^2 \gg \lambda$, Eqn. (2.24) becomes:

$$x'_{\max} = r_p^2 / \lambda \quad (2.26)$$

The position of the last axial maximum marks the transition between the Fresnel and Fraunhofer diffraction zones, or the near and far field. In the near field, energy is mainly confined within a cylinder of diameter D_0 , but the distribution

across the beam diameter at any distance x from the transducer is non uniform (which is apparent from eqn. (6.1)) whereas in the far field, the beam diverges (intensity distribution being described by a first order Bessel function) and intensity falls off in accordance with the inverse square law, Figure 2.22.

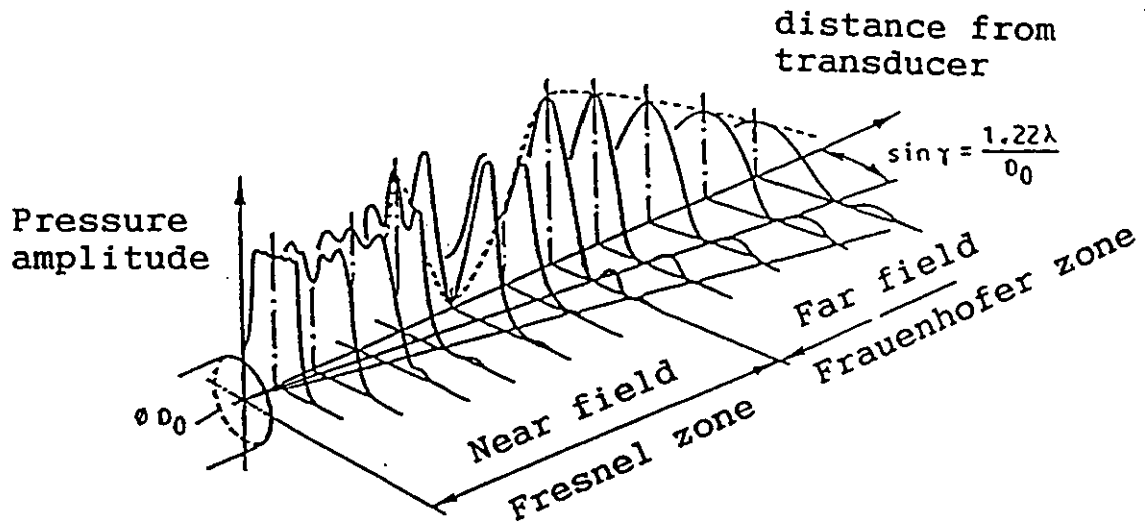


Figure 2.22. Cross-profile of sound field of circular transducer in different distances [76].

Nowadays in process industries exist solid/liquid separation equipment that removes only bulk water. For more efficient production, energy saving and environmental aspects demand more efficient dewatering methods to use in processes. During 1980 – 1990 research and development work has carried out to develop electro-acoustically aided dewatering methods. Several articles have published and mainly all the research has done only in a batch and/or small scale. Even the results have mainly been encouraging, dewatering enhanced over 4-fold, so far there is not any commercial electro-acoustic dewatering equipment in the market. Scientists have noticed in their experiments the ultimate need to develop sonic/ultrasonic transducers for bigger scale equipment. Also electrode spacing in the electrically assisted dewatering needs more precise understanding in a bigger scale. In latest publications scientists have also given more attention to the basic understanding of the electro-acoustic phenomenon, electrode and

sonic/ultrasonic transducer development work and combined use of electric and acoustic fields. Some electro-acoustic dewatering experiments have already been carried out in the PILOT-scale. An intensive research work in this area is going on and it is expected that after 4 or 5 years there will be the first electrically and/or acoustically enhanced dewatering equipment on the market.

Nowadays in process industries exist solid/liquid separation equipment that removes only bulk water. For more efficient production, energy saving and environmental aspects demand more efficient dewatering methods to use in processes. During 1980 - 1990 research and development work has been carried out to develop electro-acoustically aided dewatering methods. Several articles have been published and mainly all the research has been done only in a batch and/or small scale. Even the results have mainly been encouraging, dewatering enhanced over 4-fold, so far there is no commercial electro-acoustic dewatering equipment in the market. Scientists have noticed in their experiments the ultimate need to develop sonic or ultrasonic transducers for larger scale equipment. Also electrode spacing in the electrically assisted dewatering needs more precise understanding in a larger scale. In latest publications scientists have also given more attention to the basic understanding of the electro-acoustic phenomenon, electrode and sonic/ultrasonic transducer development work and combined use of electric and acoustic fields. Some electro-acoustic dewatering experiments have already been carried out in PILOT-scale. An intensive research work in this area is going on and it is expected that after 4 or 5 years there will be the first electrically and/or acoustically enhanced dewatering equipment on the market.

3 SUSPENSION CHARACTERISATION

The suspensions used in the experiments in this project were bio/fiber, pyrite and post-feculent phosphoric acid. The reason for using 3 different suspensions in the experiments were due to the technical needs of the partners of the project in the paper and pulp, mineral and chemical industries. So every industrial partner introduced one of their suspension samples for the project. Also these three different industrial areas, and at the same time three different suspensions, were selected to get a wider coverage of experimental results of the main industrial areas which were having problems with solid/liquid separation in their processes.

Various properties of the suspensions were determined, including the particle size distribution, surface tension, electrophoretic movement of the particles, pH and conductivity values, acoustic impedancies, densities and viscosities. Before and after every filtration experiment, the dry solid content (D.S. content) of the suspension and the filter cake were determined in mass percent (m-%).

For the experiments a large amount of suspension was needed; all the required amount was prepared before the batch of experiments were started. All the suspensions were stored in a cool room ($T = 6^{\circ}\text{C}$). In this way, the same kind of suspension was used with similar properties in every experiment. Once per week the particle size distribution of suspensions was measured by a Malvern particle size analyzer to ensure that the mean particle size value (D_{50}) had not changed more than 5 % from the original value.

3.1 Particle distributions

Mineral, bio, fiber and bio/fiber suspensions' particle size distributions were measured by laser based size analyzer (Malvern Instruments MASTER Particle Sizer M3.0) and by an image analysis method (PGT Imagist System 4plus). The particle size distribution of the post-feculent phosphoric acid was measured only

by the image analysis method. In these analyses only a small portion of solid matter mixed with large amount of water were needed for measurements. All preparations of samples for analysis were based on the Instruction Manual of the measurement equipment.

The Malvern Particle Sizer is based on the principle of laser diffraction, sometimes also known as ensemble light scattering. It falls into the category of non-imaging optical systems due to the fact that sizing is accomplished without forming an image of the particle onto a detector. The basic optical experiment is shown diagrammatically in Figure 3.1 /81/.

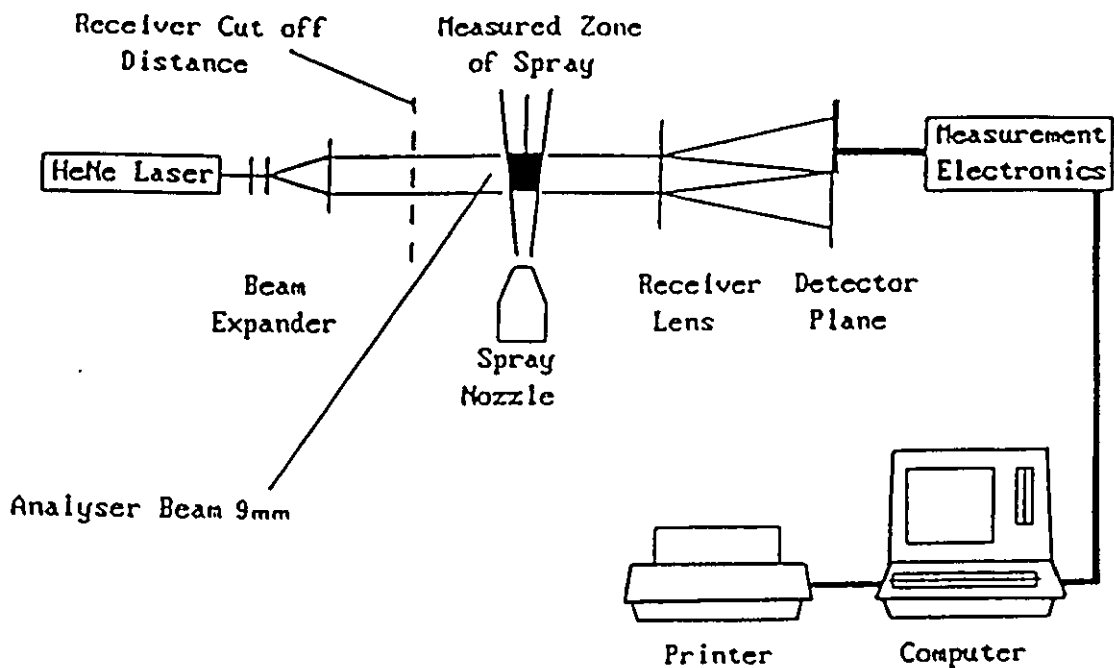


Figure 3.1. Malvern laser diffraction measurement principle./81/.

The light from a low power Helium-Neon laser is used to form a collimated and monochromatic beam of light, typically 1 cm in diameter. This beam of light is known as the analyser beam and any particles present within it will scatter this laser light. The particles are introduced to the analyser beam by the sample presentation modules or by direct spraying through the measurement area. The light scattered by the particles and the unscattered remainder are incident onto a

receiver lens, also known as the range lens. This operates as a Fourier Transform Lens forming the far field diffraction pattern of the scattered light at its focal plane. Here a designed detector, in the form of a series of 31 concentric annular rings, gathers the scattered light energy over a range of solid angles of scatter. The unscattered light is brought to a focus on the detector and passes through a small aperture in the detector and out of the optical system. The total laser power passing out of the system in this way is monitored as it allows the sample volume concentration to be determined. The range lens configuration has a property that wherever the particle is in the analyser beam its diffraction pattern is stationary and centered on the range lens optical axis.

In practise many particles are simultaneously present in the analyser beam and the scattered light measured on the detector is the sum of all individual patterns on the central axis. Thus the system inherently measures the integral scattering from all particles present in the beam. When a particle scatters light it produces a unique light intensity characteristic with angle of observation. So particle scatters light predominantly at a favoured scattering angle which is related to its diameter. Large particles scatter light into small angles of scatter and vice versa.

Over the size range of interest, typically 1 μm and upwards, the scattering with angle is independent of the optical properties of the material or the medium of suspension. Thus it is possible for the computer to deduce the volume size distribution that gives rise to the observed scattering characteristics. In addition to this treatment of the fundamental volume measurement it is possible to derive further information using numerical transformations. The result may be transformed to the equivalent surface or number distribution. The fundamental instrument measurement is one of volume, all other outputs are numerical transformations of this basic form assuming spherical particles /81/.

The PGT IMAGIST SYSTEM 4plus image analyse system consists of video camera, EVI-digitizer circuit, 13 inch high resolution monitor, computer with

peripheral equipment and software, printer and image display board, Figure 3.2. The central processor of the image analyse system allows for maximum handling of 680 particles during one analysis /82/.

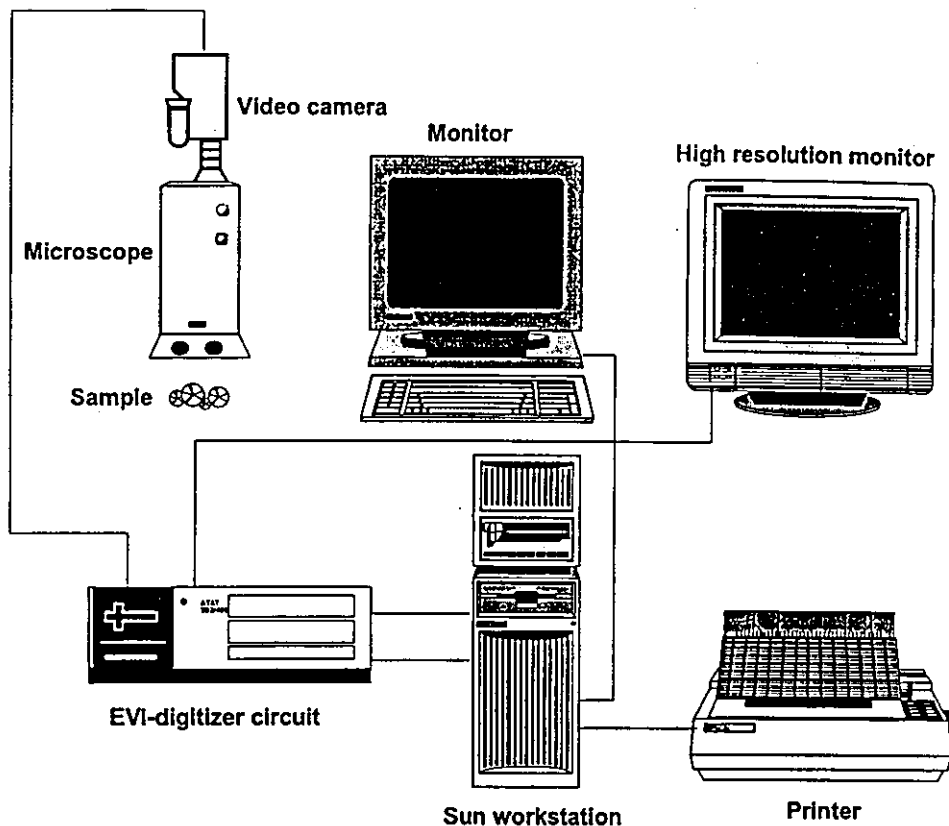


Figure 3.2. PGT IMAGIST SYSTEM 4plus image analyse system. /82/.

A photograph or a sample under examination in a microscope is transferred to the memory of the computer by video digitizer. With the high resolution of the signal of the video camera (1000 line/s) the examined object can be divided to 1024 x 800 pixels and also coloured to 256 different gray colours by the video digitizer. From the video digitizer the image will be transferred to the central memory of the computer, and to the high resolution monitor. The scaled rectangular coordinates, with their origin of the coordinates situated in the left hand corner of the image, enable all the particles appearing in the image to be sized. The examined particles are coloured and at the same time the image is transferred to the memory of the computer. After these operations it is possible to determine 20 different physical properties of the particles, e.g. average diameter, shortest dimension, longest dimension and area, in the active image /82/. Diameters

measured by the image analyser are shown in Table 3.1, and are based on the calculation of the surface area of the measured particle.

Figure 3.3 shows bio, fiber, bio/fiber and mineral suspensions particle distributions measured by laser technique (Malvern), and in Table 3.1 are shown maximum, minimum and mean size values measured by these two different methods. Bio/fiber suspension consists of 40 m-% biosludge and 60 m-% fiber suspension.

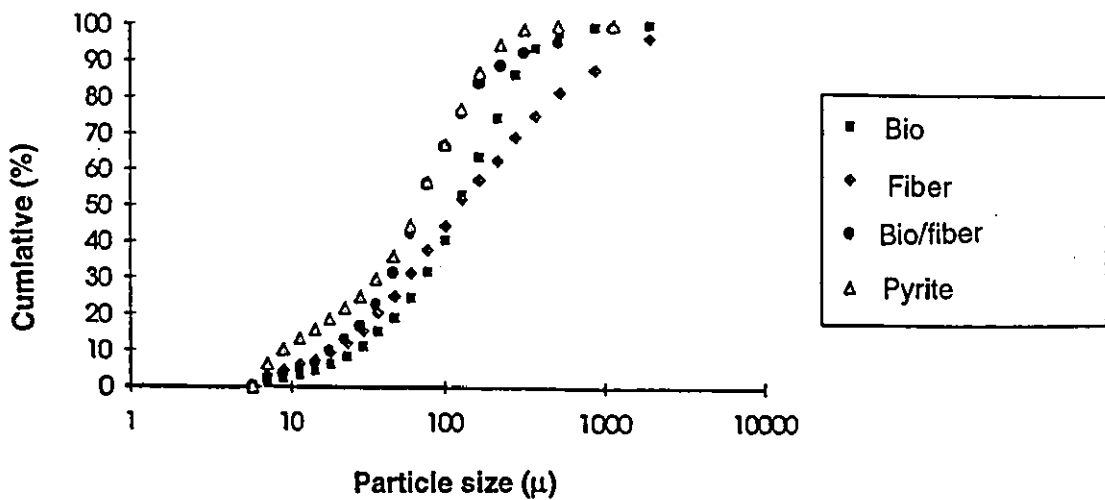


Figure 3.3. Particle size distributions of suspensions.

Table 3.1. Maximum, minimum and mean size values of particles measured by different methods.

Suspension	Malvern laser method (μm)			Image analyser (μm)		
	100 %	50 %	10 %	Max.	Mean	Min.
Bio	872	96	19			
Bio				711	94	18
Fiber	1880	97	15			
Fiber				270	43	18
Bio/fiber	1128	55	15			
Pyrite Reference	523	53	7	202	62	21
Phosphoric acid reference				236	39	21
				89	24	11
				92	27	11

3.2 Surface tension

Surface tensions of the mineral, bio/fiber and post-feculent phosphoric acid suspensions were determined as a function of the concentration of solids in the suspension. Suspensions were diluted by distilled water. In Figures 3.4, 3.5 and 3.6 are shown surface tensions of suspensions as a function of the solids concentration in the suspension. Measurements were made with a tensiometer (Haake Viscotester VT 500), which determined the force needed to pull out a platinum ring from the surface of the suspension. The analysis method is described more detail in section 3.3. The meter was calibrated with the distilled water, with a surface tension of $72,75 \text{ mNm}^{-1}$ at $20 \text{ }^\circ\text{C}$. The temperature of the suspensions was $19.5 \text{ }^\circ\text{C}$, and for each suspension several measurements were made.

In Figure 3.4 the surface tensions of the bio/fiber suspension as a function of the solids concentration in the suspension is shown. When the solids concentration of bio/fiber suspension is 1, it's D.S. content is 2 m-%. The deviations of repeat measurements were 1 to 4 %. This was due to the reason that fibers adhered to the platinum ring and then the force needed to remove the ring from the suspension varied. From the results can clearly be seen the direction of the change of the surface tension. The surface tension increases and approaches the value of distilled water when the suspension becomes more diluted.

In Figure 3.5, the surface tensions of mineral suspension are plotted as a function of the concentration of solids in the suspension. When the concentration of solids in the suspension is 1 then the D.S. content of the suspension was 78 m-%. The deviation of the repeat measurements was about 1 %. The surface tension of the mineral suspension didn't change during the dilution of the suspension.

Repeat measurement values of post-feculent phosphoric acid decreased whilst the measurement were in progress. This was due to the effect of sedimentation of the

particles in low D.S. content suspension, 5 m-%. On Figure 3.6, the measured results can be described with U-shape curve where the minimum value of the surface tension is reached when the suspension consists 50% distilled water. The minimum value is 50.75 mNm^{-1} .

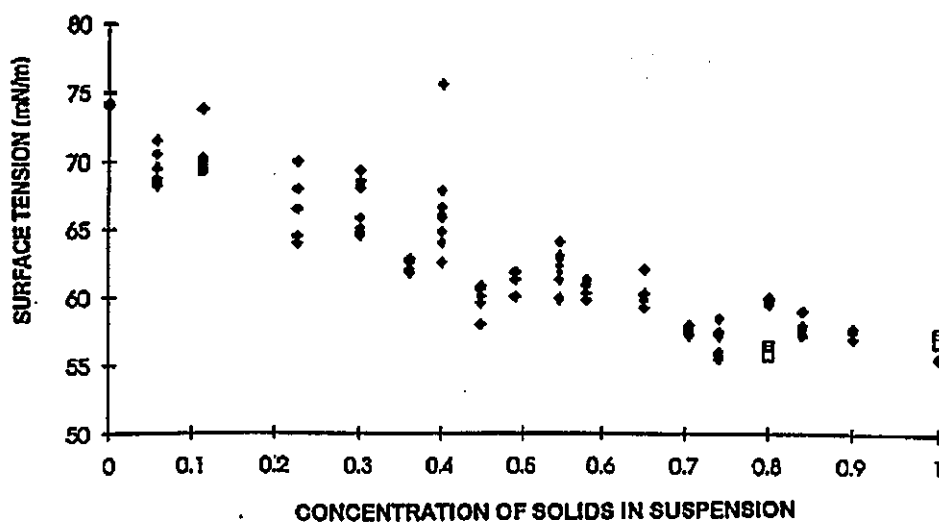
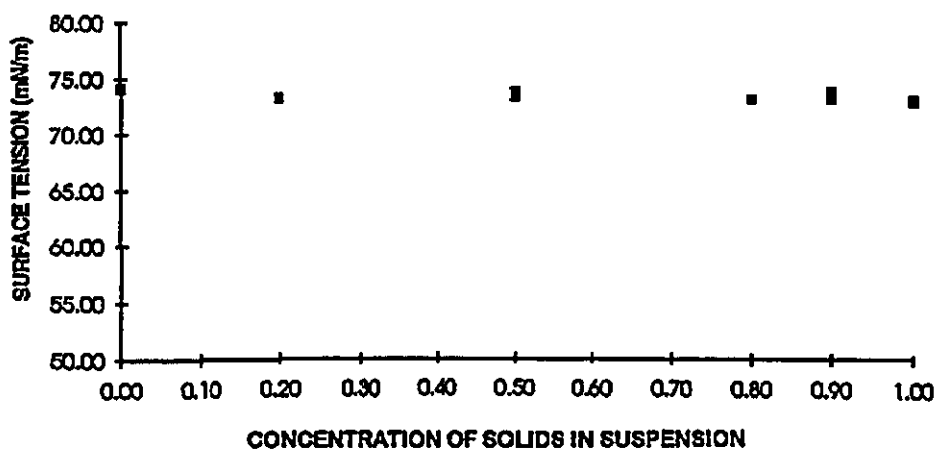


Figure 3.4. The surface tension of the bio/fiber suspension as a function of the concentration of solids in the suspension.



The Figure 3.5. The surface tension of the pyrite suspension as a function of the concentration of solids in the suspension.

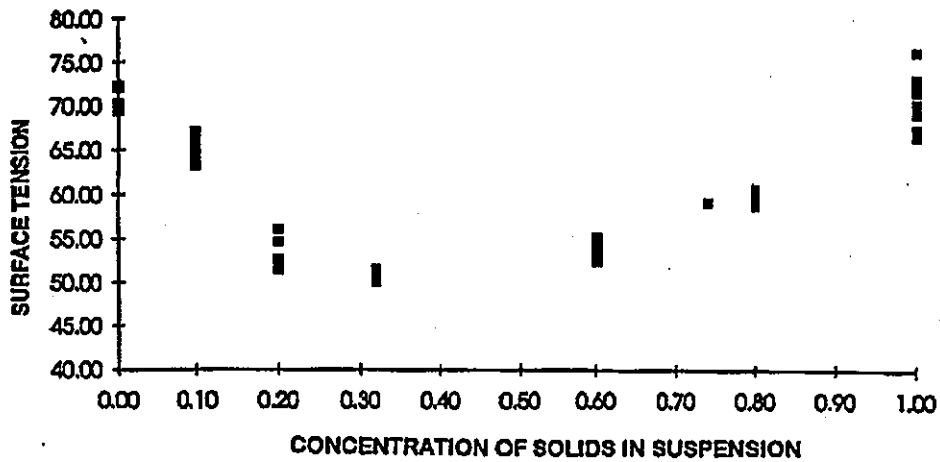


Figure 3.6. The surface tension of the post-feculent phosphoric acid as a function of the concentration of solids in the acid suspension.

In Table 3.2, surface tensions of nondiluted suspensions are tabulated.

Table 3.2. Surface tensions of suspensions (19.5 °C).

Distilled water	72.75 mNm ⁻¹
Fiber	51.90 mNm ⁻¹
Bio	64.67 mNm ⁻¹
Bio/fiber	56.36 mNm ⁻¹
Pyrite	73.17 mNm ⁻¹
Phosphoric acid	71.28 mNm ⁻¹

3.3 Densities and viscosities of suspensions

Densities were measured gravimetrically. The density of bio/fiber suspension was the same as the value of water, 1.0 kg dm⁻³. For post-feculent phosphoric acid and pyrite the corresponding values were 1.6 kg dm⁻³ and 4.1 kg dm⁻³. The densities for the solids were: bio and fiber both 1.0 kg dm⁻³, pyrite 5.0 kg dm⁻³ and post-feculent of phosphoric acid (dry solid) 1.8 kg dm⁻³.

Viscosity values were measured by a rotational viscometer Haake Viscotester VT 500, Figure 3.7. Measurements were started with maximum D.S. content of a suspension for the measurement method. The lower D.S. content measurements were based on suspensions diluted with distilled water to the desired D.S. content.

This is a Searle type rotational viscometer, where the resistance to flow of the test substance is measured as a function of selected speed. The viscosity of the sample is determined as a function of the measured torque, the instrument speed selected and the geometry of the sensor system used. The Viscotester performs these calculations and digitally displays both the results and the rough data values /84/.

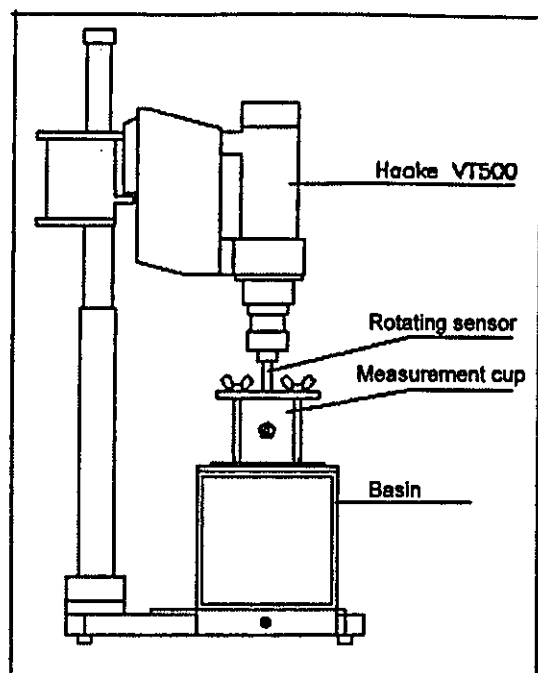


Figure 3.7. Haake Viscotester VT500 for viscosity measurements /84/.

During the first minute the speed of the spindle was increased from 0 to 30 s^{-1} , during the following two minutes the rotational speed was kept at this value. After three minutes, the speed was increased from 30 s^{-1} to 60 s^{-1} during the fourth minute and for the next two minutes the rotational speed was kept at this

constant value. The whole measurement took 6 minutes. The viscosity values in Table 3.3 are average values from these four measured values in different steps.

Table 3.3. Viscosities of bio/fiber-, mineral- and post-feculent phosphoric acid suspensions as function of D.S. content, 1 mPa s = 1 cp, water 0.001 Pa s.

Suspension	Dry solid content (m-%)	Viscosity (Pa s)
Bio/fiber	2.0%	0,150
	1.5%	0.100
	1.0%	0.080
Pyrite	8.5%	0.022
	3.0%	0.022
	1.5%	0.025
Acid	8.0%	0.130

The maximum D.S. content values of the suspensions were also the maximum measurable values in this kind of meter. From the measured results, the viscosity value of the bio/fiber suspension increases nearly linearly as a function of D.S. content. For the mineral suspension the measured values were constant over the range tested. Fast sedimentation of particles in mineral suspensions also gives some blur to the results. The viscosity value of the post-feculent phosphoric acid was due to the fluid. The fluid itself has a very high dynamic viscosity, so the solid particles had only a minor effect to the value. That's why there was no reason to measure viscosity values for different D.S. contents. Stirring time had no effect on the viscosity value but the value increased a little when the rotational speed increased. This indicated that the suspension behaved as a dilatant fluid.

3.4 Electrical properties of particles in suspensions

Electrophoretic mobility and zeta-potential describe the electrical properties of particles. For the bio/fiber suspension the electrophoretic mobility was measured using a Coulter Delsa 440 analyser.

Electrophoretic Light Scattering (ELS) is a measurement method that combines two technologies: electrophoresis (a technique that characterizes particles by their movement in an applied electric field) and laser doppler velocimetry (a method for measuring the speed of particles by analyzing the doppler shifts of scattered light). The Delsa 440 system measures the electrophoretic mobility distribution, zeta potential, specific conductivity and average hydrodynamic radius of particles in liquid suspensions. The particles can be either solid or liquid, whose size may lie between 0.01 and 30 μm . The system analyzes these particles by making independent laser doppler measurements at four different angles simultaneously with 256-channel resolution each. Comparison of simultaneous laser Doppler spectra from four angles allow the detection of very small particles as well as the separation of effects due to electrophoretic inhomogeneity, thermal and flow inhomogeneity./83/.

The system consists of four main assemblies; sample chamber, optical bench, computer and remote power supply, as shown in Figure 3.8.

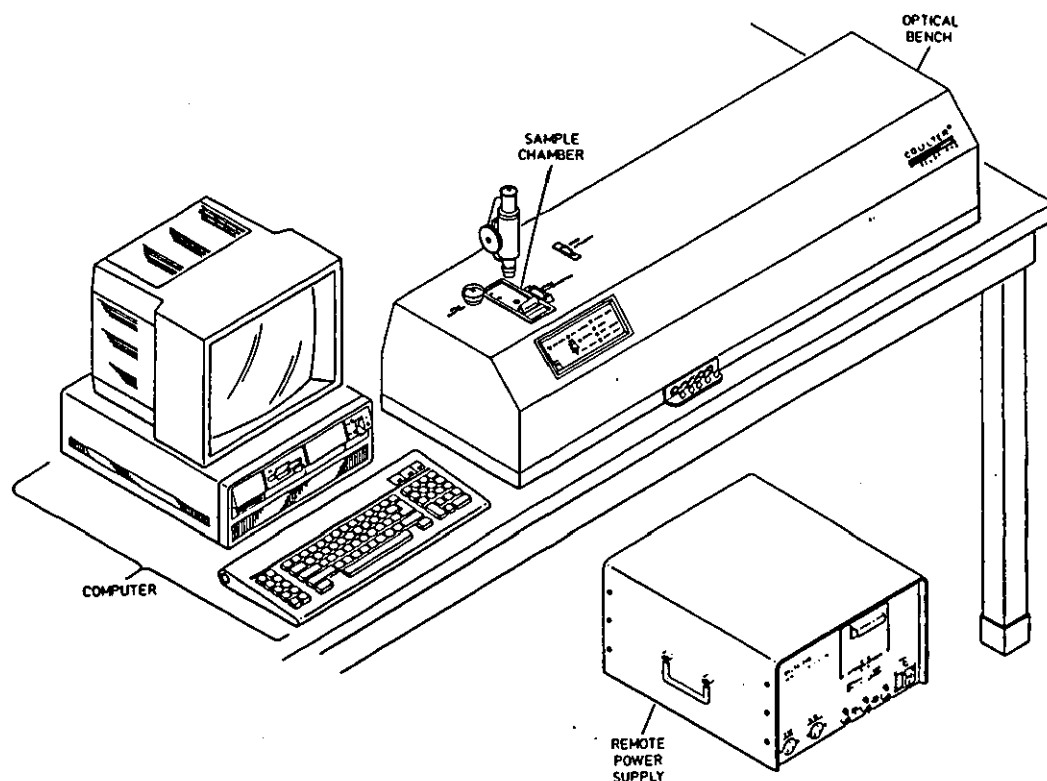


Figure 3.8. Coulter Delsa 440 analyzer for electrophoretic mobility distribution measurements. /83/.

The sample is analyzed in the sample chamber, Figure 3.9. The data is sent to the computer for analysis. The remote power supply provides regulated voltages to the optical bench. Total sample volume is about 1 ml. A rectangular channel runs through the 5 mm thickness of the insert, connecting the hemispherical cavities in each electrode. Sample is injected through a fill tube, filling both hemispheres and the channel. During electrophoresis the silver surfaces of the hemispheres act as electrodes. Light scattering data is collected from the sample in the channel. /83/.

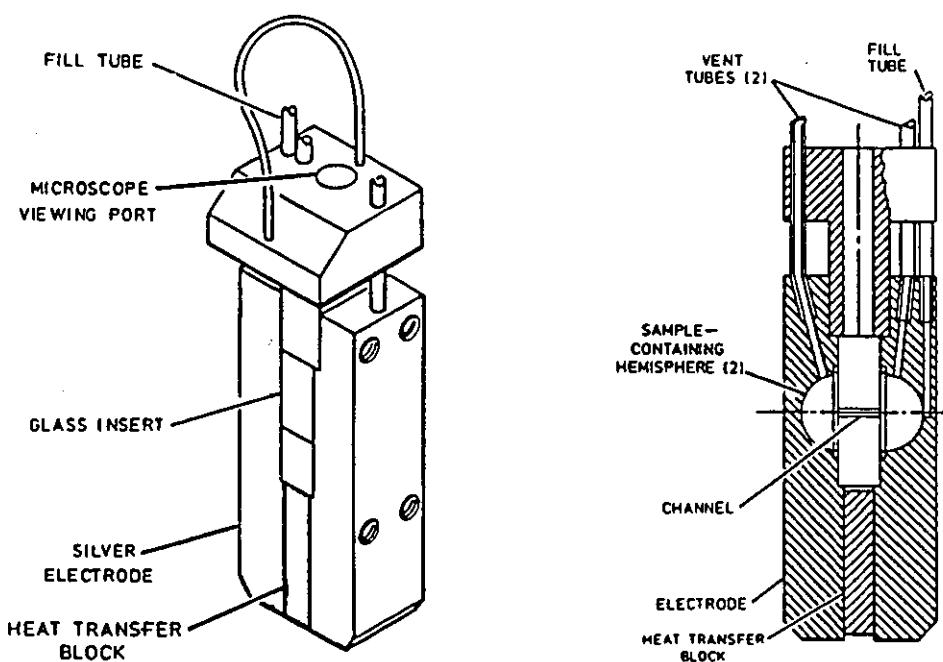


Figure 3.9. Sample chamber assembly /83/.

Particle movement is measured in the sample chamber by Laser Doppler Velocimetry (LDV). In the system, the main beam and the four reference beams are generated from the same laser using a single optical element (a diffraction grating). The beams pass through common collimating and focusing optics before entering the sample. After the sample area, four detectors sense the scattered light at four angles to the main beam. Before reaching the sample area, the main beam passes through a frequency shifter that changes the main beam's frequency by a controlled amount with respect to the reference beams. This difference allows

detection of the direction of particle motion and, thus, the sign (positive or negative) of mobility./83/.

The zeta potential value of mineral particles at a lower concentration was measured by the Malvern Zetasizer IIc system which offers the added capability of submicron particle size analysis to complement the electrophoretic capability, Figure 3.10.

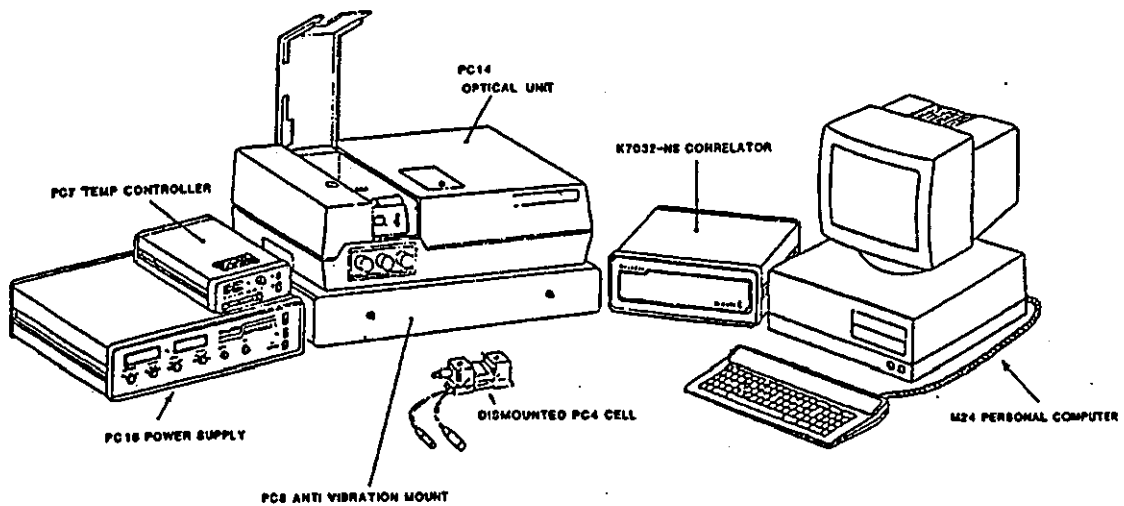


Figure 3.10. Malvern Zetasizer IIc analyse method /44/.

In the Zetasizer IIc, two coherent beams of red light, derived by splitting the output of a low power He-Ne laser, are focused and made to cross within the precision quartz capillary cell containing the particle suspension, Figure 3.11. /44/.

At the intersection of the two beams, a pattern of interference fringes is formed. Particles moving across the fringes under the influence of the applied electric field scatter light whose intensity fluctuates with a frequency that is related to their velocity. The signals resulting from individual photons of scattered light detected by the fast photomultiplier are fed to an 8 x n bit, 72-channel digital

correlator, and the resulting correlation function is analyzed to determine the frequency spectrum. From this, the mobility spectrum and hence zeta potential are calculated and displayed. The complete measurement takes only a few seconds but, more importantly, it is made over a sample consisting of many particles. The sensitivity of the system is such that particles as small as 50 nm up to several microns can be measured.

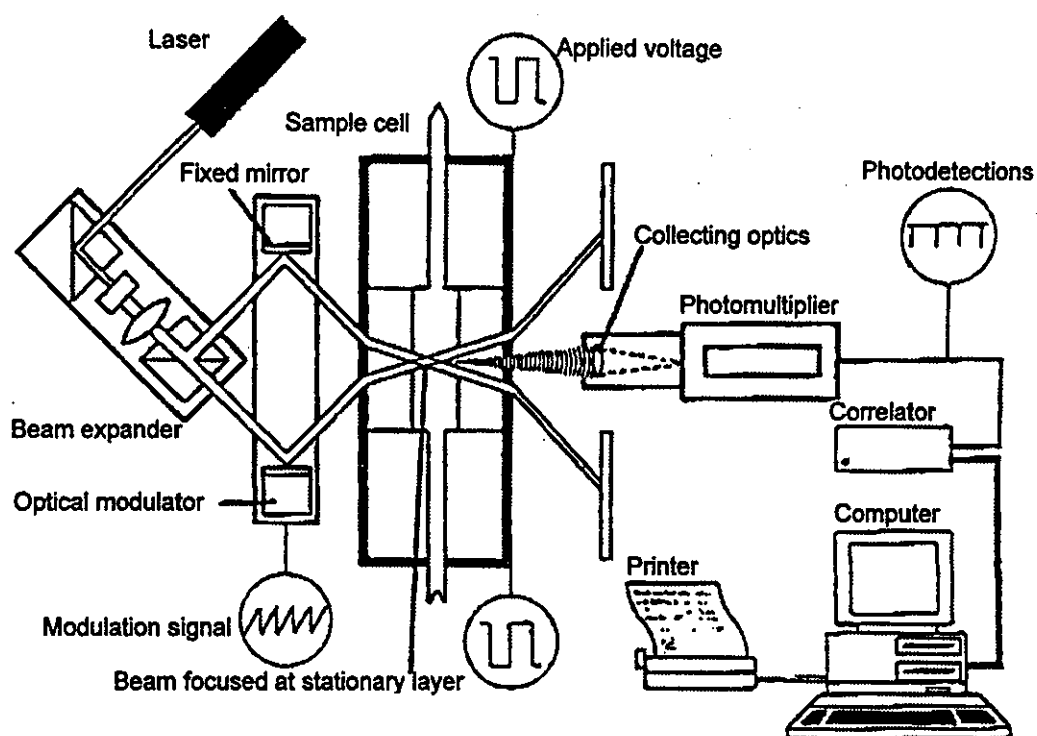


Figure 3.11. Schematic diagram of Malvern Zetasizer Ilc. /44/.

In order to determine whether the zeta potential is positive or negative in the Zetasizer Ilc, a modulation is applied to one of the laser beams by oscillating one of the mirrors in the optical system. This causes the fringe pattern to oscillate with a known frequency. The observed Doppler frequency of the light scattered by particles moving through the fringes can thus be measured by reference to the applied modulation frequency and will be either higher or lower than the applied frequency, depending upon the direction of movement. The modulation frequency is greater than any shift in frequency that could result from electrophoretic motion of the particles, so the determination is unequivocal. A

further substantial benefit of this use of an imposed base frequency is that particles with very low or zero charge that would otherwise produce very tiny Doppler shifts now give rise to substantial signals that can be measured with high accuracy. /44/.

The measured electrophoretic mobility and calculated zeta-potential of the bio/fiber suspension (Coulter Delsa 440) was $u_E = -0.6 (\mu\text{ms}^{-1})/(\text{V cm}^{-1})$, $\zeta = -17.5 \text{ mV}$ at pH 5.8. For a mineral suspension at such a high D.S.content (78 m-%) it was not possible to measure the electrophoretic mobility. So to obtain a figure for the pyrite particles' electrical properties, the zeta-potential value was measured (Malvern Zetasizer IIc) for them at a lower concentration - at pH 7.1 $\zeta = -5.9 \text{ (mV)}$ and corresponding calculated electrophoretic mobility $u_E = -0.2 (\mu\text{m s}^{-1})/(\text{V cm}^{-1})$. Post-feculent phosphoric acid at pH 1 was impossible to measure with these analysers.

3.5 Movement of bio/fiber suspension particles in electric field

Particle movements in an electric field were only measured for bio/fiber suspension. The measurements were done in a plastic tube with height 20 cm and with diameter 5 cm. At the bottom of the tube situated the cathode and 13 cm above that situated the anode. The cathode was stainless steel and the anode was aluminium. The electrodes were connected to the adjustable power supply. The measured suspension was placed into the tube between the electrodes. When the desired voltage was connected, the time to move solid particles to the anode was measured by a clock.

For mineral suspensions at such a high concentration (D.S. content in feed 78 m-%) there is no potential for particles to move in the electric field. Also, in the post-feculent phosphoric acid suspension the movements of the particles are insignificant (very slow) due to the high dynamic viscosity of the fluid. In Table 3.4 the results for the bio/fiber suspension are presented showing the time needed

to collect solid particles to anode, strength of electric field, particle speed in used electric field and electrophoretic speed.

Measurements were started in the original D.S. content of bio/fiber suspension and measurements in a lower D.S. contents were done with suspensions diluted with distilled water to the desired D.S. content.

Table 3.4. The effect of electric field strength and the D.S. content of bio/fiber suspension on the electrophoretic phenomena. Distance between electrodes 13 cm.

D.S. content	Electric field, $V\ cm^{-1}$	Time to collect particles to anode, min	The separation speed of two different phases, $\mu m\ s^{-1}$	Electrophoretic velocity, $\mu m\ s^{-1}$
1.0%	30	7	309.5	18
	20	12	180.5	12
1.5%	30	7	309.5	18
	20	10	216.7	12
2.2%	30	10	216.7	18
	20	14	154.8	12

Measured and calculated values of electrophoresis show that in these experiments, as also in real electric pre-treatment processes, electroflotation (movement of gas bubbles created by electric field in a suspension) has a major effect on particle movements. The measured times to separate bio/fiber suspension to two different "phases" were much shorter than the calculated times shown based on the values of electrophoretic mobility. During electrolysis, water breaks down and on the surface of the cathode hydrogen is released which moves like a normal gas bubble upwards, and at the same time the gas bubbles take solid particles with them. When fibers are moving upwards, smaller particles stick to the fibers and so all sizes of particles are moving with the gas bubble upwards faster than the particles alone. Actually, in this process the movement of the particles is due to joint work done by electrophoresis and electroflotation. When

the D.S. content increases, the conductivity, current and electric power increases. When electric power increases the release of hydrogen from the surface of the cathode increases.

Measurements of viscosity and particle movements in the electric field showed for bio/fiber suspension to use in electric field enhanced dewatering experiments lower concentrations, D.S. content ≤ 1.5 m-%. But also the properties of experimental rig and filter medium affected the final experimental D.S. content of the suspension in each experimental scale. For pyrite and post-feculent phosphoric acid the D.S. contents for the experiments were already fixed due to the process conditions. In so high D.S. contents it was impossible to make all the same analysis than it was done for the bio/fiber suspension due to the reasons mentioned in each chapter of analysis done for the suspensions.

3.6 Choice of acoustic properties for the experimental separators

Ultrasound propagates in suspensions mostly by longitudinal wave motion. In a porous material, for example a filter cake, sound can also propagate by transverse waves and by surface waves. The propagation speed of longitudinal waves in a homogeneous medium can be described by /37/

$$c = \sqrt{E_m / \rho} \quad (3.1)$$

where: E_m = elasticity coefficient of medium
 ρ = density of medium, (kgm^{-3}).

For the planar wave the acoustic impedance of the medium Z is /37/

$$Z = \rho c \quad (3.2)$$

where : c = sound velocity, (ms^{-1}).

The acoustic impedance of dilute suspensions does not normally differ from the value of the corresponding suspending medium, but a small amount of dry solid content and/or gas bubbles can have a remarkable effect on the attenuation of sound. Attenuation is affected by many factors, e.g. reflection, real adsorption and scattering. In a classical way the attenuation of sound has been described by /85/

$$I(x) = I(0)e^{-2\alpha x} \quad (3.3)$$

where: $I(x)$ = acoustic intensity at a distance x from the source, (Wm^{-2})
 $I(0)$ = acoustic intensity at point $x=0$, (Wm^{-2})
 α = coefficient of adsorption or attenuation (m^{-1}).

Possible powerful adsorption in a target material, e.g. in a suspension, has to be taken into account during the specification of ultrasound transmitters and processes. The acoustic properties of different suspensions are best determined by measurement; models do not give accurate results. There are methods to evaluate the adsorption, e.g. scattering theory, but solution of adsorption models can be difficult because in many cases there is a lack of measured physical properties what are needed for calculations.

3.6.1 Acoustic drift

Besides entrainment by the vibratory motion of the medium, suspended particles are also subject to sound-related time-averaged forces. These forces cause particles to drift along the direction of medium (e.g. fluid) vibration. The magnitudes of these forces depend on the particle sizes. The larger a particle, the larger the acting force will be. Thus different sized particles will drift with different velocities. The relative drift velocities increase the probability of particle collisions, and enhance the acoustic agglomeration rate.

The most important of these forces is the acoustic radiation pressure force. The acoustic radiation pressure force is associated with a variation of the time-averaged momentum carried by acoustic waves. In the interaction of a wave with a particle, a transfer of time-averaged momentum from the wave to the particle takes place on account of the scattering and absorption of acoustic energy by the particle, which results in a net force on the particle.

In a travelling wave field, these radiation pressure forces are in the direction of the wave propagation. Therefore they play a similar role in acoustic agglomeration as the gravitational forces. In a standing wave field, however, the radiation pressure forces are directed toward the velocity antinodes (the locations where the acoustic velocity amplitude has a peak). In this case, besides the direct increase of particle collision probability as in the case of the travelling wave, the radiation forces can bring an additional benefit to acoustic agglomeration by pushing particles toward the velocity antinodes where the orthokinetic and hydrodynamic interactions are at a maximum /52/.

In Figures 3.12 - 3.15 particle entrainment factors for spherical particles at different conditions are shown, where account is taken of Newton's second law and Stoke's viscous drag /65/.

PARTICLE ENTRAINMENT FACTOR

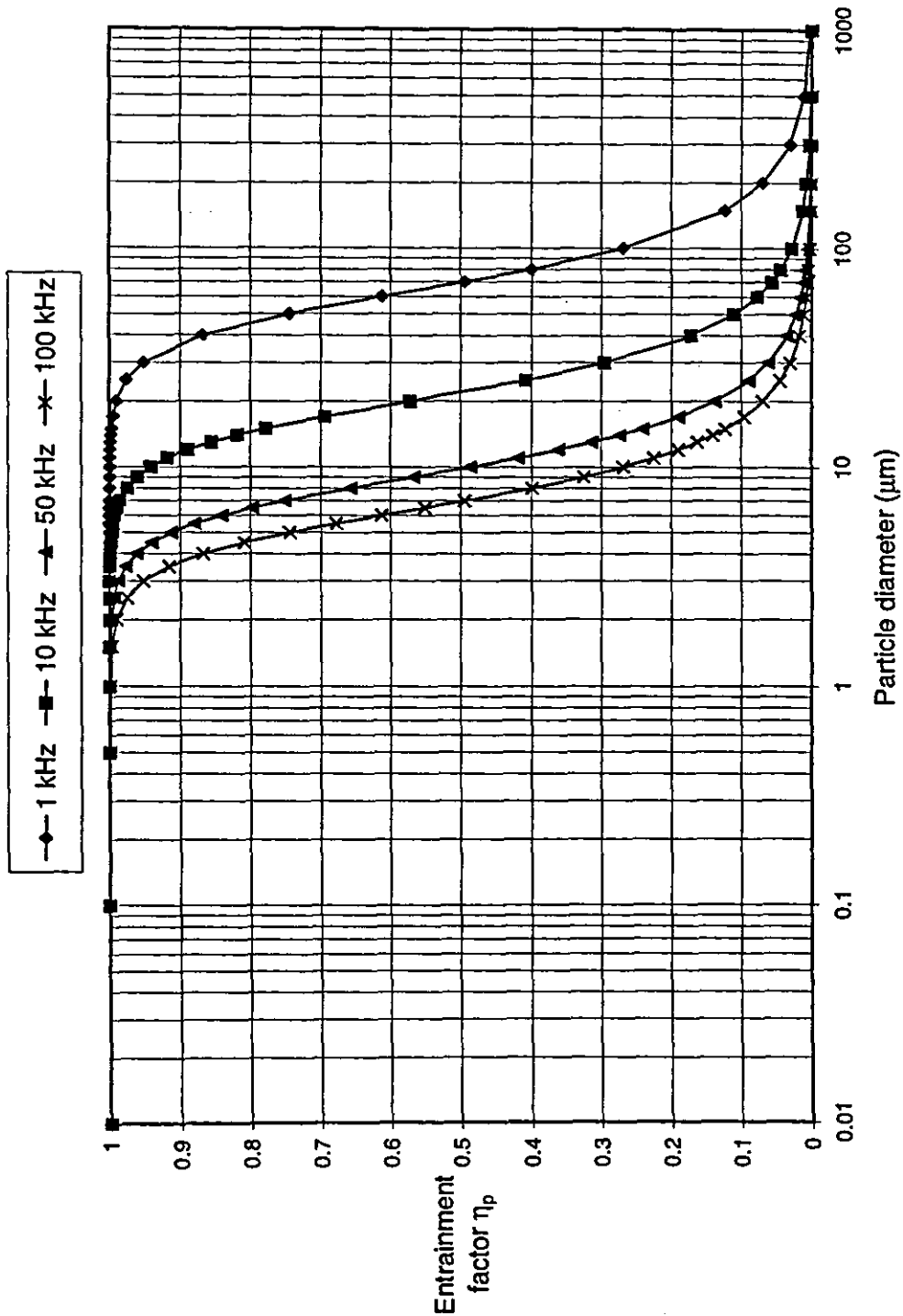


Fig. 3.12. Particle entrainment factor η_p in an acoustic field, in water (17.5 °C), when Stoke's law and Newton's second law are taken into account. The density of the particle is 1100 kg m⁻³ /65/.

PARTICLE ENTRAINMENT FACTOR

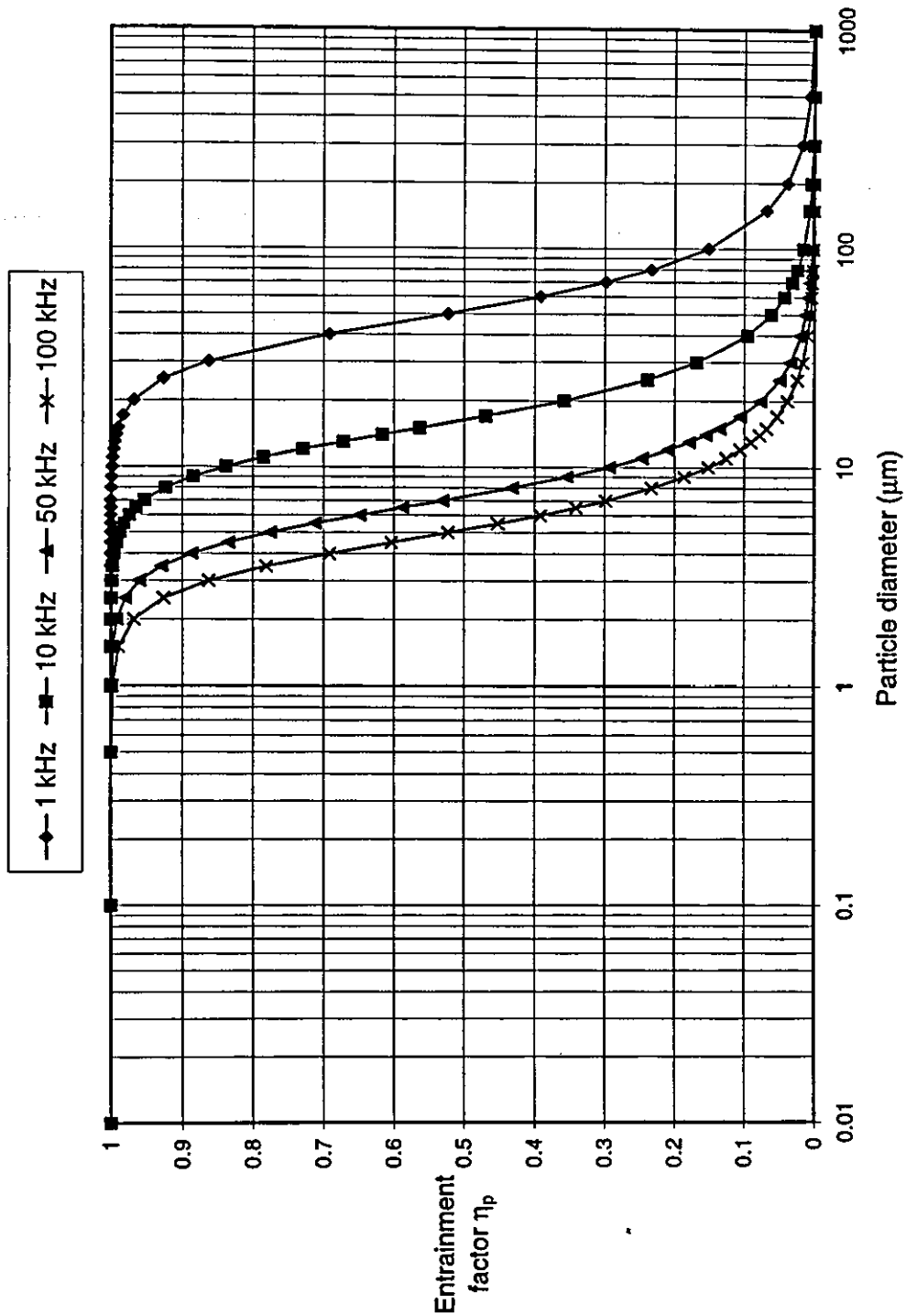


Fig. 3.13. Particle entrainment factor η_p in an acoustic field, in water (17.5 °C), when Stoke's law and Newton's second law are taken into account. The density of particle is 2000 kg m⁻³ /65/.

PARTICLE ENTRAINMENT FACTOR

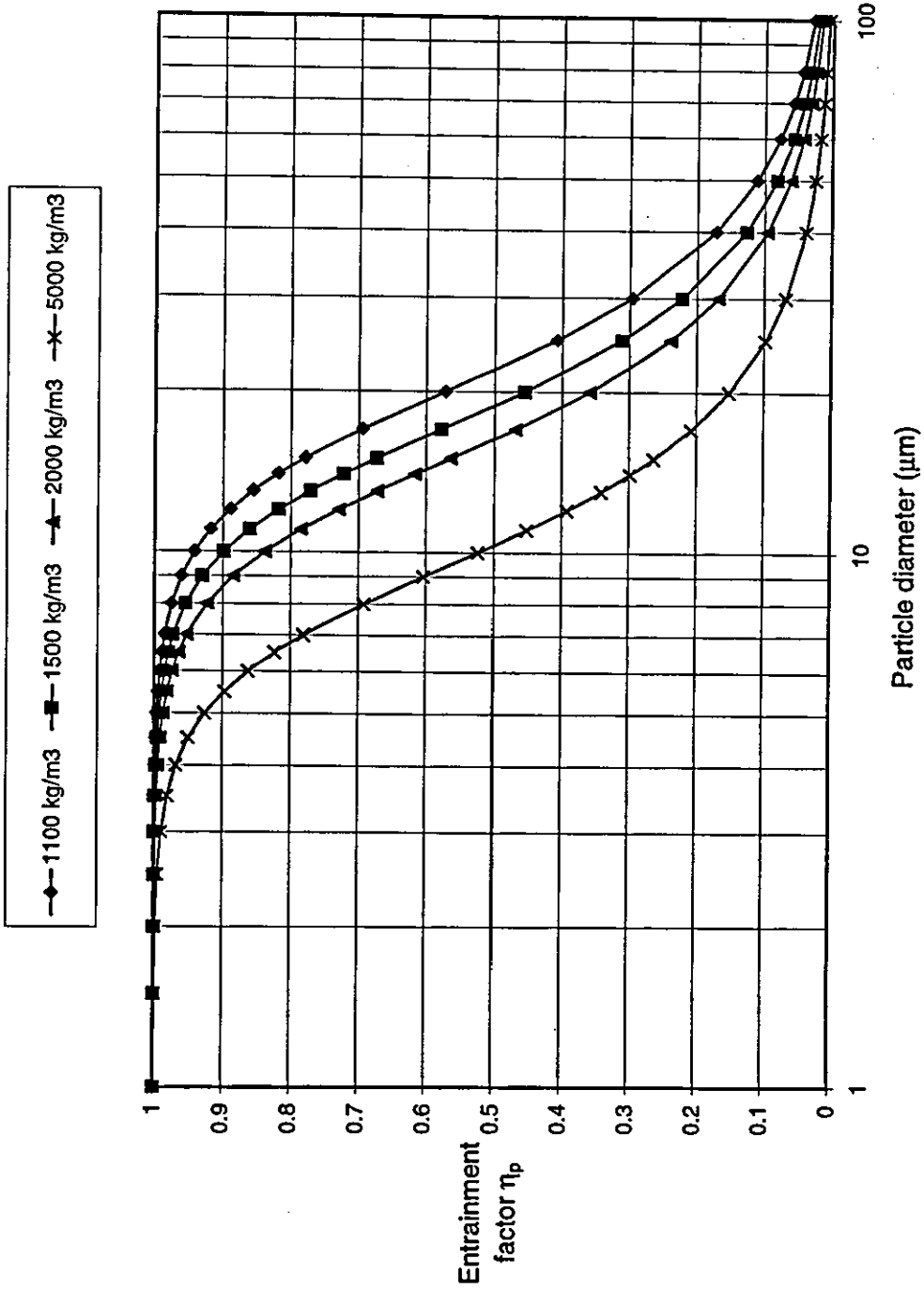


Fig. 3.14. Particle entrainment factor η_p in an acoustic field (10 kHz), in water (17.5 °C), when Stoke's law and Newton's second law are taken into account. The density of particle varies /65/.

PARTICLE ENTRAINMENT FACTOR

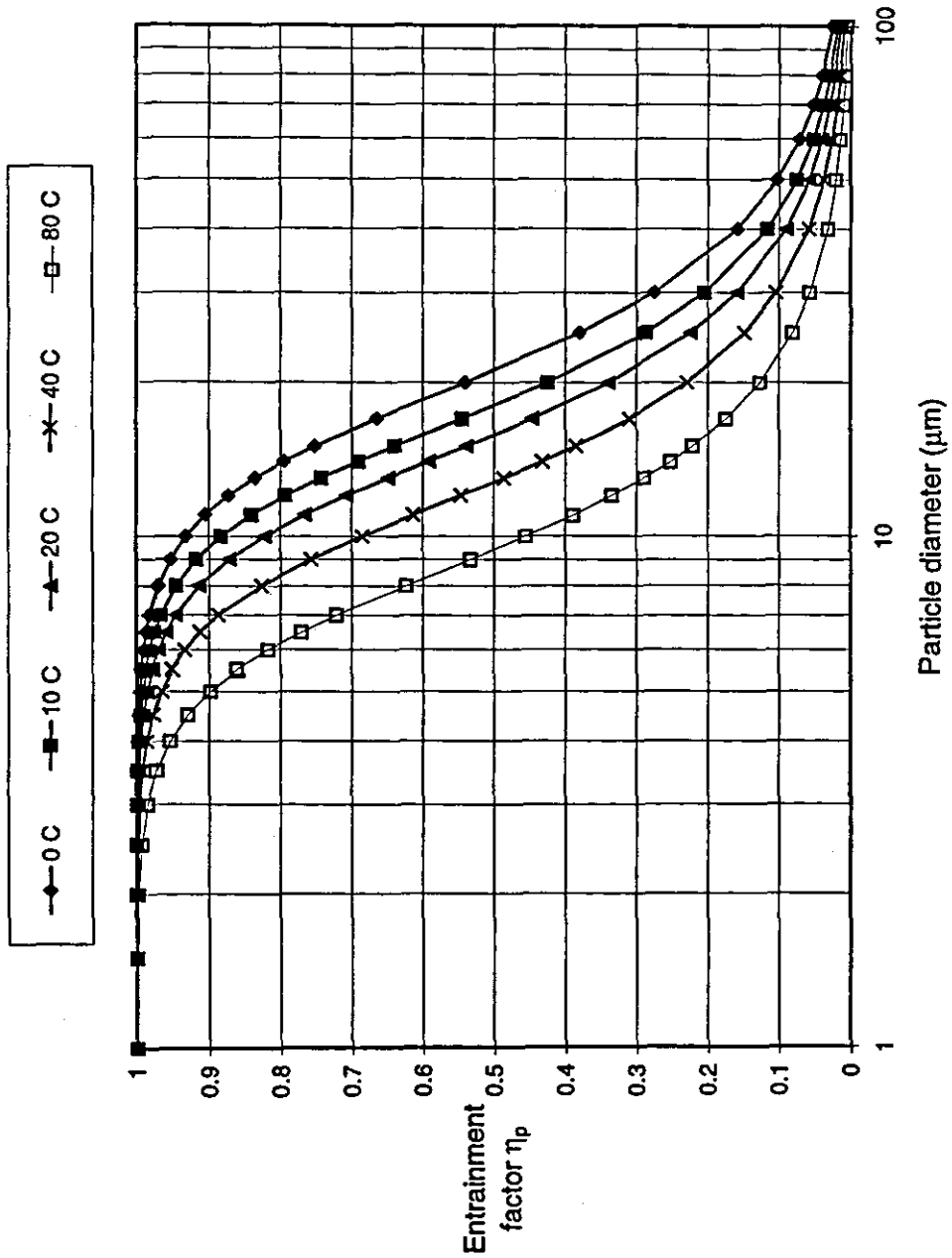


Fig. 3.15. Particle entrainment factor η_p in an acoustic field (10 kHz), in water, when Stoke's law and Newton's second law are taken into account. The density of the particle is 2000 kg m^{-3} , the temperature of water varies /65/.

3.6.2 Basset-Boussinesq-Oseen equation

Newton's second law and Stokes viscous drag force are suitable for calculations of particle entrainment factors if the fluid is a gas. More accurate results can be reached if the Basset-Boussinesq-Oseen (BBO) equation is used as the starting point for the total fluid force on the particle, when the fluid is water. Then the total force F_p due to the fluid impressing to the spherical particle can be described as follows /66/.

$$F_p = -\left(\frac{1}{\rho_p}\right)m_p \Delta(p - p_0) + \frac{1}{2}\left(\rho_f / \rho_p\right)m_p \frac{d(u_f - u_p)}{dt} + 3\pi\mu d_p(u_f - u_p) + \frac{3}{2}d_p^2 \sqrt{\pi\mu\rho_f} \int_{-\infty}^t \frac{d(u_f - u_p)}{d\eta} \frac{d\eta}{\sqrt{t - \eta}} \quad (3.4)$$

where

- μ = dynamic viscosity of fluid, (Ns m⁻²)
- d_p = diameter of particle, (m)
- u_f = velocity of fluid, (m s⁻¹)
- u_p = velocity of particle, (m s⁻¹)
- ρ_f = density of fluid, (kg m⁻³)
- ρ_p = density of particle, (kg m⁻³)
- m_p = mass of particle, (kg)
- p = pressure, (N m⁻²).

In equation (3.4) the first term is the pressure gradient force, the second term represents the "apparent mass" effect on the particle due to its acceleration relative to the fluid, the third term is Stokes viscous drag and the last one represents the contribution of the so called "history time" effect. At the starting point in the calculations, this last term can be neglected.

If the velocity variation of a fluid u_f is sinusoidal due to the acoustic field according to the equation (3.5);

$$u_f = U_f \sin(\omega t) \quad (3.5)$$

where U_f = amplitude of the fluid velocity (i.e. the velocity of the fluid, m s^{-1})
 t = time, (s)
 ω = acoustic angular frequency, (rad s^{-1})

we get the following representations of the particle entrainment factors shown in Figures 3.16 - 3.19.

In practice, the problem of connecting the ultrasonic field to the filtration equipment lies in obtaining the desired motion of the particles and then moving them in particular directions in the ultrasonic field. We need to decide the optimum frequency in order to obtain this particle motion.

The use of the BBO equation will give the first answers to this problem. On the basis of this study it was noticed that the BBO equation describes well the ability of particles to follow the movements of liquid in an acoustic field. This equation takes into account particle density, fluid density, dynamic viscosity of fluid and sound frequency.

From the Figures 3.16 - 3.19 it can be seen the entrainment factor η as a function of particle diameter with the curves of variables of frequency, density and temperature. Entrainment factor value 1 means that the particles follow the acoustic field totally and values less than 1 means that the entrainment of particles in an acoustic field is poorer .

PARTICLE ENTRAINMENT FACTOR

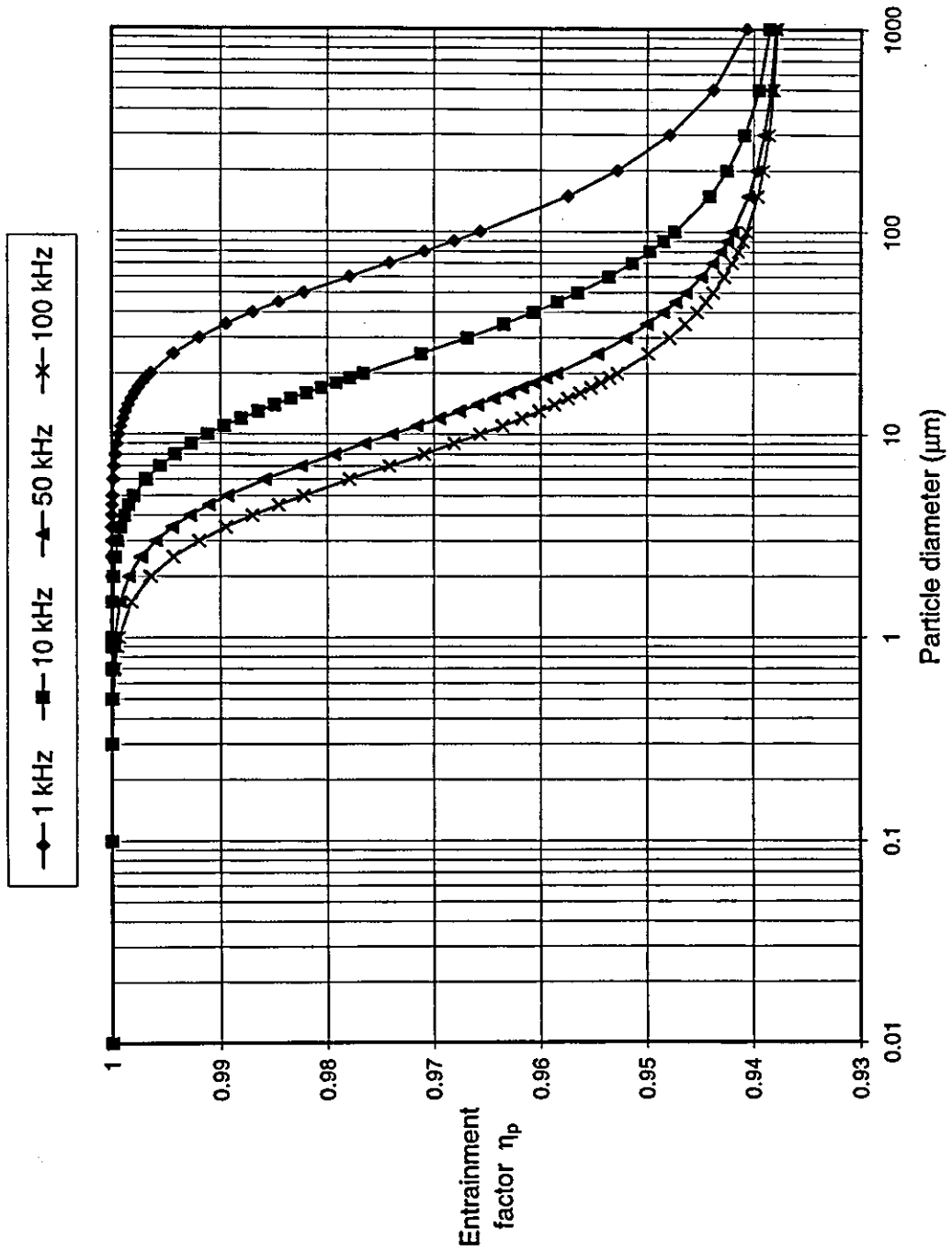


Fig. 3.16. Particle entrainment factor η_p in an acoustic field, in water (17.5 °C), when the BBO equation is the starting point for the calculations. The density of the particle is 1100 kg m⁻³. The frequency varies /65/.

PARTICLE ENTRAINMENT FACTOR

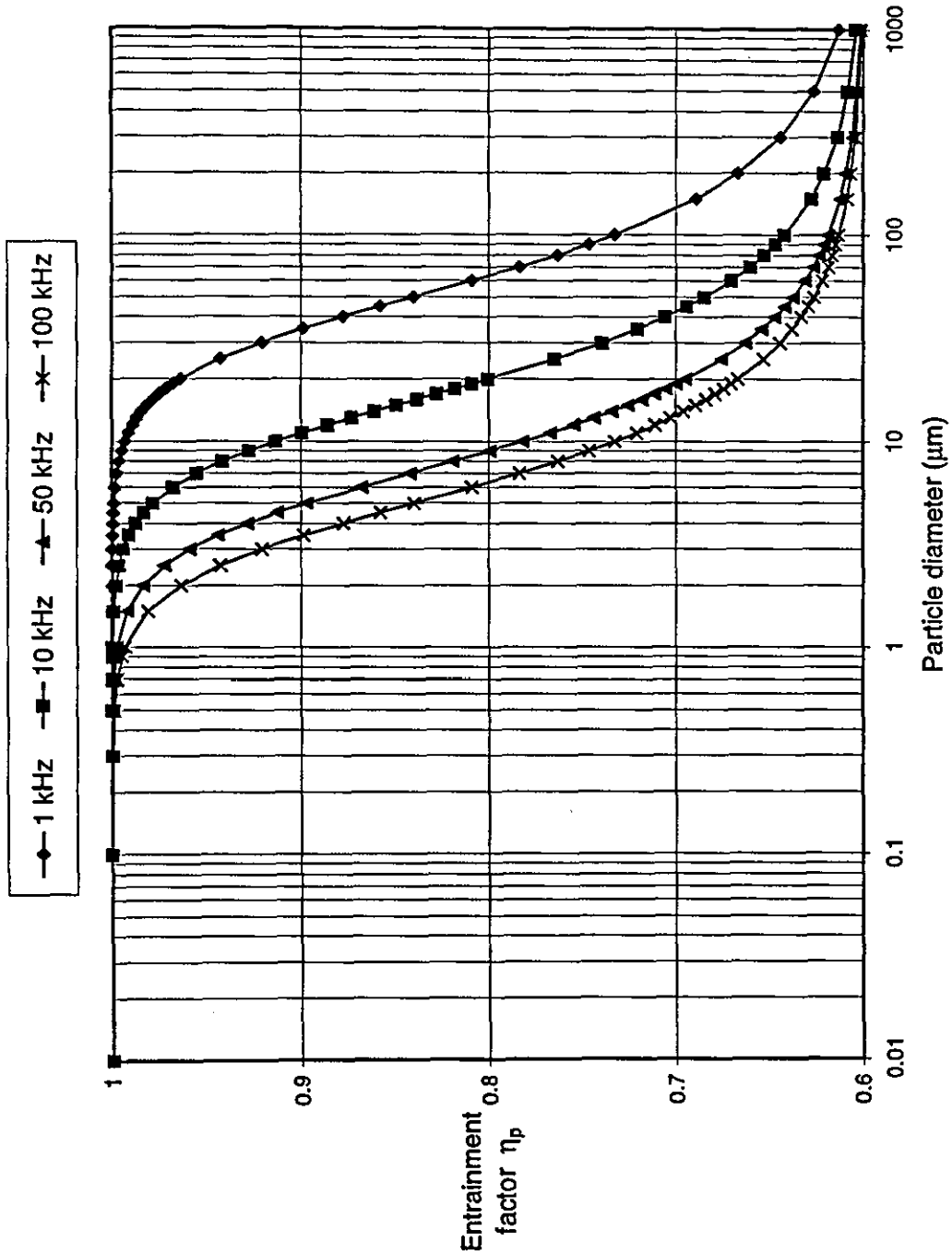


Fig. 3.17. Particle entrainment factor η_p in an acoustic field, in water (17.5 °C), when the BBO equation is the starting point for the calculations. The density of the particle is 2000 kg m⁻³. The frequency varies /65/.

PARTICLE ENTRAINMENT FACTOR

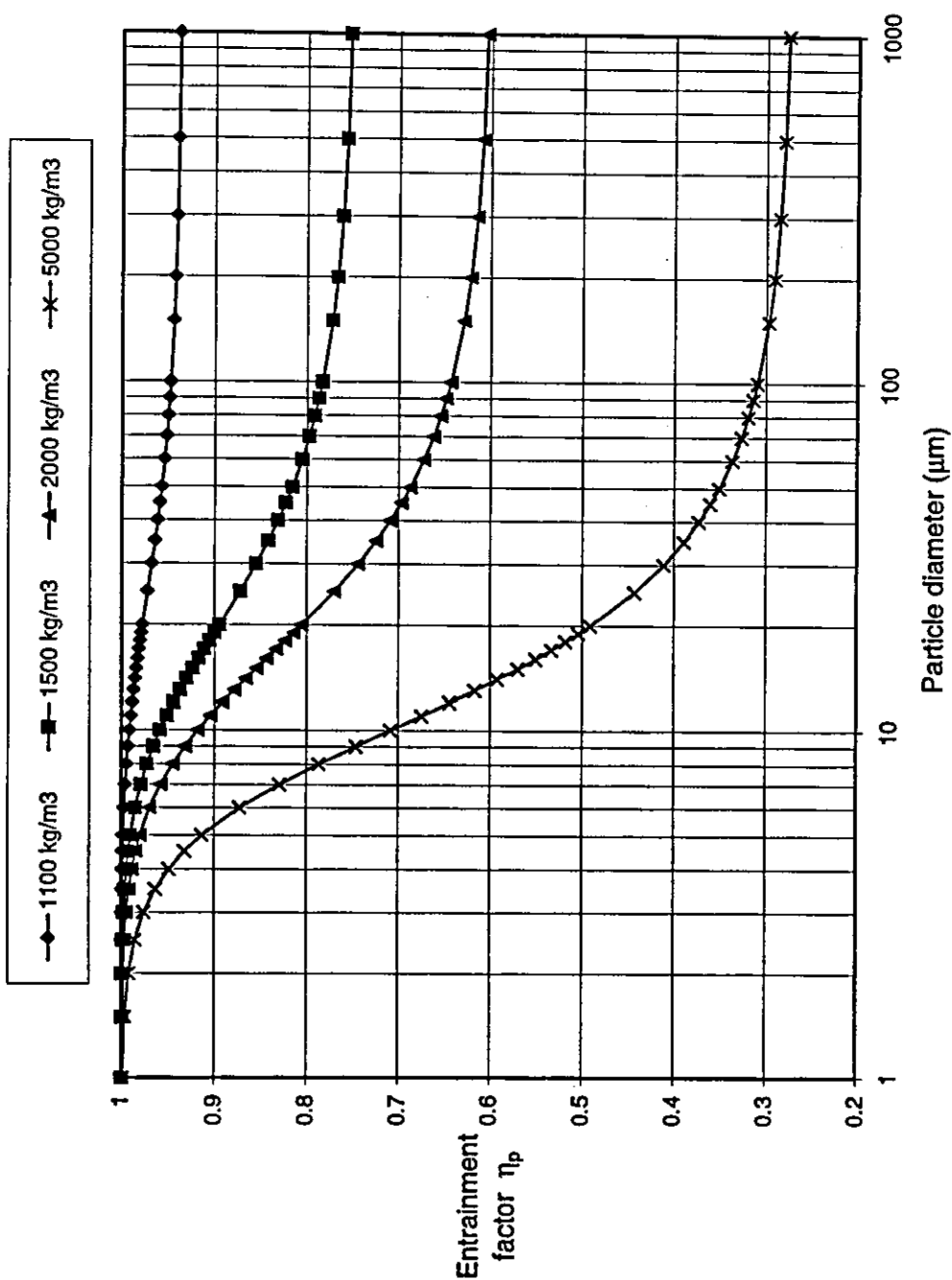


Fig. 3.18. Particle entrainment factor η_p in an acoustic field (10 kHz), in water (17.5 °C) for particles of various density, where the BBO equation is the starting point for calculation /65/.

PARTICLE ENTRAINMENT FACTOR

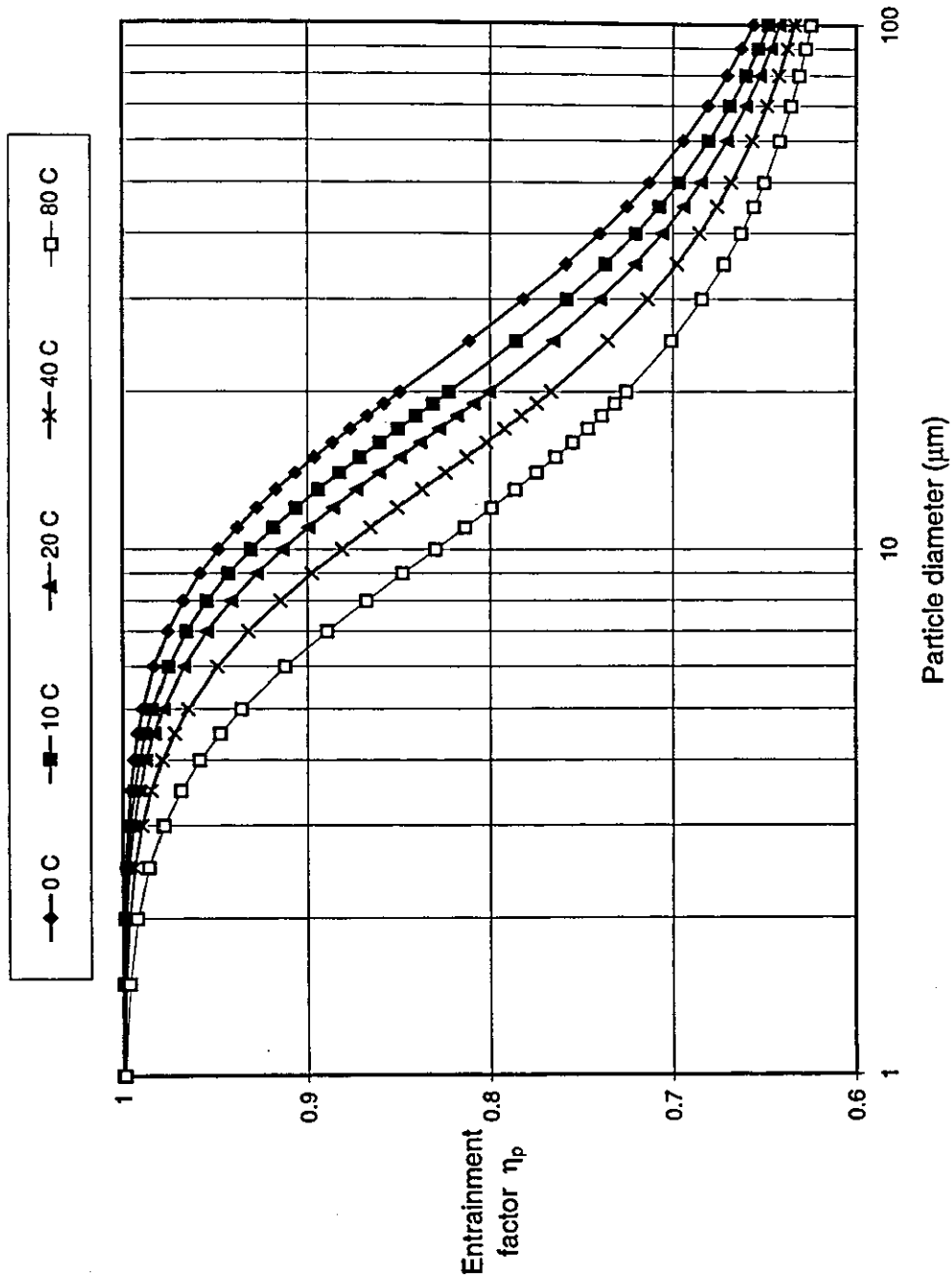


Fig. 3.19. Particle entrainment factor η_p in an acoustic field (10 kHz). The density of the particle is 2000 kg m^{-3} , the temperature of the water varies. BBO equation is the starting point for the calculations /65/.

Normally if the entrainment factor is over 0.5 in the chosen conditions, particles follow the ultrasonic field well enough and the hoped for effects of moving the particles in a particular way can be reached. But we have to remember that the above mentioned happens in ideal circumstances and at steady state; these are no additional movements of particles due to additional forces acting on the particles or fluid movement, there is no sound wave scattering etc. All the additional forces on the particles and any additional fluid movements will affect to particles movements in a fluid in an ultrasonic field.

Calculations based on combined Stoke's law and Newton's second law shows that small particles, diameter $< 5 \mu\text{m}$, follow reasonably well or totally the acoustic or ultrasonic field between 1 – 100 kHz. Bigger particles, diameter $> 5 \mu\text{m}$, follows better at lower frequencies (1-10 kHz) than at higher frequencies (50-100 kHz). In the fixed acoustic or ultrasonic field and at constant temperature the entrainment factor η_p becomes poorer when the density of particle increases. The same effect is seen also when temperature increases. The best entrainment factor η_p values are reached with lower temperatures. So based on the combined Stoke's law and Newton's second law to move bigger particles than $5 \mu\text{m}$ by diameter, the best circumstances are to use lower frequencies (sonic field 1-10 kHz), lower densities (entrainment increases when the density of particle becomes nearer the density of water) and lower temperatures (below 20°C). Smaller particles than $1 \mu\text{m}$ by diameter follows totally ($\eta_p = 1$) acoustic or ultrasonic field in any above mentioned conditions.

If the entrainment factor η_p has a value of 0.5 or more it is expected that the particle follows reasonably well the acoustic or ultrasonic field and there is a benefit to use these fields to move particles to the desired places or to get them to agglomerate.

These calculations also show that particles with diameter $> 20\text{-}30 \mu\text{m}$, or especially over $100 \mu\text{m}$, are impossible to move with acoustic or ultrasonic field.

Calculations based on Basset-Boussinesq-Oseen (BBO) equation, which is more accurate to use when particles are suspended in a fluid, shows that particles with diameter $> 100 \mu\text{m}$ (or even $1000 \mu\text{m}$) follows extremely well the acoustic or ultrasonic field. But also in this case lower frequencies are better than higher ones. The density of particle has a great effect on the entrainment factor η_p . Particles with lower densities follow better acoustic field than particles with higher densities. Particles with a density of 1100 kg m^{-3} follow the acoustic field nearly totally even when the diameter of the particle is $100 \mu\text{m}$, but for particles with a density of 5000 kg m^{-3} the entrainment factor η_p goes below 0.5 with the diameters of particle $> 20 \mu\text{m}$. At different temperatures between $0-80^\circ\text{C}$, all particles with the diameter $< 100 \mu\text{m}$ follow the acoustic field (10 kHz) reasonably well, smaller particles better than bigger ones. But at lower temperatures the particle entrainment with the acoustic field is better than at higher temperatures.

So the BBO equation shows that the best circumstances to move suspended particles are similar to the case when Stoke's law and Newton's second law are combined; lower frequencies, lower densities and lower temperatures are preferred. But the importance results from these two equations are that the more accurate BBO equation for suspended particles gives much higher (better) entrainment factor η_p values than the other. In all these calculated circumstances ($f = 1-100 \text{ kHz}$, $\rho_p = 1100-5000 \text{ kg m}^{-3}$, $T = 0-80^\circ\text{C}$) the η_p value is well above 0.5 with particles of diameter $100 \mu\text{m}$ or over, except particles with high densities e.g. 5000 kg m^{-3} . Then η_p falls down to the value of 0.5 with particles diameter $20 \mu\text{m}$.

So in conclusion it can be said that not only particles with smaller diameter ($< 5 \mu\text{m}$) but also particles with bigger diameters ($> 100 \mu\text{m}$) can be moved with acoustic or ultrasonic field very well to desired places and to get agglomerate. It has to be notice that these calculations are valid under cavitation level of bulk suspension.

3.7 Acoustical properties of suspensions

A plane wave perpendicularly incident on a boundary layer of two matters 1 and 2, and which passes through and into the matter 2, is attenuated according to the following relation $T = 2/(1+Z_1/Z_2)$, where Z_1 and Z_2 are acoustic impedances of matters 1 and 2. The experimental set up used in these measurements is described in Figure 3.20.

Dimensions of the measurement pool are 37 x 29.5 x 24 cm (volume about 26 l). An ultrasonic transducer is placed on one of the walls of the measurement pool. The position of a hydrophone moving on a bar can easily be changed to give different distances from a transmitter. The hydrophone measures acoustic pulses transmitted by the ultrasonic transducer. A sound velocity and a connection between the transducer and a suspension compared to a connection of the distilled water and the transducer can be measured by this experimental set-up. The ultrasonic transducer used in these experiments had a radius of 19 mm and an operating frequency 75 kHz.

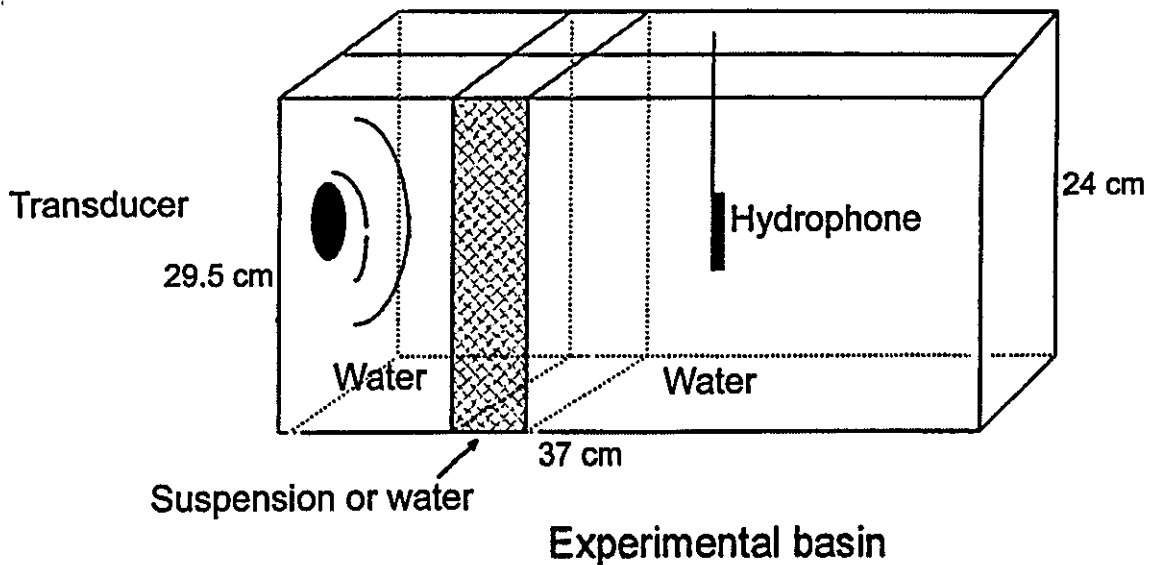


Figure 3.20. Measurement pool for acoustic impedancies, suspension in separated vessel.

In Figure 3.20, the measurement pool was divided by aprons into different parts. In this way a 56 mm thick suspension layer could be arranged inside the

experimental basin. Ultrasound attenuates when passing through the suspension layer. The reference situation was arranged by filling the space between the aprons with water. Thin plastic walls between suspension and water cause no significant attenuation of the sound propagation. Measurements with and without plastic walls are presented in the Figure 3.21. The first and the second plastic walls were situated 22 mm and 78 mm from the ultrasonic transducer.

The Sound pressure in the experimental basin after the aprons, the position of the last apron about 80 mm

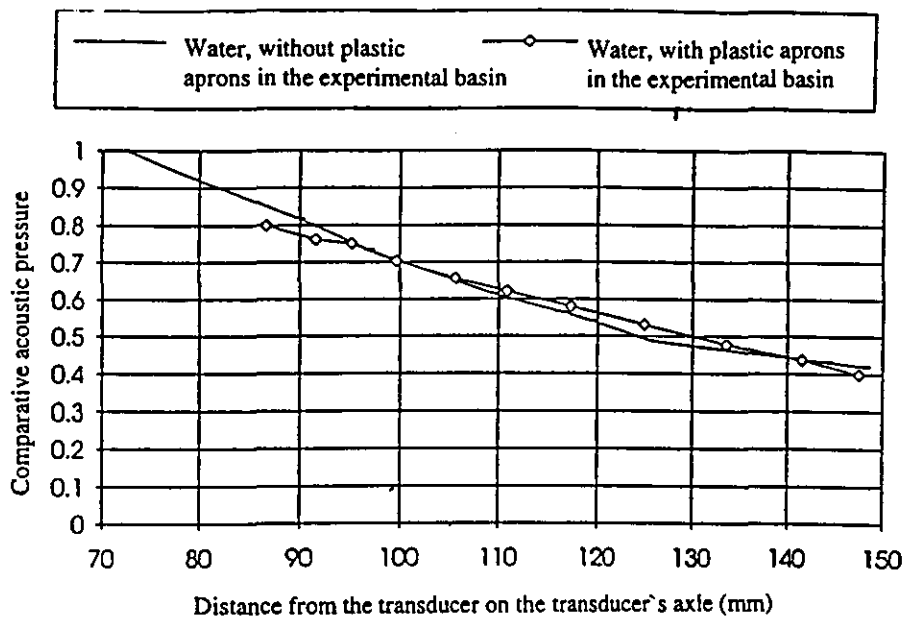


Figure 3.21. Attenuation of pressure amplitude in measurement pool in water (19.5°C) with and without plastic walls.

The amplitude of the sound wave attenuates by the following equation $T_1 = 2/(1 + Z_1/Z_2)$ when it propagates from water to suspension and vice versa by the equation $T_2 = 2/(1 + Z_2/Z_1)$, where Z_1 and Z_2 are the acoustical impedance of the water and the suspension. Overall the attenuation of the pressure amplitude of the short sound pulse is $1 / (T_1 T_2)$ from the original when it propogetes from water to suspension and then again to water. If attenuation still happens in suspension, the total attenuation of the pressure amplitude is $1 / (T_1 * T_2 \exp(-\alpha d))$ from the original value where α is the adsorption coefficient and d is the thickness of the suspension layer.

In these experiments the sound pulse was long, 30 cycles after every 60 ms, so that the tail of the pulse propagates partly in resonance through the medium layer or generally in the continuous phase. In these experiments the thickness of the medium layer was 56 mm, which means that generally the sound pulse propagates in the continuous phase through the bio/fiber- and phosphoric acid suspensions and it resonates through the mineral suspension. The intensity of the continuous pulse should propagate through the suspension layer without adsorption, with T_1 attenuated according to (Kinsler et al., 1980 modified):

$$T_1 = 1/((1+1/4(Z_2/Z_1-Z_1/Z_2)^2(\sin k_2d))^2) \quad (3.6)$$

where

- Z_1 = acoustic impedance of water
- Z_2 = acoustic impedance of suspension
- d = thickness of suspension layer
- k_2 = wave number connected to suspension, $\omega/c_2 = 2\pi f/c_2$
- c_2 = sound velocity in suspension
- T_1 = sound intensity after medium layer / sound intensity before medium layer.

If we forget the effects of the plastic walls and we use equations as for plane waves, we get the acoustic impedances of suspensions relative to the water by equation (3.6). The calculated values are presented at the Table 3.5. The acoustic impedance of the distilled water in 20 °C is $1.48 \times 10^6 \text{ Pa s m}^{-1}$. Measurements were started with the shown highest D.S. content and measurements in lower D.S. contents were based on diluted suspensions with distilled water to the desired D.S. content. The intensity is equal to the square of the pressure amplitude. Acoustic impedances presented in the following Table are not absolute values, they are so called realistic "apparent" values of the acoustic impedance. These values are exact enough for the design purposes of the transducers for filtration applications. For the exact values you should examine

the complex impedances of the suspensions $Z = r + j\sigma$, where r is the real- and σ imaginary part.

Table 3.5. "Apparent" acoustic impedances of suspensions relative to water ($1.48 \times 10^6 \text{ Pa s m}^{-1}$)

Water	1
Phosphoric acid	2.4
Pyrite 63 m-%	2.4
Pyrite 76 m-%	6.2
Pyrite 84 m-%	170
Fiber 0.8 m-%	1.1
Fiber 1.7 m-%	2.0
Fiber 2.5 m-%	2.3
Fiber 4.8 m-%	3.4
Biosludge 0.4 m-%	1.0
Bio/fiber 0.9 m-%	2.4

From equation (3.2) it can be seen that acoustic impedance of medium matter Z is dependent on the product of the density (ρ) of the medium and the sound speed (c) in that medium, $Z = \rho c$. The dynamic viscosity of post-feculent phosphoric acid fluid is higher than water and also the density of this suspension is higher than water, so the acoustic impedance compared to water increases. For pyrite and fiber suspensions it can be seen that when the dry solid content (m-%) increases, viscosity increases (Table 3.3.) and also acoustic impedance for those suspensions increases due to the above mentioned relationship between Z , ρ and c . In the case of fiber, bio and bio/fiber suspensions they are quite "thick" (higher viscosity) suspensions even in a low dry solid concentration compared to water. But in bio/fiber suspensions the dry solid matter is an organic deposit where density is very near the density of water. So the main reason for the increase of the acoustic impedance for these suspensions is their higher viscosities, and also partly the dry solids content in water.

Pyrite, which is inorganic, does not mix with water in the same way as bio/fiber matter. In a pyrite suspension water and solid particles do not mix together, they are in a suspension in two different phases. As to dry solid content of the suspension increases, the acoustical properties of the medium (suspension) comes nearer to those of the pure dry solid matter. As can be seen from Table 3.5., at a certain dry solid content (here 84 m-%) the properties of the suspension changes dramatically and the acoustic impedance increases remarkably. At this point the suspension is already so concentrated that the sound speed will increase towards the sound speed of the pure solid matter. The suspension starts to act more like a rigid matter behaviour and due to the equation (3.2) also the acoustic impedance increases towards higher values compared to water.

Three different kind of suspensions were characterised for the reason of storage to ensure that in all experiments the used suspension samples were similar and also to determine electrical and acoustical properties of the suspensions. Measurements for electrophoresis with bio/fiber suspension showed that using electric field to move particles, the movement is caused by combined effects electroflotation and electrophoresis. These measurements showed also that electroflotation is a major effect to move particles in a bio/fiber suspension. Basset-Boussinesq-Oseen (BBO) theoretical equation to describe particle entrainment in an acoustic field was more accurate than combined Newton's second law and Stoke's law when particles were suspended. The calculations based on BBO equation showed also that particles smaller than 1 μ m with diameter will follow totally acoustic field in water. "Apparent" acoustic impedance of bio, fiber and post-feculent phosphoric acid were quite similar or few folds higher in measured concentrations than water itself. "Apparent" acoustic impedance of pyrite suspension in a higher concentration (84 m-%) was nearly two hundred folds greater than the similar value for water. This described that this kind of suspension in a high concentration act more like a rigid body than a suspension with the manners of acoustic properties.

4 THE ELECTRO-ACOUSTIC FILTRATION EQUIPMENT

Suspensions used in the electro-acoustic filtration experiments were the same as those whose properties were analyzed in Chapter 3; bio/fiber, pyrite and post-feculent phosphoric acid. Filtration experiments were divided into three different equipment scales: small, miniPILOT and PILOT scale.

In the experiments there were used totally 7 different experimental equipment. Small scale equipment was used for all three suspensions, Figure 4.1. These experiments were done to determine basic electro-acoustic dewatering properties of suspensions. Dewatering experiments were based on gravitation or a low (-0.2 bar) under pressure. For miniPILOT scale experiments it was used 4 different equipment, Figures 4.2.-4.5. The first one was for bio/fiber suspension experiments, the second and the third one for pyrite suspension and the last one for pyrite and post-feculent phosphoric acid. This was due to the reason that two different equipment manufactures were involved, Larox Oy and outokumpu Mintec Oy. Larox Oy was interested about bio/fiber suspension and willing to connect electro-acoustic method to their rotary vacuum drum filter. Outokumpu Mintec Oy was interested about pyrite and post-feculent phosphoric acid and at the same way willing to connect electro-acoustic method to their ceramic filter unit CERAMEC®. So miniPILOT equipment in Figure 4.2. was for experiments to get dewatering results in this scale but also to get needed information to design and build PILOT scale equipment. Pyrite suspension was more difficult to use (ultra)sonic field to enhance dewatering due to the high attenuation of acoustic waves in a higher concentrations. That is why it was needed two different kind of preliminary miniPILOTs, Figures 4.3-4.4, to get dewatering results and to get information to design and build the final miniPILOT equipment, Figure 4.5. Based on the achieved information from the smaller scale experimental equipment, the PILOT scale equipment were designed and constructed. Equipment for bio/fiber suspension simulated the rotary vacuum drum filter built

by Larox Oy, Figure 4.6. PILOT equipment for pyrite and post-feculent phosphoric acid simulated CERAMEC® filtration equipment built by Outokumpu Mintec Oy, Figure 4.7.

Small scale filtration experiments were static filtration experiments based on gravity or vacuum. There was no suspension movement before filtration. The apparatus was constructed of Perspex tube, the diameter of which was 14 cm and height 50 cm. The area of the filter medium was 0.015 m^2 and the maximum amount of suspension filtered was 7 liters. Suspension was fed at the top of the apparatus over the filter medium, the volume below the filter medium was kept full of water before the filtration experiments. The ultrasonic transducer (diameter 5 cm) was connected through the Perspex tube so that the acoustic field covered the hole area of the filter medium, see Figure 4.1. In the electric field enhanced filtration experiments, the anode was a floating type electrode over the suspension and the cathode was metallic wire which was the filter medium itself or wire was connected to filter media made from different materials. All the filtration experiments were based on gravitation or vacuum, so there was no need for experiments to use the over pressure. The apparatus was also equipped with heat regulation and cooling systems, but the duration of all the filtration experiments were so short that there was no need to use the cooling system to avoid over heating. Normally during the filtration, suspension temperatures increased between 20 to 30 °C as measured by thermometer. In the volume below the filter medium, a hydrophone was used to measure acoustic pulses. This was used to ensure that an acoustic connection between transmitter and suspension existed. The distance between the ultrasonic transmitter and the filter medium was changeable between 0 and 15 cm.

In the filtration experiments the volume below the filter medium was full of water and the volume was connected with the tube to a smaller bottle which was connected to a vacuum pump. This smaller bottle was placed on a balance such that before the filtration experiments, vacuum was sucked first into the smaller

bottle. Vacuum was measured by vacuum meter. When the required vacuum level (0,15 - 0,90 bar) was reached, then the balance was tared and after that the valve in the filtrate tube was opened and the filtration started. The permeate was led through the filtrate tube to the smaller bottle over the balance. The balance measured in real-time the mass of water separated during the filtration experiment.

These experiments describe mainly the maximum effects of electric and/or ultrasonic fields on filtration.

For small, miniPILOT and PILOT scale experiments, the apparatus used filter media cut to the required dimensions, connected and sealed with glue into position. The filter media used varied depending on the suspensions being filtered. For bio/fiber suspension in the small scale experiments nylon cloth with pore size 10 μm (72-1134-L2 Tamfelt) was used and in the miniPILOT scale experiments woven wirecloth with pore size 2 mm was used. This was due to higher ultrasonic field attenuation with tighter filter media. For pyrite suspension a ceramic plate with pore size 1 μm (main component aluminium oxide, more details not given) was used, and for post-feculent phosphoric acid metallic membrane plate with a pore size of 3 μm (BEKIPOR ST3AL3SS, acid-proof) was used. In the electric field assisted filtration experiments when the filter media was used as a cathode, in the case of nylon cloth the woven wirecloth was connected above the nylon wire. The pore size of metallic wire was at least 3-folds greater than the pore size of the nylon cloth. When ceramic plate was used as a cathode, the plate was cut in half and a woven wirecloth with a pore size much more greater than the pore size of the ceramic plate was placed between these two halves. The halves were glued together. Because metallic membrane plate was already conductive (metal), it can be used as a cathode itself without any changes. In the case of cathode filter media, the conductive woven wirecloth was connected straight to a power supply to an earth potential.

scale apparatus was used to determine the dewatering parameters and apparatus design information for a next scale of experimental rig.

Small scale experiments for bio/fiber suspension showed that ultrasonic intensity had to be increased for the next scale mainly due to the bigger volume of suspension to dewater. Also the miniPILOT scale rig was designed so that it was possible to transmit the ultrasonic field through the filter media from the filtrate side and avoid filter media blocking. The distance between the ultrasonic transducer and the filter media was fixed based on the small scale experiments. Polarity and the distance between electrodes for the miniPILOT scale was determined also with the small scale apparatus.

The miniPILOT scale equipment, Figure 4.2., for bio/fiber suspension filtration was constructed of Perspex with rectangular shape. The dimensions of the vessel were 25 x 30 x 30.5 cm and the volume 20 l. Filter media with the area of 0.03 m² was placed in the middle of the vessel. For ultrasonically enhanced filtration tests an ultrasonic transducer was led through the other end of the vessel and sealed well to avoid any leaks. The distance between the transducer and the filter media was changeable between 0 and 10 cm. For electric field filtration experiments the filter media was used as a cathode and an anode was placed into the vessel. The distance between the filter media and the anode was 5 cm. All the filtration experiments were started at room temperature 20 °C and after the filtration, the temperatures of the suspensions were at a maximum 30 °C due to mainly the use of the electric field.

In the beginning of an experiment the suspension vessel was filled with the suspension and vacuum was sucked first into the bottle over the balance. Vacuum was measured by vacuum meter. When the required vacuum level (0.15 – 0.90 bar) was reached, the balance was tared and the valve in the filtrate tube was opened and the filtration started. The permeate was led through the filtrate tube to the bottle over the balance.

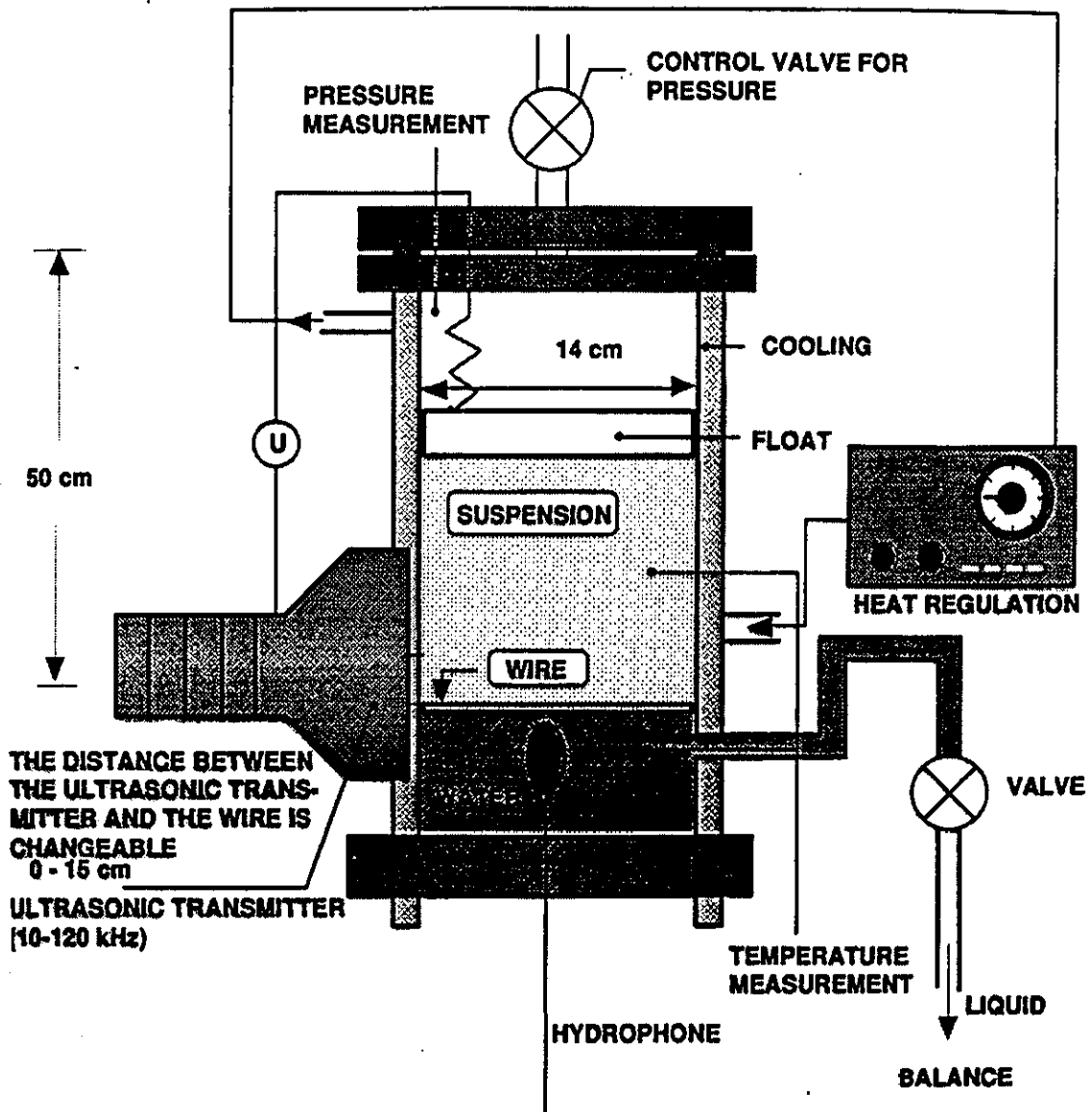


Figure 4.1. Small-scale electro-acoustic filtration apparatus and its mode of operation.

MiniPILOT experiments were also static filtration experiments based on a negative pressure, maximum -0.9 bar. Experiments with the small-scale apparatus described above gave the first experimental results to enhance filtration by electrically and/or acoustically assisted force fields. The final aim of the development work for bio/fiber suspension dewatering was to simulate a drum filter. The development work was planned to proceed by step by step, from smaller scale apparatus via miniPILOT scale towards PILOT scale. The smaller

The same computer program was used to calculate the filtration parameters and the program for the balance as in the miniPILOT apparatus, manufactured by Outokumpu Mintec Oy. The filtration parameters filtration time and the period of application of the ultrasonic and/or electric field during the filtration were set by the computer. The balance starting time, data collection sequence and calculation of a dry solid content in the slurry vessel (based on the starting parameters of the filtered suspension) were controlled by the computer. The miniPILOT scale filtration equipment for bio/fiber suspension experiments is shown in Figure 4.2.

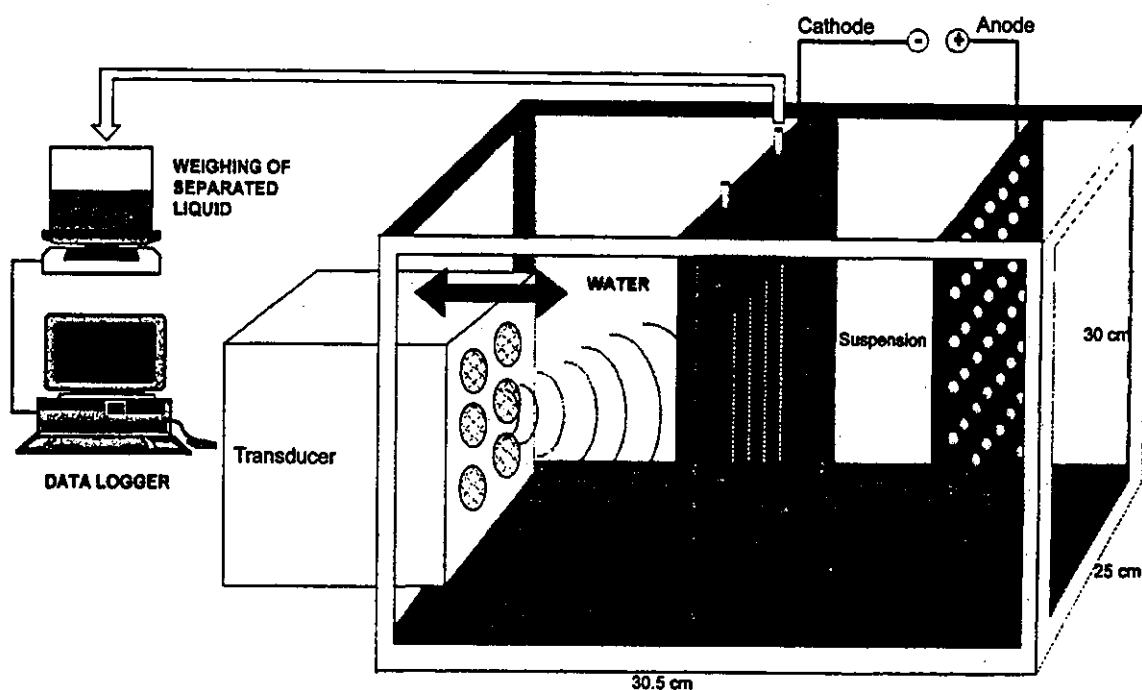


Figure 4.2. MiniPILOT scale filtration equipment equipped with electro-acoustic accessories.

Enhanced miniPilot scale filtration of a pyrite suspension with a sonic field was studied using two different test set-ups. In the first set-up a nylon cloth with pore size $6 \mu\text{m}$ was used as the filtration medium together with an ultrasonic transmitter which was bigger in terms of the oscillating surface, Figure 4.3. The dimensions of the Perspex suspension tank were $25 \times 30 \times 35 \text{ cm}$ and volume 26 l. The filtration area ($7,1 \text{ cm}^2$) was smaller than the area of the oscillating

surface of the transducer (19.0 cm^2), to cover the whole filtration area with ultrasonic field. The ultrasonic transducer was fitted inside the Perspex tube and sealed to avoid leakages during immersion. The distance between the transducer and the filter media was changeable between 0 and 10 cm.

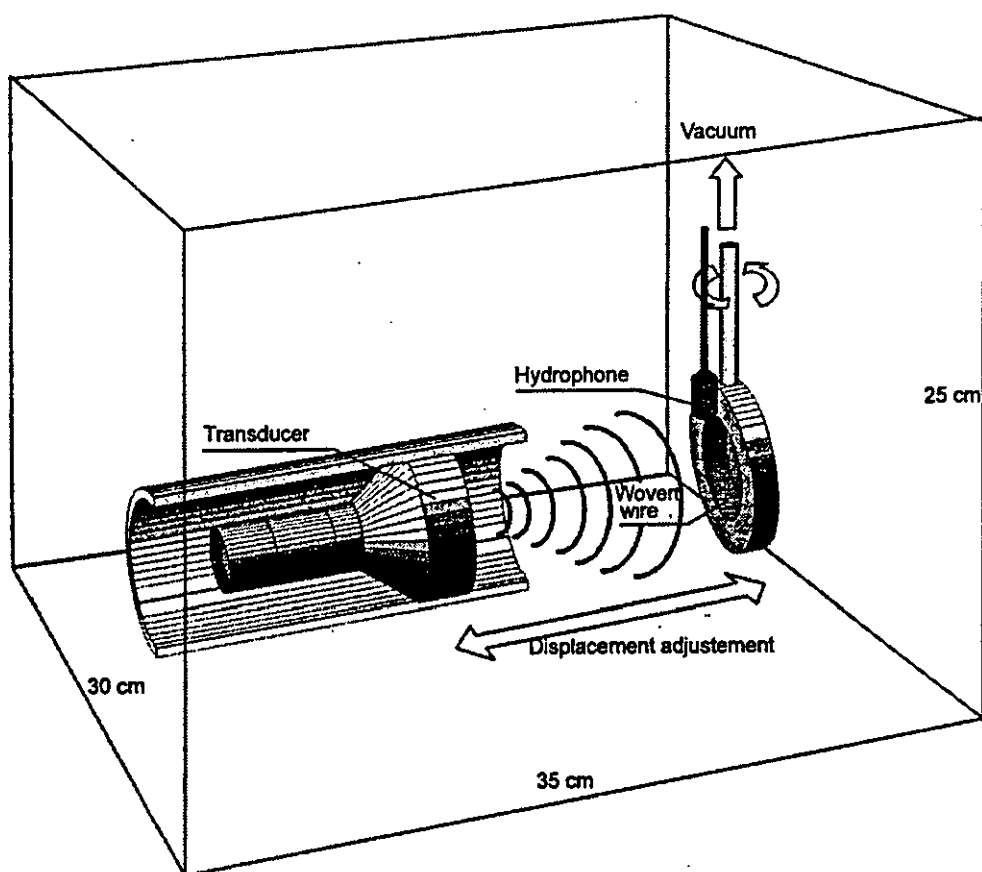


Figure 4.3. The first experimental set-up used in pyrite suspension filtration tests enhanced by ultrasonic field.

The experimental rig used in the second test set-up is described in Figure 4.4. The ceramic plate filtration tests were done with this system. The dimensions of the suspension tank were 37 x 16 x 15 cm and the volume 9 l. The ultrasonic transducer was connected to the other side of the suspension tank and the filter plate was glued together with the transducer. The plate was connected to vacuum and filtration measurements were done in the way described previously. The transducer consisted of six piezo-ceramic elements. The transducer was originally designed and constructed for ultrasonic cleaning purposes. The reason

to use this kind of transducer was to get higher output powers from the transmitter as mentioned after the small-scale experiments. The area of the ceramic plate was 33 cm^2 and the pore size $1 \mu\text{m}$. The total area of the ultrasonic transducer was 140 cm^2 .

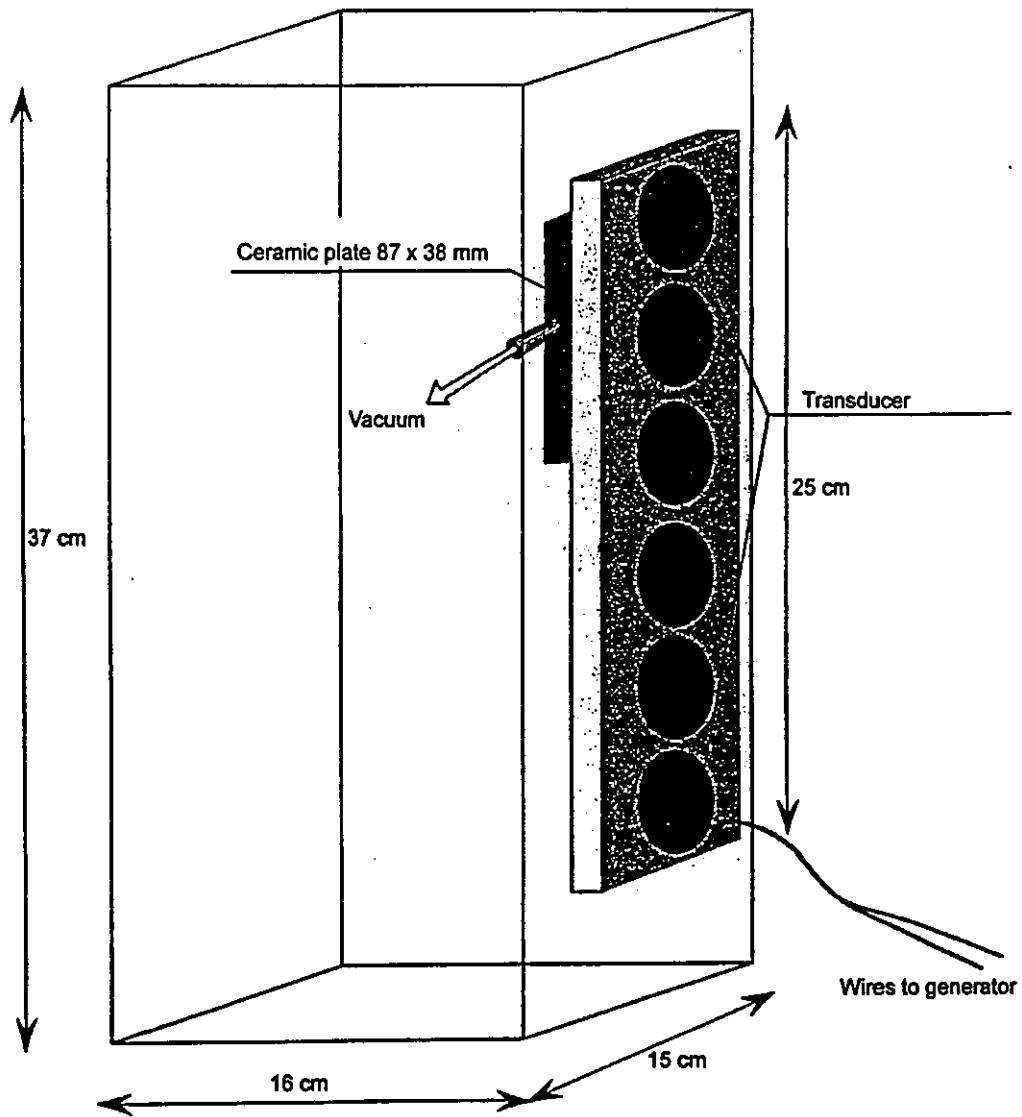


Figure 4.4. Ceramic plate filtration unit for ultrasonically enhanced pyrite suspension experiments.

For pyrite and post-feculent phosphoric acid suspensions the final aim for the experimental apparatus was the PILOT scale equipment which simulated the rotary ceramic filter equipment CERAMEC® manufactured by Outokumpu Mintec Oy. The small scale experimental rigs were used to determine the best

electrically and/or acoustically assisted filtration parameters for the miniPILOT scale rig. With the first experimental apparatus, described in Figure 4.3, the direction and distance between the ultrasonic transducer and the filter media was determined. In these experiments the hydrophone was used in front of the filter media to measure ultrasonic intensities approximately on the surface of the filter media. With the second small scale experimental rig, described in Figure 4.4, preliminary filtration tests were done with a more powerful ultrasonic transducer connected to the ceramic plate. In this stage, for the first time it was possible to use the small scale ceramic filter plates which were totally similar to the plates used in the commercial equipment manufactured by Outokumpu Mintec Oy. The first small scale experiments showed that the best direction for the ultrasonic field to enhance filtration was through the ceramic plate in the direction of filtration. These miniPILOT scale experiments showed that ultrasonic transducers originally designed and constructed for ultrasonic cleaning purposes could be used in the PILOT scale experiments such that the acoustic connection between the transducer and the ceramic plate was acceptable. Preliminary electric field enhanced filtration parameters were based on those experiments done with the small scale apparatus shown in Figure 4.1.

A miniPilot scale filtration unit for pyrite and post-feculent phosphoric acid experiments was constructed and delivered by Outokumpu Mintec Oy to VTT Energy at this stage. The system was used in the first stage of the pyrite suspension filtration experiments enhanced by electric field, and also for the post-feculent phosphoric acid experiments. The experimental rig is shown in Figure 4.5. Ultrasonic transducers and electrodes were connected to the equipment at VTT Energy. The body of the unit was stainless steel. The ceramic plate was connected with an arm to the body. The arm was movable and the movements of the plate to a suspension tank (Perspex) and out of the tank was controlled by the control panel, so the filtration and drying times of the whole cycle were adjustable. Dimensions of the rectangular suspension tank were 17.5 x 17.5 x 12.5 cm and the volume ~ 4 l.

The experimental miniPILOT filtration apparatus simulated the operation of the CERAMEC® vacuum filter, in which the main operational functions are cake filtration over a ceramic plate by vacuum in a slurry vessel (filtration mode), cake drying by vacuum when a plate is in the air (drying mode), scraping the cake off the surface of the plate after drying (scraping mode) and plate washing with water by counterpressure. The main parts for the operation of the apparatus are a control panel, computer programs for the filtration parameters and balance.

In the control panel there are switches and signal lights for the full operation of the apparatus. Emergency shutdown switches the voltage off from the output of control panel. With a MANUAL/AUTO switch the manual mode can be selected for all the different modes. Parameters for filtration can only be selected from the computer in this mode. In auto mode the filtration process can be started with the START-button. In this mode the apparatus will automatically do the filtration process based on parameters selected in the computer. In the control panel there are also ultrasound and electric field buttons, and a desired time during the filtration for which the functions can be used.

Before starting a filtration experiment, the filtration parameters filtration time, drying time, counterwashing, time to use ultrasound and/or electric field during the filtration had to be set by the computer. Also, the program for the balance contents the start time, data collection sequence and calculation of a D.S. content (based on suspensions D.S. content in the beginning of the experiment) of a cake during the filtration will be started by the computer.

The ceramic plates, area 0.015m^2 , were connected by a tube straight to a filtrate bottle over the balance, which was connected to a vacuum pump. Before the filtration experiments, vacuum was sucked first into the filtrate bottle. Vacuum was measured by vacuum meter. When the requested vacuum level (- 0,90 bar) was reached, then the balance was tared and after that the valve in the filtrate tube was opened and the filtration started. The permeate was led through the

filtrate tube to the filtrate bottle over the balance. The balance measured in real-time the mass of the water separated during the filtration experiment.

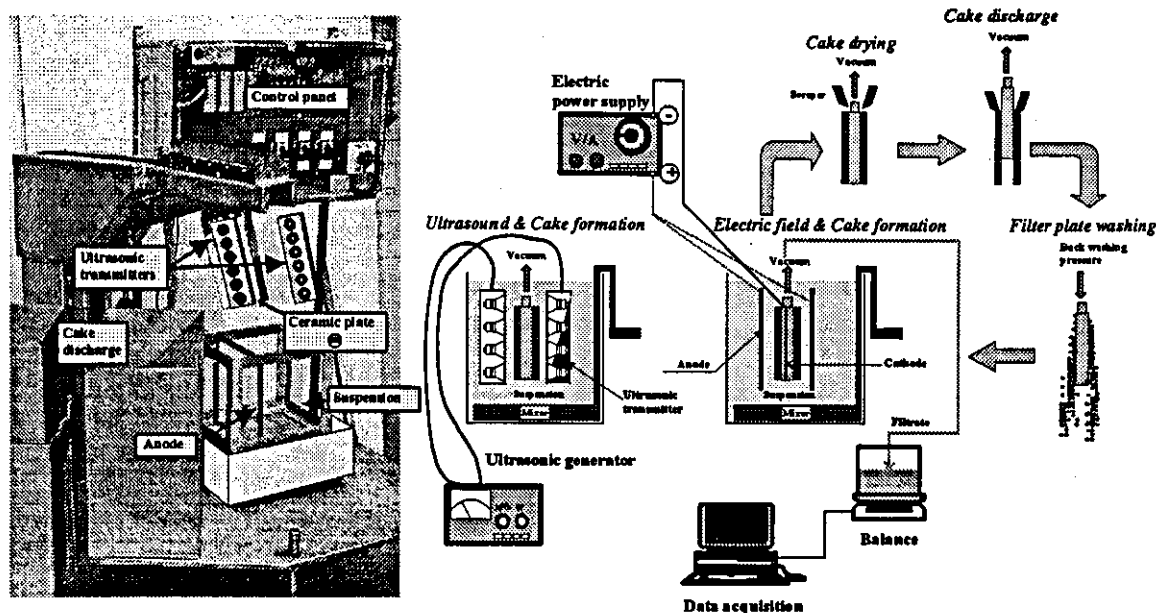


Figure 4.5. MiniPILOT filtration rig with ceramic filter plate rig manufactured by Outokumpu Mintec Oy.

Enhancements of ultrasonic and electric fields on the bio/fiber suspension filtration were studied with the PILOT scale equipment manufactured by Larox Oy. The experimental rig is shown in Figure 4.6. The body of the equipment was steel and the woven wirecloth (filter media, pore size 1 mm) was set to go over the rolls situated in the corners of the body construction. Over the woven wirecloth above the body of the rig was placed a suspension vessel (Perspex) sealed well to avoid any leaks. The bottom of the vessel was rectangular with dimensions of 17 x 17 cm, area $\sim 0.03 \text{ m}^2$, height 25 cm and volume 7 l. The filtration area was the same as the area of the bottom of the suspension vessel. The vacuum, 0.8 bar, was sucked with a vacuum pump under a filter element. The filter element was an underpressure chamber, whose top was the filter medium. The ultrasonic transducer was situated under the suspension vessel and under the filter media. In the electric field assisted filtration tests the cathode was the filter medium. The anode was aluminium with a spiral shape construction. The distance between the electrodes was 2 cm and during the experiments the

current was kept at 3 A by adjusting the voltage. Separated water was collected in the vessel over the balance, which was connected to the data acquisition system. The experiments were run and the filtration data was collected in the same way as in the smaller scale experiments described before. All the filtration experiments were started at room temperature (20 °C) and after the filtration the suspension maximum temperature was 30 °C, mainly due to the use of the electric field.

The bio/fiber suspension PILOT scale filtrations were batch operated experiments. Filtration circumstances were similar to the real process conditions of feed concentration, particle/fluid movements and sedimentation effect. The results achieved will describe electro-acoustic filtration in a batch operating filtration mode, simulating real process equipment and are a starting point to scale-up the method towards commercial equipment.

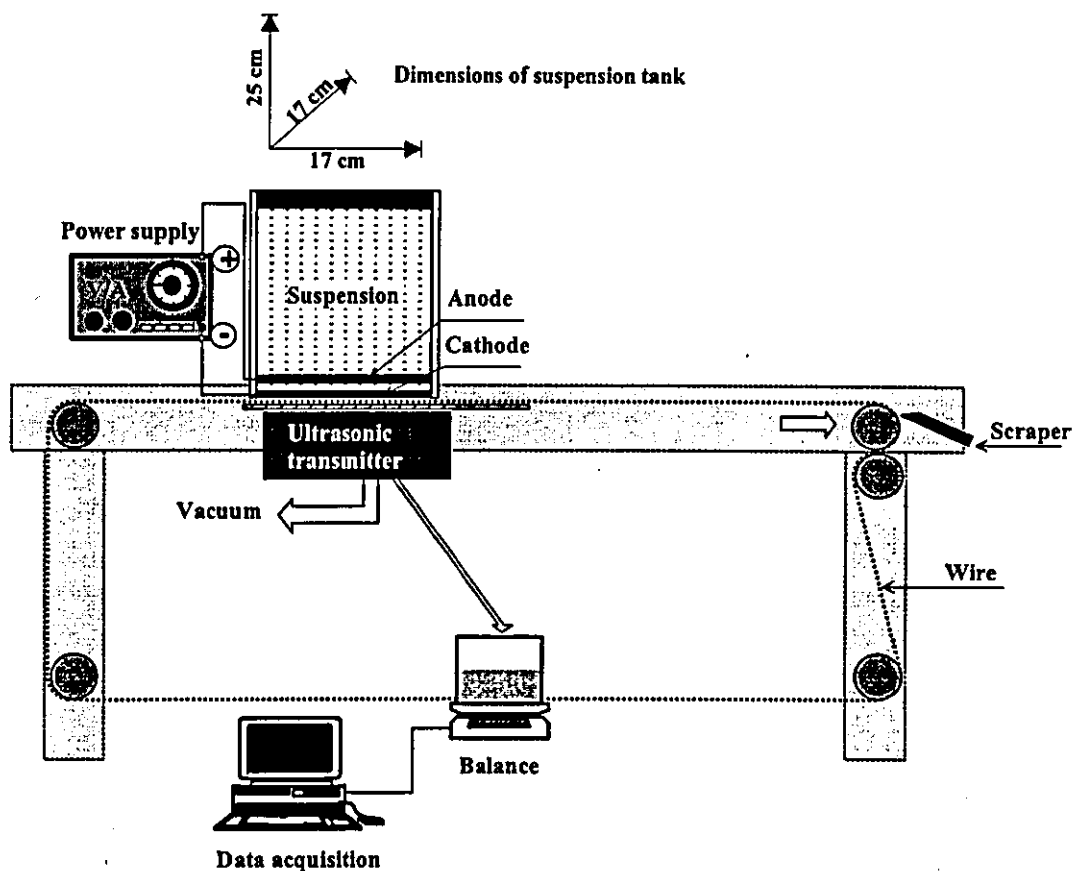


Figure 4.6. PILOT-scale underpressure filtration unit for bio/fiber suspension tests equipped with electro-acoustic accessories.

The Pilot scale filtration unit for pyrite and post-ferment phosphoric acid experiments is described in Figure 4.7. The rig was manufactured by Outokumpu Mintec Oy. The equipment was logic operated making all the same functions as the process-scale equipment, including suspension mixing in the suspension vessel. The operation was divided into four different sections; filtration, drying, cake scraping and filter plate cleaning. Ultrasonic transducers and electrodes were connected to the equipment at VTT Energy. The body of the unit was stainless steel. The ceramic plate was connected with an arm to the body. The arm was movable and the movements of the plate to a suspension tank (Stainless steel) and out of the tank were controlled by the control panel, so the filtration and drying times of the whole cycle were adjustable. Dimensions of the rectangular suspension tank were 40 x 40 x 53 cm and the volume ~ 85 l. The ceramic plates, area 0.015m² and pore size 1 µm, were connected by a tube straight to a filtrate bottle over the balance, which was connected to a vacuum pump. Before filtration experiments, vacuum was sucked first into the filtrate bottle. Vacuum was measured by vacuum meter. When the required vacuum level (- 0,90 bar) was reached, then the balance was tared and after that the valve in the filtrate tube was opened and the filtration started. The permeate was led through the filtrate tube to the filtrate bottle over the balance. The balance measured in real-time the mass of the water separated during the filtration experiment.

Using an ultrasound field to enhance the dewatering in these experiments, the transducer was connected to the other side of the filter plate. So in all experiments only one side of the plate was used for filtration, the other permeable side of the plate (transducer side) was blocked.

For electric field enhanced filtration experiments the cover box of the ultrasonic transducer was connected to the power supply to the earth potential (cathode) and the anode was placed in the suspension tank. The gap between both electrodes was 5 cm. During the filtration cycle the current was kept at the constant value of 5 A.

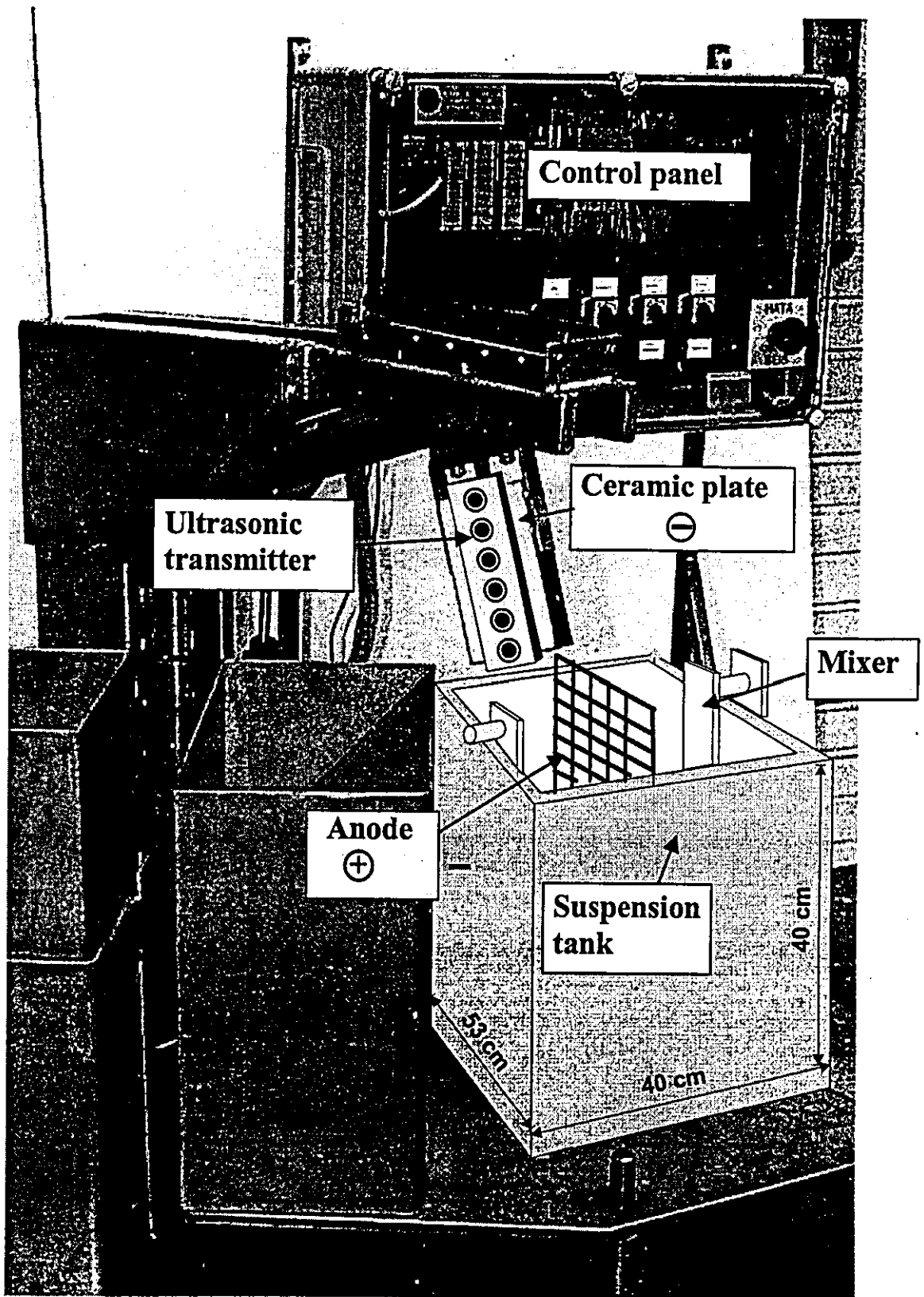


Figure 4.7. PILOT scale ceramic filtration unit equipped with electro-acoustic accessories.

All the experiments were started at 20 °C and after the experiments the suspension temperature was at a maximum 30 °C, measured by thermometer, mainly due to the use of the electric field.

5 FILTRATION - RESULTS AND DISCUSSION

5.1 Small-scale dewatering tests enhanced by an electric and/or ultrasonic field

The outline of the experimental small-scale apparatus is shown in Figure 4.1. The lower electrode was set at the bottom of a Perspex tube. Metallic wire was used as the lower electrode which was also the filter media itself, or wire was connected to filter media when made from other materials. The upper electrode was set up in contact with the surface of the suspension. This electrode was made of a perforated steel plate with hole diameter of 1 mm in order to remove the small volume of gas produced by electrolysis. As the height of the surface of the suspension decreased with the dewatering of suspension, the position of the upper electrode was always adjusted so as to contact with the upper surface of the suspension. In these experiments the suspension was not compressed by the upper electrode. The polarity of both electrodes was determined in consideration of the polarity of δ -potential of the particles. The voltage applied to the suspension was adjusted by the power supply. The amount of the filtrate was measured by the balance connected to the PC giving real time information of the dewatering experiment.

Small-scale static filtration tests enhanced by an electric and/or ultrasonic field were carried out with bio/fiber suspension (40 m-% biosludge and 60 m-% fiber suspension), pyrite suspension and post-feculent phosphoric acid. Before starting the experiments the initial D.S. contents of these three suspensions were determined using an oven to dry the sample totally. In the beginning of the experiment a desired amount of suspension was measured by a balance. Before starting the dewatering experiment, dewatering parameters (dewatering time, time to use ultrasound and/or electric field during the dewatering) were set by the computer. Also, the program for the balance (starting time, data collection sequence after every second and calculation of a D.S. content (based on suspensions D.S. content in the beginning of the experiment) of a cake) during

the dewatering was started by the computer. The real time information gathering was switched on at the same time as the dewatering experiment was started. When the dewatering of the suspension ended, the experiment was stopped and the information measured by the PC was saved to disk for later analysis. Also, a sample was taken from the filter cake to measure the final D.S. content of the cake. This was done using an oven to dry the sample totally. The result of the real time information (D.S. content) and the result after oven drying were compared and if the difference between these values were more than 1 % D.S., the experiment was repeated.

Curves showing the dewatering results were drawn by an Excel-programme with a PC. In the figures the curves have been fitted to go through every measurement point. After the experiments the dewatering capacity was calculated based on the information obtained from the experiment; namely mass of filtrate (kg), mass of filter cake (kg), area of filter medium (m^2) and filtration time (h). When ultrasound was used to enhance the filtration, the input power of the transducer (W) and the time of the operation (h) were measured. During filtration experiments enhanced by an electric field the operating values connected to the use of electric field, voltage (V) and current (I), distance between electrodes (cm) and time of operation (h) were also measured. The enhancement of the electro-acoustic dewatering capacity was compared to the reference (no electro-acoustic field) dewatering using in calculations the value of 90% of the maximum capacity value from the corresponding results. On the basis of these small-scale dewatering tests, energy consumptions associated with the various means of enhancement were calculated.

For the filtration experiments the suspension samples had to be conserved for a long period in a cool room and also later on if there was a need to pick up more samples. Particle distribution measurements and electrical properties of the suspensions (electrophoretic mobility and zeta-potential) were measured. When a new suspension sample for the experiments was taken from the cool room, the

above mentioned properties were measured to ensure that the sample was similar to the original one. Other analyses (surface tension, acoustic impedance, density and viscosity presented in Chapter 3) were measured to give more information about the suspensions, especially compared to the corresponding properties of water. With bio/fiber suspension, also the measured and calculated values of the rate of the electrophoresis were compared (Table 3.4). For the calculations of these values measurements the zeta-potential and the viscosity of the fluid were also needed, results presented in Chapter 3.

One of the aims with the small-scale experiments were to show the enhancement of the electro-acoustic method of dewatering, to optimise the use of the acoustic and the electric field in the miniPILOT-scale.

5.1.1 Bio/fiber suspension

In the small-scale filtration tests of the 1.5 m-% bio/fiber suspension it was found that the best enhancement of the filtration has been reach by using electric field of 30 V/cm as a pre-treatment 15 minutes. The quantity of filtrate obtained using this electric field was increased 20-fold and the speed of filtration increased 9.5-fold compared to vacuum (20 kPa negative pressure) filtration without an electric field, Figure 5.1. Electric field pre-treatment brought the bio/fiber suspension into two different “phases”, clear water and consistency solid matter, as earlier described in Chapter 3. In this case it could be avoid filter media blocking during the dewatering a longer period and to separate a larger amount of water from the suspension also with a higher separation (filtration) speed. Energy consumption for this means of improving efficiency was 0.024 kWh/kg of filtrate. In ultrasound filtration tests conducted with the bio/fiber suspension the best improvement was achieved when gravitational filtration of a 1 m-% bio/fiber suspension was subjected to a sonic field of 11.3 kHz and 100 W input power. In this case the quantity of filtrate was increased 7.5-fold and the speed of filtration increased 18-fold compared to the reference filtration and the energy consumption 0.001 kWh kg⁻¹ of filtrate, Figure 5.2. In this case a sonic field

moved particles out of the surface of the filter media and even increased the speed of filtration but did not keep the filter media unblocked during the dewatering as long as in the case of using an electric field as a pre-treatment. When the gravitational filtration of 1 m-% bio/fiber suspension was boosted using both an electric field and ultrasound a 7.1-fold quantity of filtrate and 7.3-fold rate of dewatering were obtained. In this case the energy consumption was 0.019 kWh kg⁻¹ of filtrate.

In the small-scale filtration experiments enhanced by ultrasonic field the efficiency of the transducer was so poor that all these experiments were effectively by gravitational filtration. If vacuum was used, forces connected to Δp overcame all the acoustical forces produced by the transducer. So it was impossible to obtain any enhancements of ultrasonically enhanced filtration experiments using vacuum. In the further experiments at the bigger scales it was necessary to get better ultrasonic transducers (higher output power and efficiency) for the experiments.

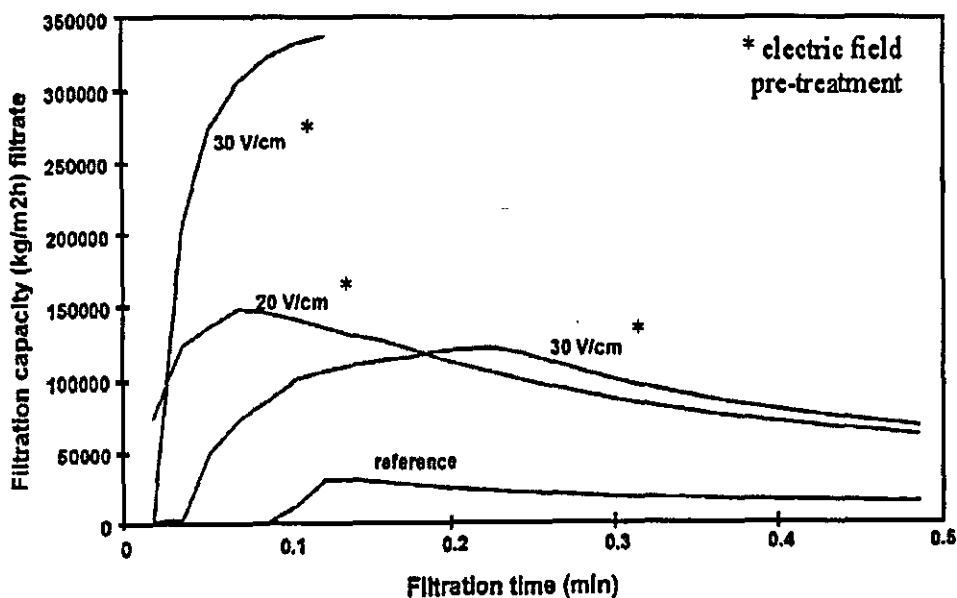


Figure 5.1. Effects of an electric field on the filtration of bio/fiber suspension of 1.5 m-% with an underpressure of 20 kPa.

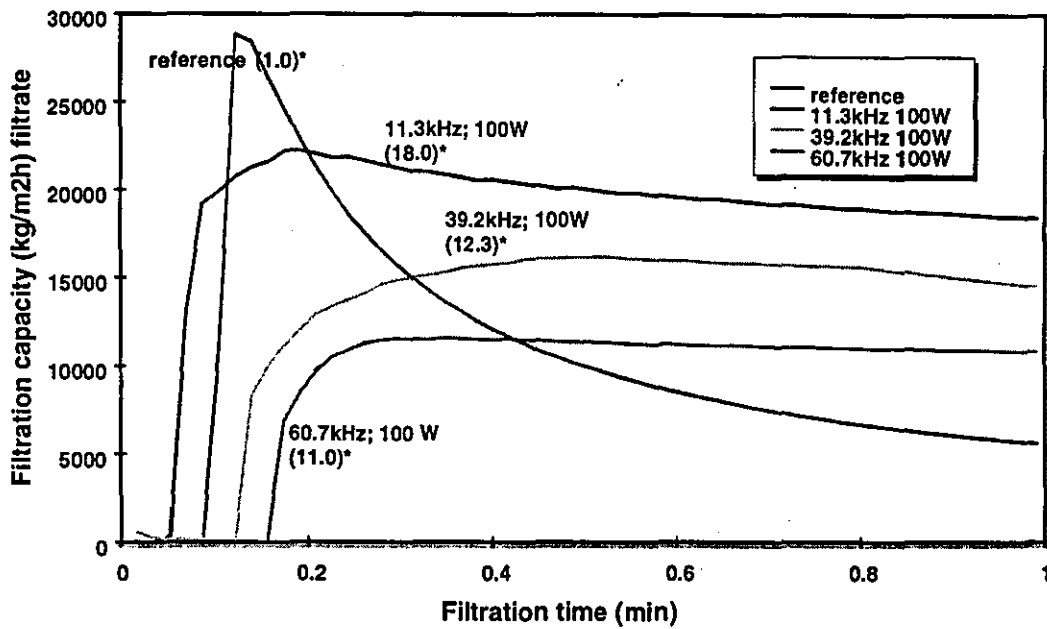


Figure 5.2. Effects of an ultrasonic field on the filtration of bio/fiber suspension of 1 m-% with gravitation.

For the best dewatering result using electric field (30 Vcm^{-1}) as a pre-treatment (Figure 5.1.), a plot of t/V was drawn vs. V figure, where t is the dewatering time (s) and V (m^3) is the volume of filtrate. From Figure 5.3. cake resistance and filter medium resistance were calculated. Cake resistance is obtained from a value of the slope of the straight line passing through the measurement points. The filter medium resistance is calculated from the value of the intersection of the t/V -axis.

The calculated resistance values based on the Figure 5.3 are the following; cake resistance (slope of the curve) 1.2×10^9 (m kg^{-1}) and filter media resistance (intersection of the t/V -axis) 3.5×10^8 (m^{-1}). For the reference dewatering (no electric field) the calculated cake resistance was 8.1×10^{11} (m kg^{-1}). From the results it might be concluded that electric field caused particle agglomeration in a suspension and the filter cake was more porous than in the reference case.

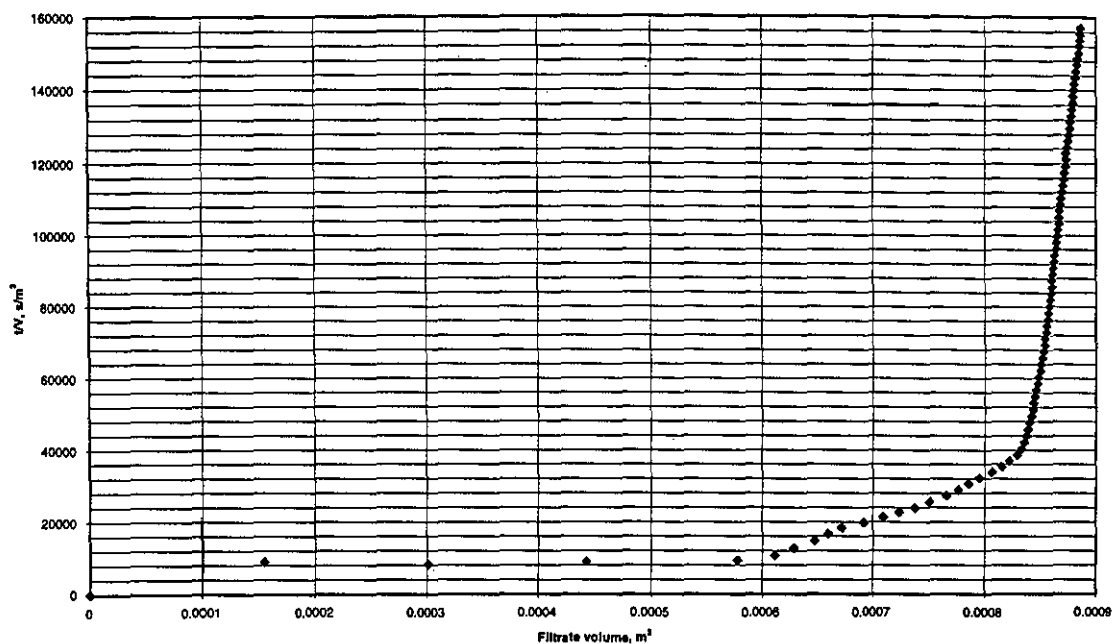


Figure 5.3. t/V vs. V plot for bio/fiber suspension dewatering using electric field ($30 Vcm^{-1}$) as a pre-treatment to calculate cake and filter media resistances.

Similar cake and filter medium resistance calculations were also done based on the results described in the Figure 5.2. For the best dewatering result, 11.3 kHz sonic field to enhance dewatering, the calculated resistance values were the following; cake resistance 2.0×10^7 ($m kg^{-1}$) and filter media resistance 2.1×10^8 (m^{-1}). In the reference filtration, no sonic field, the cake resistance was 7.7×10^9 ($m kg^{-1}$). Cake resistance in both experiments were 2 orders of magnitude less than the similar values in the experiments where electric field was used as a pre-treatment method to enhance the dewatering. This is due to the difference of these experiments, electric field enhanced dewatering experiments were based on underpressure and sonic field enhanced dewatering experiments were based on gravitation. Also electric and sonic fields have to have different effects to the particles in the suspension and at the final stage also different kind of effects to the structure of the dewatering cake. This conclusion is based on the information described the effects of electric and (ultra)sonic fields in suspensions and in connection to dewatering, explained more detailed in Chapters 2 and 3. These results support the observations done during the experiments. Using a sonic field

to enhance dewatering, in the beginning of the filtration cycle the sonic field prevented cake formation.

5.1.2 Post-feculent phosphoric acid

In the experiments to enhance the filtration of post-feculent phosphoric acid with an ultrasonic field, the following frequencies were tried; 16, 33 and 53 kHz all with the same input power of 100 W, Table 5.1. A 16 kHz frequency and 100 W input power was the best of the combinations in the terms of filtrate mass investigated in the small-scale static filtration tests enhanced by an ultrasonic field for post-feculent phosphoric acid. This was one of the main aims of the enduser, to get as much as possible enough clean (D.S. content < 0.5 m-% in filtrate) phosphoric acid from the post-feculent phosphoric acid using deliquoring. With the assistance of sound field the quantity of filtrate obtained by means of gravitational filtration was increased 6.9-fold and the relative rate of deliquoring increased by 5.9-fold compared to the reference filtration. The energy consumption of this efficiency boost was 0.008 kWh/kg of filtrate. The solid matter content of the sample suspension in the tests was 8 m-%.

Table 5.1 The effect of different ultrasonic frequencies and input powers to the filtration of post-feculent phosphoric acid.

Measured parameters	Gavitational filtration	33kHz/100W	53kHz/100W	16kHz/100W	16kHz/125W
Filtration rate (kg min ⁻¹)	0.017	0.169	0.025	0.097	0.126
Filtrate (kg)	0.085	0.162	0.556	0.586	0.212
Relative filtration rate	1.0	10.2	1.5	5.9	7.6
Relative mass of filtrate	1.0	1.9	6.5	6.9	2.5
Energy consumption/ kg separated fluid	0.000	0.020	0.003	0.008	0.010

Particle size distribution measurements in Table (3.1) give the mean particle size value for post-feculent phosphoric acid as 24 to 27 μm . Based on the particle entrainment factors, η_p in Figures 3.16 and 3.17 shows that with lower frequencies (16 kHz) the particle entrainment of sonic field is remarkably better than with higher frequencies (53 kHz). Also in these experiments with the lower frequencies it was more efficient at keeping the filter medium open than was the case with the higher frequencies. Also, with the lower frequencies the vibration amplitude is greater than with higher frequencies and thus the ultrasonic power in the suspension is greater and the effects more powerful.

5.1.3 Pyrite suspension

Gravitational small-scale filtration of the pyrite suspension was most efficient at a power of 125 W (input) and a frequency of 16 kHz, filtration speed of 3 m-% pyrite suspension was improved 23-folds. The effect was similar to the experiments with post-feculent phosphoric acid. During ultrasonic enhancement the energy fed to the suspension was 0.008 kWh/kg of filtrate when employing a sonic field of 52 kHz and 100 W (input) and 0.002 kWh/kg of filtrate when using a sonic field of 16 kHz and 125 W input, Figure 5.4.

Cake and filter medium resistance values for pyrite suspension were based on an experiment where filtration was enhanced by a sonic field 16 kHz and input power 50 W. The resistance values as were follows; cake resistance 2.0×10^7 (m kg^{-1}) and filter media resistance 2.5×10^8 (m^{-1}). Cake resistance for the reference dewatering, no sonic field, was 2.3×10^{10} (m kg^{-1}). The experiment with lower input power could be described better by the t/V plot and the actual values of resistance were then calculable.

Ultrasound and electric fields had significant influence both on the speed of dewatering/deliquoring and the quantity of fluid removed. From the experiments it was clearly apparent that during filtration ultrasound can be employed to keep the filter medium (e.g. nylon cloth, ceramic plate, woven wirecloth) open. Using

an electric field the bio/fiber suspension can be brought into two different "phases", solid matter and water. In this case the second of these "phases", the water, can be removed easily and quickly through the filter medium. When enhancing filtration by means of ultrasound in the case of the ceramic plate, many difficulties were encountered with the pyrite suspension and post-feculent phosphoric acid during the tests. Either the ultrasonic transmitters used were too weak in terms of power (general transmitters, efficiency 30%) to generate sufficient movement of the particles in the pyrite suspension or the ceramic plate was unsuitable for filtration tests involving post-feculent phosphoric acid.

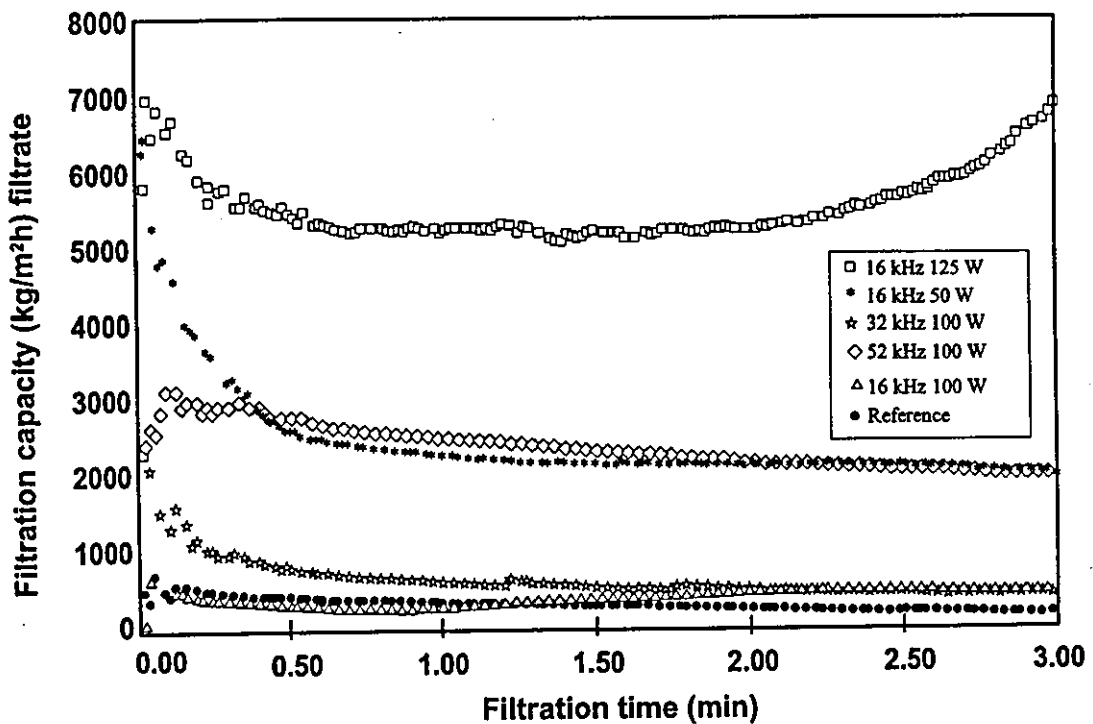


Figure 5.4. Effects of an ultrasonic field on the filtration of pyrite suspension of 3.0 m-% with gravitation.

In all small-scale dewatering experiments using a sonic field to enhance dewatering, lower frequencies of 11.3 kHz for bio/fiber suspension and of 16 kHz for pyrite and post-feculent phosphoric acid suspensions produced the best results. In these experiments the sonic field kept the filter media open most effectively. These results are fully supported by the theoretical examinations presented in Section 3.6.2. Particles with diameter greater than $20 \mu\text{m}$ (d_p average

for bio/fiber about 55 μ m, pyrite about 60 μ m and post-feculent phosphoric acid about 27 μ m) have a higher entrainment factor ζ_p in the sonic field than in the ultrasonic field. Maximum, minimum and mean size values of particles measured by different methods are presented in Table 3.1 in the Chapter 3.1.

In the small-scale experiments using electric field to enhance filtration the results were very promising. Electrical effects (particle movement, agglomeration) are quite slow compared to the normal dewatering time of 30 to 60 seconds. The best dewatering result was achieved using an electric field, 30 V cm⁻¹ as a pre-treatment method. But the pre-treatment time of 15 minutes seemed to be too long for normal applications. So the next aim for the larger scale experiments was to develop electrode material and electrode geometry and overall to enhance the use of electric field and markedly decrease the time needed for pre-treatment.

The results achieved in enhancing dewatering by electric or ultra(sonic) field were similar, showing the same kind of tendency as ultrasonic- and electric fields published in the literature e.g. references /3/, /10/, /11/ and /36/.

The calculated values of cake resistance and filter media resistance in the experiments of bio/fiber and pyrite suspensions showed that electric or sonic fields created more porous filter cakes than in the reference experiments without electric or sonic fields. Using an electric field or a sonic field to enhance bio/fiber suspension, in both cases the values of cake resistance was approximately 2 decades smaller than in the reference filtration. Using a sonic field to enhance pyrite suspension dewatering, the value of the cake resistance was approximately 3 decades smaller than in the reference case.

The values of cake and filter media resistance for post-feculent phosphoric acid were determined using PILOT scale experiments. Before these experiments the final filter media BEKIPOR ST3AL3SS was not absolutely determined and also the electrode material and configuration needed some verifications. The values of

cake and filter media resistance were as follows; cake resistance 2.1×10^{10} (m kg^{-1} , with electric field), 1.5×10^9 (m kg^{-1} , with ultrasonic field) and 2.0×10^{11} (m kg^{-1} , reference without additional force fields). The filter medium resistance value for BEKIPOR ST3AL3SS (used in all these experiments) was 9.77×10^9 (m^{-1}). From the results it can be seen that the value of cake resistance is smallest when ultrasonic field is used to enhance dewatering. In the experiment for electric field dewatering the cake resistance is approximately 1 decade greater than in the ultrasonic field dewatering.

5.2 MiniPILOT-scale dewatering tests enhanced by an electric and/or ultrasonic field

The miniPILOT experiments were mainly carried out to test different kinds of available sonic transducers for the PILOT scale experiments. The best dewatering results are presented here and also the achieved data from the experiments for (ultra)sonic transducer positioning was taken to account in the design work of PILOT scale apparatuses.

5.2.1 Bio/fiber suspension

When a 1 m-% bio/fiber suspension was pre-treated before a miniPilot filtration for 15 minutes with a 30 V cm^{-1} electric field, volume of filtration was improved almost 4-fold. The main mechanism responsible for this enhancement was pre-treatment by electroflotation as a result of which the solid matter was collected to the anode and the fluid was below the solid matter layer. Also, based on Table 3.4, electroflotation has a major effect on particle movements. Electrophoresis also occurs using an electric field in a suspension but, for example, in these experiments the movement of gas bubbles are faster than the movements of particles. The gas bubbles produced catch fibers and small particles as they move upwards, and by that way they have the main effect to bring the bio/fiber suspension into two "phases".

During the miniPilot-scale filtration tests of the 2.0 m-% bio/fiber suspension enhanced by sonic field, at a frequency of 16.3 - 17.1 kHz, the boost in filtration capacity was at best 12.3-fold (0.15 bar negative pressure, filter medium woven wirecloth with pore size 2 mm). Under the conditions limited by the power of the (ultra)sonic transmitter it was possible to keep the filter medium open by means of the sonic field or to open a filter medium clogged by solid matter, and thus to enhance filtration significantly. In the equipment construction used it was observed that the optimal enhancement occurred when the sonic field was supplied from directly in front of the filter medium. Ultrasonic filtration of the electrically pre-treated suspension weakened filtration, because in the electric field the small particles join together to form large flocs, which the ultrasound breaks up. The flocs move more weakly in the ultrasonic field than the individual small particles.

5.2.2 Post-feculent phosphoric acid suspension

For the miniPilot filtration of phosphoric acid a sonic frequency of 16.5 kHz, input power 100 W and negative pressure of 0.9 bar were used. It was noticed that the sonic field kept the filter medium open and improved filtration 2.1-fold when the field was directed at the filter medium from straight in front. Enhancement of the filtration of phosphoric acid in an electric field is based on electro-osmosis and electrophoresis, observation done visually. Gas bubbles generated during electric treatment also kept the filter medium open by breaking up the cake that was forming. Electric filtration capacity was 3-fold compared to the reference filtration. Joint use of electric and ultrasonic fields boosted filtration as much as 8-fold. This result was influenced by the positive combined effects of the above-mentioned fields during filtration. The electrophoresis and electro-osmosis caused by the electric field and the ability of the ultrasonic field to move particles kept the filter medium open and possibly caused a change in the viscous characteristics of the fluid (a decrease of the dynamic viscosity).

5.2.3 Pyrite suspension

In the miniPILOT-scale the best improvement in filtration capacity of 3 m-% pyrite suspension was 19-fold when the negative pressure was 15 kPa and the oscillating frequency 16.2 - 17.3 kHz. It was possible to demonstrate experimentally the ability of a sonic field to open an already clogged nylon cloth and keep it open. With the equipment construction used it was also observed in this case that the optimal transmitting direction was from directly in front with respect to the filtration medium, Figure 5.5.

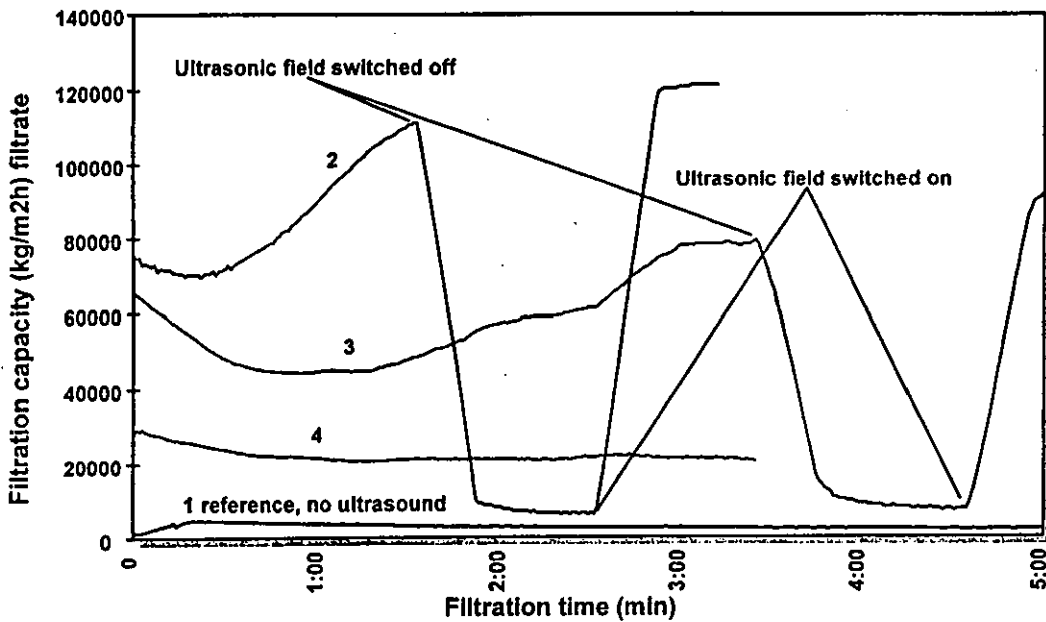


Figure 5.5. Effect of an ultrasonic field on the filtration of pyrite suspension of 3.0 w-% with an underpressure of 15 kPa. Ultrasonic field in front of filter media $I = 0.4 \text{ W cm}^{-2}$ (curve 2), behind $I = 0.2 \text{ W cm}^{-2}$ (curve 3) and from the side $I = 0.4 \text{ W cm}^{-2}$ (curve 4).

During filtration tests a variety of difficulties were encountered. The only possibility with the transmitter used was a situation in which the ultrasonic field was directed at the plate directly from behind and in such a manner that the plate was fixed in the transmitter coverbox. This in turn brought with it the problem of acoustic coupling between the plate and the transmitter. However, in ultrasound-enhanced filtration tests of a pyrite suspension at 6 m-% solid matter content,

negative pressure 15 kPa, it was possible to demonstrate the ability of ultrasound to open a plate already clogged in several successive cycles. The effect corresponded to that shown in Figure 5.5 .

The electric field significantly enhanced negative pressure miniPilot filtration ($\Delta p = 90$ kPa) of 78 m-% pyrite suspension. Electro-osmosis improves the movement of liquid droplets to the plate through the cake formed over the filter medium. After 10 filtration cycles (0.5 min. filtration in a suspension and 0.5 min. filtration in an air) the increased filtration capacity was 7-fold and the cake capacity 2-fold compared to a reference filtration.

For bio/fiber and pyrite suspensions, as well as for post-feculent phosphoric acid, filtration tests enhanced using electric and/or ultrasonic fields were carried out at miniPILOT scale. On the basis of these tests enhancement values for filtration capacity and specific energy consumption associated with the enhancement techniques were calculated, laboratory-scale PILOT filtration equipment was designed and operating parameters associated with the use of the electric and/or ultrasonic fields determined and energy consumptions calculated.

5.3 PILOT-scale dewatering tests enhanced by an electric and/or ultrasonic field

The filtration equipment manufacturers involved in the research project, Outokumpu Mintec Oy and Larox Oy, built PILOT scale rigs for use in this research based on the findings obtained at the two smaller scales. Electro-acoustic assessories were connected to the equipment at VTT Energy.

The aim of the experiments was to optimise the use of the acoustic/electric field in the PILOT-scale experiments and also to optimise the state of the suspensions for process-scale filtration enhanced by electro-acoustic force fields. The calculated enhancement values represent the average increase of the filtration capacity.

5.3.1 Bio/fiber suspension

In filtration tests involving enhancement of a bio/fiber suspension with an electric field different electrode materials were tried, aluminium and acid-proof plates or meshes. The gap between the anode and filter medium connected with the cathode was optimized, together with dry solid load over the filter medium and dry matter content of the suspension. Previously it had already been established that when filtering a bio/fiber suspension it is advisable to use only an electric field as a pre-treatment.

The best filtration result was achieved using an electric field as the pre-treatment for filtration in the following manner. Both electrodes were placed above the filtration medium (nylon cloth, 72-1134-L2 Tamfelt) with the cathode fixed to the cloth and the anode located at a distance of 2 cm from the cathode. For the anode a ringlike aluminium rod (rod diameter 1.3 cm) was used and for the cathode a stainless steel plate. The initial D.S. content of the suspension was 0.5 m-% in a ratio of 40 m-% biosludge and 60 m-% fiber sludge, pre-treatment time

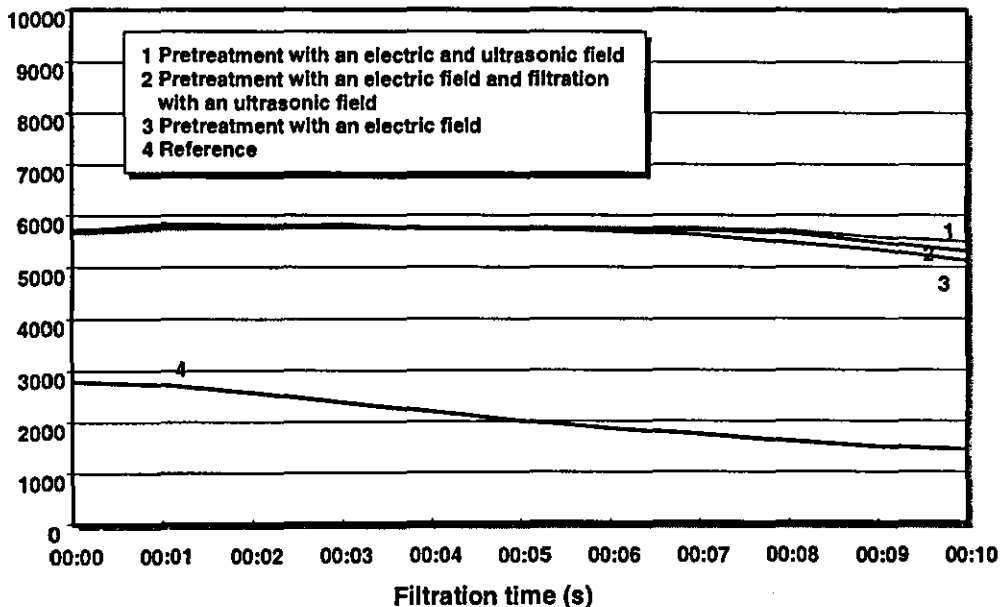


Figure 5.6. Effects of an electric, ultrasonic and combined fields on the filtration of bio/fiber suspension of 0.5 w-% with an underpressure of 90 kPa.

5 min., electric current constant 3 A, dry solid load 0.3 kg D.S. m⁻² and negative pressure 90 kPa. In this case the filtration capacity was increased approximately 4-fold compared to the reference filtration. From the filtration tests it was discernible that the cake formed well and detached easily from the cloth. The final dry matter content of the product was 23 m-%. Without electric pre-treatment, in the reference filtration the final dry matter content of the product was less than 2 m-%, Figure 5.6.

Ultrasound, with or without an electric field, did not further increase the amount of water separated during filtration or the speed of dewatering.

5.3.2 Pyrite suspension

In filtration tests conducted with pyrite suspension (78m-%) the best results were obtained when only ultrasound was used. After trying out a variety of locations for the transmitter it was established that the enhancing effect was greatest when the transmitter was situated behind the ceramic plate. The best driving parameters obtained were as follows: 15 s negative pressure filtration at 90 kPa, 15 s negative pressure filtration with 22 kHz ultrasound at 200 W power (input power) pulsed (0.5 s ultrasonic burst), 20 s filtration in an air with negative pressure. The use of continuous ultrasound for the whole duration of filtration clogged the plate. Compared to the reference filtration the cake capacity (kg D.S. m⁻² h⁻¹) in ultrasonic filtration was 4 times greater, the moisture content being 7 % while that of the reference cake was 14 %, Figures 5.7 and 5.8.

After numerous electric pre-treatment and filtration tests it was established that 30 s pre-treatment and 30 s electric filtration time were best. When the sludge was 78 m-% and the current and potential gradient of the DC electric field were 7 A and 11 V cm⁻¹ respectively the electric field filtration capacity (kg D.S m⁻² h¹)* was higher and the capacity* decreased slower than the reference filtration capacity*. After 15 filtration cycles (60 s cycle) the filtration capacity* was over 10-fold compared to the reference filtration. Unfortunately electric pre-treatment

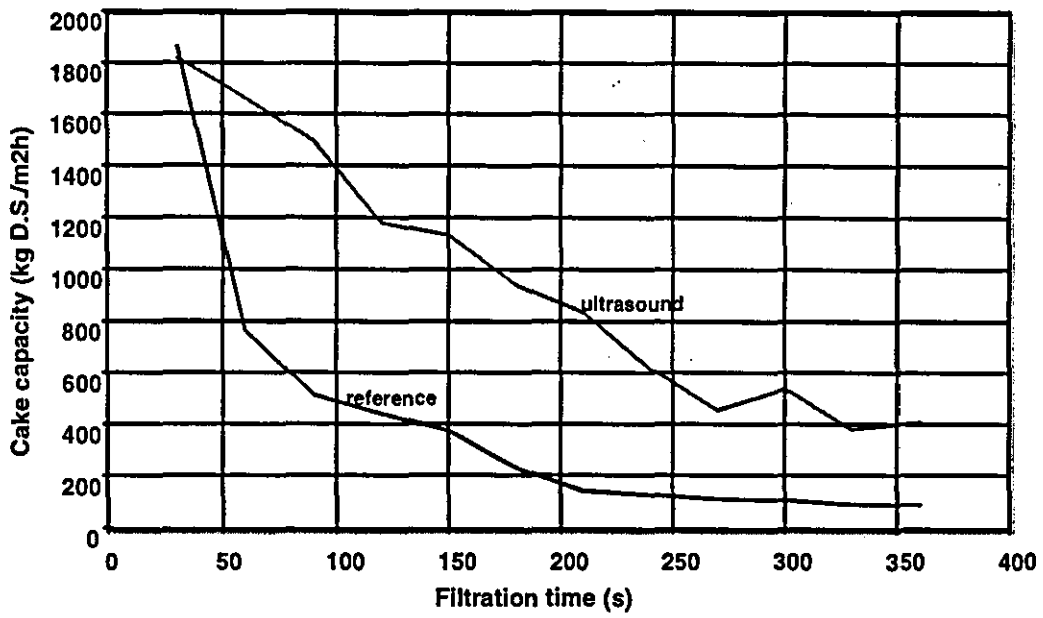


Figure 5.7. Effect of an ultrasonic field on the cake capacity of pyrite.

and filtration times added to a normal drying time (20 - 30 s) were too long to increase the total capacity* of the system enough compared to the ultrasonically enhanced filtration, and the cake capacity* was increased only 3-fold. Electric treatment also increased the cake capacity* of the pyrite to some extent. One factor limiting the increase in cake capacity* was the mixture in the sludge

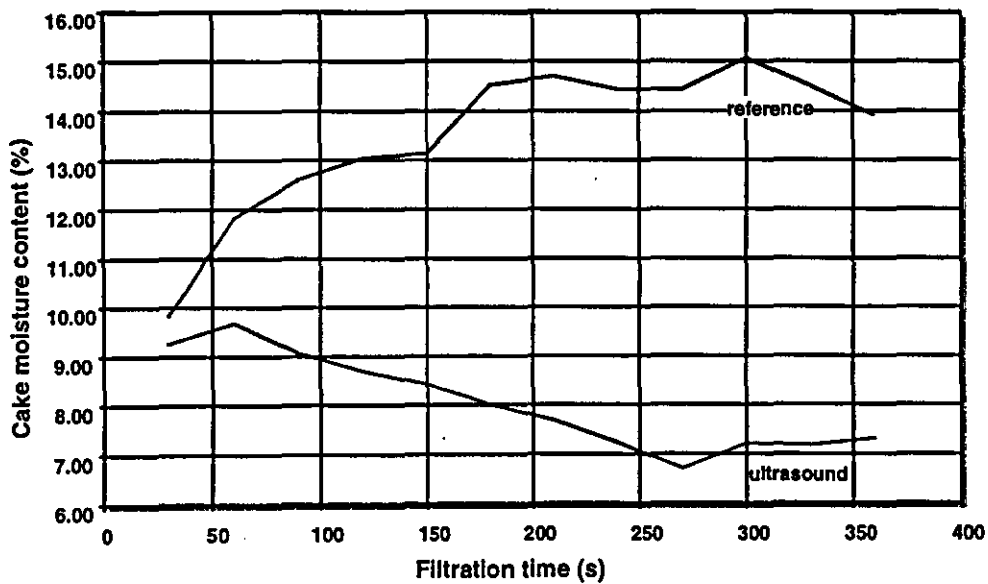


Figure 5.8. Effect of an ultrasonic field on the cake moisture content of pyrite.

vessel, which affected the movement of the particles more than the electric forces, even though according to preliminary particle size distribution measurements the average particle size (D_{50}) in the proximity of the plate became slightly bigger in the electric field. Combined use of ultrasonic and electric fields, under the same conditions than they were used separately, as filtration enhancements in this case even gave negative results.

5.3.3 Post-feculent phosphoric acid suspension

For post-feculent phosphoric acid a suitable filter material was found, BEKIPOR ST3AL3SS steel membrane (3 micron pore size, acid-proof steel). The dimensions of the filter plate were 21 x 7 cm, area ~ 0.015 m². This type of filtration medium does not dissolve under the influence of strong acid and the purity of the filtrate is clearly below the target value (solid matter content <0.5 m-%).

The best filtration results were obtained for phosphoric acid when combined use was made of ultrasound and an electric field. Almost as good results were achieved when using ultrasound alone. Combined use of these enhancement measures improved the filtration capacity 15-fold, use of ultrasound on its own more than 10-fold and of an electric field alone 2-fold, Figure 5.9.

For ultrasonic filtration of phosphoric acid two transmitters were used. Of the locations for the transmitters tried the best was found to be when one transmitter was placed on the back of the filter itself and the other directed straight at the filter 1.8 cm away (1/2-wave length of the pressure maximum). The other tried combinations were that both transmitters were either on the both sides of the filter medium or one transmitter above the filter medium and the other one below it. Both were 40 kHz transmitters and used to transmit continuous ultrasound at 400 W input power. The use of a lower frequency (16 kHz) transducer was neglected for the reason of noise in the hearing area. When the electric field was used (DC, 5.5 A, 5V) the steel anode was positioned between the transmitters.

The steel anode best enhanced the filtration capacity of phosphoric acid, but using this type of anode the acid also precipitated most. The reason for that is mainly due to Cr^{2+} dissolution and the temperature increases more than with other anodes. With the steel anode, the filtrate was greener than in other cases when the colour was brownish. The carbon anode and IrO-covered titanium anode were not much worse.

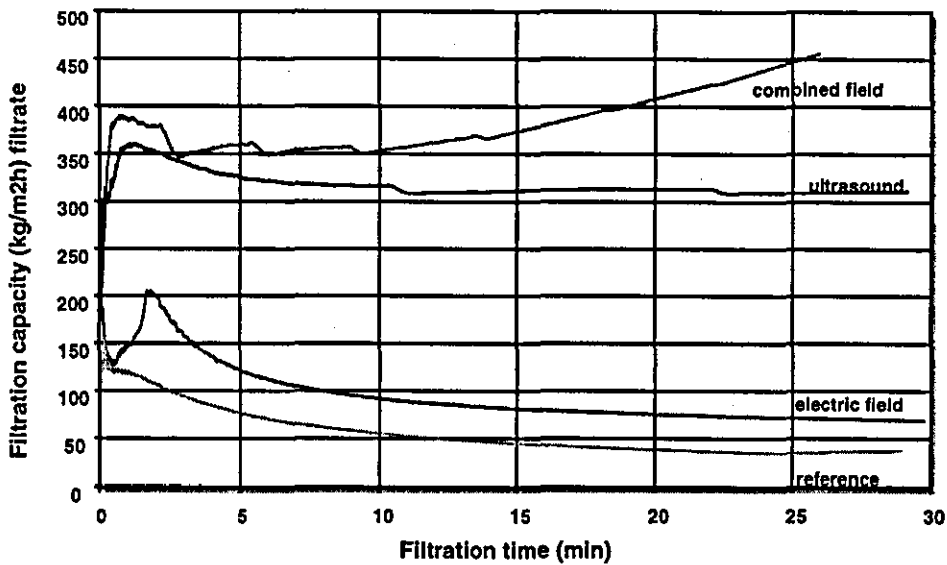


Figure 5.9. Effects of electric, ultrasonic and combined fields on the filtration of 3 m-% of phosphoric acid with post-deposit.

In the filtration tests involving a bio/fiber suspension enhanced with an electric field the best result was achieved using the electric field as pre-treatment in the following manner. Both electrodes were placed above the filtration medium (nylon cloth Tamfelt, 72-1134-L2) with the cathode fixed to the cloth and the anode located at a distance of 2 cm from the cathode. For the anode a ringlike aluminium rod was used and for the cathode a stainless steel plate. The pre-treatment time was 5 minutes, the electric current 3 A constant, and the negative pressure 90 kPa. The filtration capacity in this case was 4-fold compared to reference filtration. The final dry matter content of the product was 23 m-% and the solid matter content of the filtrate less than 0.1 m-%. In the reference case the final dry matter content of the product was only 2 m-%.

In filtration tests conducted with pyrite suspension the best results were obtained when ultrasound was used as follows: 15 s negative pressure filtration at 90 kPa, 15 s negative pressure filtration with a 22 kHz ultrasonic burst (0.5 s) and 20 s filtration in an air with negative pressure. The cake capacity was then 4 times greater than in the reference case, the moisture content being 7 % while that of the reference cake was 14 %. The aim value of the moisture content of the product was 6 - 7 %.

Use of the electric field in the filtration of a pyrite suspension, 78 m-%, gave the best results when employing a DC field of 7 A and 11 V cm⁻¹ for 30 s as pre-treatment and 30 s in connection with filtration. After 15 filtration cycles the filtration capacity was over 10-fold compared to the reference filtration. At best the improvement in cake capacity was 3-fold compared to the reference case. During the tests it could be clearly seen that mixing in the dipping tank disturbed the electrophoretic phenomenon and thus the formation of the cake. In future it will be most sensible to conduct electric field-enhanced filtration of a pyrite suspension in such a manner that mixing of the suspension takes place in a different tank to the one in which electric field-enhanced filtration occurs. In electrically enhanced filtration the plate thus stayed open better and became clogged significantly more slowly than in filtration without the electric field. Light ultrasonic cleaning (5 s, 16 kHz, 100 W input power) of a plate which had become clogged during electric filtration lifted the filtration capacity almost back to what it was originally.

For post-feculent phosphoric acid a suitable filter material has been found, BEKIPOR ST3AL3SS steel membrane. Using this the purity of the filtrate is clearly below the target value (solid matter content <0.5 %).

The best filtration results were obtained for phosphoric acid when combined use was made of ultrasound and the electric field. Combined use of these enhancement measures improved the filtration capacity 15-fold. Use of

ultrasound on its own increased the filtration capacity 10-fold and of the electric field by itself 2-fold.

For a bio/fiber suspension the best form of enhancement is use of the electric field as pre-treatment. This will not mean changes to the current conventional negative pressure filtration equipment itself. The pre-treatment unit is technically easy to add on to the current equipment, which further filters the suspension dewatered in the first phase led in from pre-treatment. Use of ultrasound in the filtration of a pyrite suspension still requires further development of the ultrasonic transmitters. For use in a practical set-up the ultrasonic transmitter needs to be made so thin that it can be fitted inside the ceramic plate. The second transmitter can be a rectangular and even oscillator of the current type. In the filtration of post-feculent phosphoric acid the highest capacity of filtration (filtrate volume) can be achieved with the filtration material discovered in the research to work well plus combined use of the electric and ultrasonic fields. In this case, too, the means of enhancement can be added to conventional methods of filtration by the same filter media and transducer set-up than in the pyrite filtration case.

PILOT scale dewatering results were very promising. All the results fully support the aim of the work; dewatering can be enhanced by electric and/or (ultra)sonic field(s). Previous published experimental work to enhance dewatering was based on batch or small-scale continuous dewatering experiments. But the results published in the literature (references /3/, /8/, /11/, /22/ and /29/) support the results presented here. The tendency and expectations seemed to be similar to the experimental results proved in this thesis; dewatering/filtration can be enhanced even remarkably using electric and/or acoustic force field(s). It was expected also, based on the information from the literature, that values of enhancement will decrease in the bigger scale compared to the smaller-scale experiments. The results presented in this thesis are a starting point for more R&D work which is needed towards commercial equipment with electro-acoustic accessories. The

main R&D work in the future should concentrate to develop output power and geometry of (ultra)sonic transducers to treat larger volumes of suspensions in process applications.

5.4. Energy consumptions of PILOT scale filtration

Energy consumptions of the PILOT scale filtrations with and without electric or ultrasonic field were calculated for all three suspensions used in the research. The energy consumptions are shown in Table 5.2, 5.3 and 5.4.

Table 5.2. Energy consumptions of bio/fiber suspension filtration

	Vacuum pump (kWh)	Electric field (kWh)	Total (kWh/kg separated water)
Vacuum filtration	0.040	-	0.027
Electric pre-treatment + vacuum filtration	0.006	0.044	0.034
Vacuum filtration + thermal drying *	0.040	-	0.197

* To reach same final D.S. content (23 m -%) than in electric pre-treatment experiment

Table 5.3. Energy consumptions of different filtration methods for pyrite suspension

	Vacuumpump (kWh)	Electric field (kWh)	Ultrasonic field (kWh)	Drying to 7% humidity (kWh)	Total (kWh kg ⁻¹ D.S.)
Electric pre- treatment and filtration	0.04	0.01	-	0.03	0.08
Vacuum filtration	0.18	-	-	0.05	0.23
Electric drying (surface anode)	0.02	0.002	-	0.03	0.05
Vacuum filtration	0.02	-	-	0.03	0.05
Ultrasonic filtration	0.03	-	0.0004	0.00	0.03
Reference	0.07	-	-	0.06	0.13

Table 5.4. Energy consumption of post-feculent phosphoric acid filtration

Filtration method	Energy consumption [kWh/kg filtrate]
Vacuum filtration	2.1
Electric filtration	1.1
Ultrasonic filtration	0.4
Ultrasonic- and electric field filtration	0.2

5.4.1 Energy consumption comparison between small- and PILOT scale experiments

PILOT scale experiments were done with the best set-ups found in earlier experiments. With bio/fiber suspension the best enhancement to filtration was found to be the use electric field as a pre-treatment. Pyrite suspension dewatering enhanced by ultrasonic field gave the highest dewatering capacity ($\text{kg D.S. m}^{-2} \text{ h}^{-1}$). Post-feculent phosphoric acid filtration enhanced by ultrasound or the combined electric- and ultrasonic fields, gave very good results in both cases but using combined fields the result was the best. It was even 50 % better than ultrasonic field alone. Energy consumptions of the best filtration set-ups in small- and PILOT scale for the used suspensions with electric and/or ultrasonic fields are shown in Table 5.5.

Table 5.5. Small- and PILOT-scale electro-acoustic filtration energy consumptions in the best filtration set-ups.

	Small / PILOT -scale	
Suspension	Energy consumption (kWh kg^{-1} filtrate) *(kWh kg^{-1} D.S.)	Enhancement (filtration volume)
Bio/Fiber	0.024 / 0.034	20 / 4 electric field
Pyrite*	0.008 / 0.030	23 / 4 ultrasonic field
Acid**	0.008 / 0.40	7 / 10 ultrasonic field

** For the acid the energy consumption was calculated only for the use of the ultrasonic field. The owner of the acid process believed that the use of the electric field will be impossible in their process conditions.

The results confirm what was anticipated. The energy consumptions are higher in the PILOT scale apparatus than in the small scale apparatus and enhancements of the filtration vice versa. With bio/fiber suspension, the energy consumption is nearly the same in both cases. This is due to the development of the electrodes during the research and also in the same time possibility to decrease the distance between the electrodes from 50 cm (small scale) to 2 cm (PILOT scale). Using ultrasound to enhance the filtration with pyrite and acid, the energy consumptions in the small-scale are the same because the ultrasonic field set-up was the same in the both cases. In the PILOT scale experiments the corresponding set-ups were different.

The enhancements of the filtrations were smaller in the PILOT scale than in the small scale with bio/fiber and pyrite suspensions but greater with acid suspension. This was due to the better ultrasonic field configuration in the PILOT scale than in the small scale. In the small scale it is always easier to get higher enhancements than in the PILOT scale. The volumes of the suspensions are smaller, higher ultrasonic intensities near filter media can be obtained, and particle movements are higher due to the scattering of the ultrasonic waves in the small-scale. But PILOT scale results are nearer the possible achieved enhancements in the process conditions, due to the filtration conditions and equipment dimensions being more similar compared to the process applications than in the case with the small scale experimental set-ups.

The results achieved in the PILOT scale experiments are very promising, and encourage continuation of the work towards real process solutions. The enhancements are remarkable, from 4 - 10- folds (even 15-folds with post-feculent phosphoric acid with combined field), and the total energy consumptions were only from 17 - 23 % from the reference (filtrations without electric and/or ultrasonic field) energy consumptions.

5.4.2 Connection of electro-acoustic method to filtration equipment

For bio/fiber suspension a possible electric pre-treatment unit before filter drum could be a tube-like electrical pre-treatment unit, Figure 5.10.

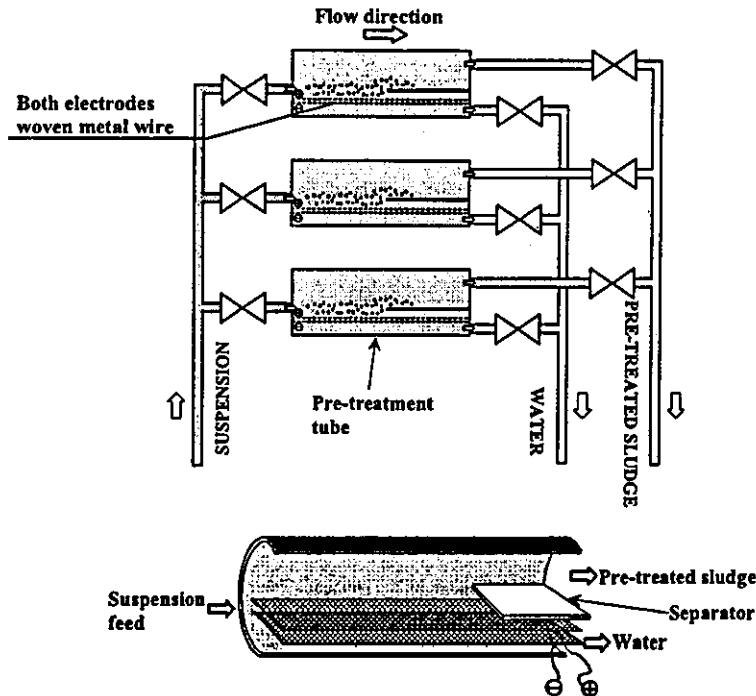


Figure 5.10. Electric pre-treatment of bio/fiber suspension in a tube.

In the Figure 5.12 the electric pre-treatment of bio/fiber suspension is based on the pre-treatment tube method. Untreated water is pumped into the tubes from the left hand side of the tubes. Both electrodes, anode and cathode, are situated at the bottom of the tubes. The distance between the electrodes is 2 cm. During the pre-treatment time inside the tube, 5 min., solid particles and fibers are led to the upper part of the tube by the electrophoresis and by the generated gas bubbles (electroflotation). Treated water is led out of the system from the right hand side of the system under the electrodes and concentrate is led out of the system also from the right hand side of the system from the upper part of the tube. This pre-treatment idea was established during the research work.

In the above case the treated water is normally so clear that it is ready to be taken out of the filtration plant. The concentrate is the suspension for later treatment

e.g. by vacuum drum filter or press filter. The idea in the tube method is that the pre-treatment happens in sequences, so that based on the speed of the vacuum drum there is always enough pre-treated concentrate to lead to the vacuum drum. So the capacity of the system determines the number of tubes needed. This pre-treatment unit can be very easily connected to the vacuum drum manufactured by Larox Oy.

For the filtration of pyrite or post-feculent phosphoric acid a new electro-acoustic ceramic plate (for pyrite) or metallic membrane plate (for acid) (the configuration of the plate is the same in both cases) has been designed during the research work, Figure 5.11. In this configuration piezo-ceramic crystals were glued to the metallic transmitter case. Filter medium (ceramic- or metallic membrane plate) was then glued or welded over the transmitter case. An electrode can be placed inside the ceramic plate or the transmitter case can be used as an electrode.

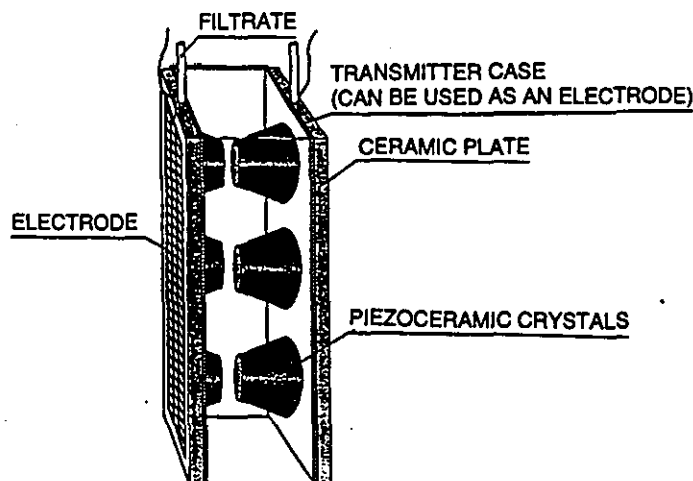


Figure 5.11. Electro-acoustic ceramic or metallic plate for vacuum filtration.

This kind of plate can be easily connected to the vacuum filtration equipment manufactured by Outokumpu Mintec Oy.

The clear filtrate is led out of the system from the filtrate tubes described in Figure 5.11, and concentrate is handled in the normal way (scraped out of the plant surface to the product store).

6 CONCLUSIONS

During the research initial inquiry was made into the interaction between the fluid and the particles in the (ultra)sonic field, the acoustic properties of suspensions were measured and the enhancing effect of (ultra)sound and the electric field during dewatering was also measured. Energy consumptions of the electro-acoustic method were measured and calculated. To conclude, initial dewatering tests involved the use of enhancement measures in some cases to affect consistency and pre-treatment, in others to keep the filter medium open, to significantly increase the dewatering speed and to raise the final dry matter content of the product. In general, however, acoustic enhancement as a process is fast and electric enhancement relatively slow, which gives some indication of their suitability in process concepts.

The mechanical effects of (ultra)sonic fields in suspensions are of relatively central importance when explaining the enhancement effects on solid/liquid separations. The chief concepts associated with the (ultra)sonic field are: radiation pressure, particle drift, acoustic agglomeration and cavitation.

The acoustic characteristics of sludges were determined in order to understand the behaviour of the suspension and give some indication of the power of the transmitters required. The (ultra)sonic speeds and pressure amplitudes at the transmitter's middle axis were determined for fiber suspensions of different thicknesses (up to 4.8 m-%), biosludge (up to 0.4 m-%), bio/fiber mixtures (up to 0.9 m-%) and a pyrite suspension (up to 84 m-%). On the basis of the measurements taken the "apparent" acoustic specific impedances of the suspensions were estimated.

Characteristics of suspensions associated with the enhancement effects of the electric and/or ultrasonic field: particle size distribution, surface tension,

electrophoretic mobility of the particles, pH and conductivity, density and viscosity were also determined.

Particle entrainment factors were calculated based on two different theoretical equations; combined Stoke's law and Newton's second law as well as the Basset-Boussinesq-Oseen equation (BBO). The BBO equation describes particle movements in an (ultra)sonic field with fluid as a medium better than Stoke's and Newton's combined laws. These equations are suitable for cases where the continuous phase is gaseous.

The filtration equipment manufacturers involved in the research project, Outokumpu Mintec Oy and Larox Oy, built PILOT set-ups for use in research. For test and equipment purposes (ultra)sonic transmitters were designed and built by the team itself as well as in co-operation with the Spanish research institute Consejo Superior Investigaciones/Instituto de Acustica. First prototypes of the transmitters were finished at the beginning of 1995, so research work using the transmitters could not be completed within the framework of the project under discussion here.

In filtration tests involving a range of suspensions and employing electric field enhancement various electrode materials and electrode geometries were tried and the gap between the electrodes optimised. The optimal conditions to use an (ultra)sonic field to enhance dewatering were established. These conditions were based on the properties of the transducers used in the experiments.

Overall the results were very promising. Using electric and/or (ultra)sonic field(s) to enhance dewatering, the dewatering capacity and filtration rate were increased several fold. The enhancement factor decreased from small scale experiments towards PILOT scale experiments, but was still for different suspensions from 4 to over 10 folds compared to the reference dewatering results. The total energy consumption were only from 17 – 23 % from the reference energy consumption.

The technology of how to connect electro-acoustic accessories to the existing equipment were described.

These experiments clearly showed the efficiency of the electro-acoustic method to enhance filtration. Basic information and the method of how to enhance dewatering with electric and/or (ultra)sonic field(s) were laid down. More R&D work is needed in the area of (ultra)sonic transducers. More powerful (output power) and more flexible transducers with alternative geometries are needed to treat larger volumes of suspensions in real industrial processes. Demonstration scale experiments should be the next step after the experiments done for this thesis. It is expected that after the next 4 or 5 years the first commercial dewatering equipment with electric and/or acoustic accessories to enhance dewatering will be in the market.

We summarise the main conclusions which should be taken into account when designing dewatering method enhanced by electric and/or acoustic force field(s). The acoustic enhancement process is fast, while the electric one is relatively slow. The main phenomena in electric field assisted dewatering are electrophoresis and electroflotation. In acoustic field assisted dewatering they are radiation pressure, particle drift, acoustic agglomeration and cavitation. To describe particle entrainment in an acoustic field, the BBO equation gives more appropriate results than Stoke's and Newton's second law combined, when particles are suspended. Stoke's and Newton's second law combined are suitable when the continuous phase is gas. In the electric field assisted dewatering normally the best enhancement will be reached by minimising the gap between an anode and a cathode. The enhancement factors which will be achieved in an assisted dewatering experiments in a small scale will decrease in a bigger scale experiments. Tailored (ultra)sonic transmitters for dewatering are not yet commercially available, so more R&D work in this area is needed. Anyway active R&D work for electro-acoustically enhanced dewatering has been done already several years in different experimental scales and a lot of know-how is

existing. The next challenge for R&D performers should be a demonstration phase to achieve commercial equipment for the market in a reasonable time.

7 REFERENCES

1. **T. Tuori, E. Järvelä**, Elektroakustiset Menetelmät Suodatuksessa, Vuorimiesyhdistyksen seminaari, Lappeenranta, 1992.
2. **R. J. Wakeman**, Filtration Post-Treatment Process, Elsevier Scientific Publishing Company, Netherlands, 1975.
3. **H. S. Muralidhara, N. Senepati, and R. B. Beard**, A Novel Electroacoustic Separation Process for Fine Particle Suspension, Advances in Solid-Liquid Separation, (Edited H.S. Muralidhara), Battelle Press, Columbus, USA, 1986.
4. **H.S. Muralidhara, D. Ensminger**, Acoustic Dewatering and Drying: State-of-the-Art Review, Proceedings IV, International Drying Technology Symposium, Kyoto, Japan, 1984.
5. **H.S. Muralidhara, N. Senepati**, A Novel Method of Dewatering Fine Particle Slurries, presented at International Fine Particle Society Conference, Orlando, Florida, USA, 1984.
6. **M. Robinson**, Early History of Electrodeposition and Deposition of Particles, in Dielectrophoretic and Electrophoretic Deposition, Electrochem. Soc., Pennington, New Jersey, USA, 1969.
7. **P. Krishnaswamy, P. Klinkowski**, Electrokinetics and Electrofiltration, Advances in Solid-Liquid Separation, (Edited H.S. Muralidhara), Battelle Press, Columbus, USA, 1986.
8. **H. Yukawa, K. Kobayashi, M. Iwata**, Studies of Electrically Enhanced Sedimentation, Filtration and Dewatering Process, Prog. Filtr. Sep., 1, 83-112, 1979.
9. **H. Yukawa, H. Yoshida, K. Kobayashi, M. Hakoda**, Electroosmotic Dewatering of Sludge under Condition of Constant Voltage, Journal of Chemical Engineering of Japan, 11(6), 475-480, 1978.
10. **R. J. Wakeman**, Effects of Solids Concentration and pH on Electrofiltration, Filtech Conference, 1981
11. **R. J. Wakeman**, Electrofiltration: Microfiltration plus Electrophoresis, The Chemical Engineer, June, 65-70, 1986.

12. **P. Zumbusch, W. Kulcke, G. Brunner**, Use of Alternating Electrical Fields as Anti-Fouling Strategy in Ultrafiltration of Biological Suspensions – Introduction of a New Experimental Procedure for Crossflow Filtration, *Journal of Membrane Science* 142, Published by Elsevier Science B.V., Amsterdam, 75-86, 1998.
13. **M. X. Porter**, Ultrafiltration, *Handbook of Industrial Membrane Technology* (Edited by M. C. Porter), Noyes, Park Ridge, NJ, USA, 1990.
14. **S. M. Finnigan, J. A. Howell**, The Effect of Pulsed Flow on UF Fluxes in a Baffled Tabular Membrane System, *Desalination* 79, 181-202, 1990.
15. **C. K. Lee, W.-G. Chang, Y.-H. Ju**, Air Slugs Entrapped Cross-flow Filtration of Bacterial Suspensions, *Biotech. Bioeng.* 41, 525-530, 1993.
16. **M. H. V. Mulder**, Polarization Phenomena and Membrane Fouling, *Membrane Separations Technology – Principles and Applications* (Edited by R. D. Noble, S. A. Stern), Elsevier, Amsterdam, 1995.
17. **G. Akay, R. J. Wakeman**, Electric Field Enhanced Crossflow Microfiltration of Hydrophobically Modified Water Soluble Polymers, *Journal of Membrane Science* 131, Published by Elsevier Science B.V., Amsterdam, 229-236, 1997.
18. **K. Okada, Y. Nagase, Y. Ohnishi, A. Nishihara, Y. Akagi**, Correlations of Filtration Flux Enhanced by Electric Fields in Crossflow Microfiltration, *Journal of Chemical Engineering of Japan*, 30(6), 1054-1058, 1997.
19. **J. Heikkinen**, Acoustically and Electrically Assisted Solid-Liquid Separation, Graduate School in Chemical Engineering – course Solid-Liquid Filtration and Separation Technology, Technical University of Lappeenranta, Finland, 1999.
20. **D. E. Ensminger**, Acoustic Dewatering, *Advances in Solid-Liquid Separation*, (Edited H.S. Muralidhara), Battelle Press, Columbus, USA, 1986.
21. **R. E. Beard, H. S. Muralidhara**, Mechanistic Considerations of Acoustic Dewatering Techniques, *Proceedings 1985 IEEE Ultrasonic Symposium*, 1072-1075, 1985.

22. **H. V. Fairbanks**, Use of Ultrasound to Increase Filtration Rate, Presented at the International Ultrasonic Conference, London, England, 1973.
23. **M. A. Grundy, K. Moore, W. T. Coakley**, Increased Sensitivity of Diagnostig Latex Agglutination Tests in an Ultrasonic Standing Wave Field, *J. Immunol. Methods*, 176, 169, 1994.
24. **R. Allman, W. T. Coakley**, Ultrasound Enhanced Phase Partion of Microorganisms, *Bioseparation*, 4, 29, 1994.
25. **O. Doblhoff-Dier, T. Gaida, H. Katinger, W. Burger, M. Gröschl, E. Benes**, A Novel Ultrasonic Resonance Field Device for the Retention of Animal Cells, *Biotechnol. Prog.*, 10, 428, 1994.
26. **S. Gupta, D. L. Feke, I. Manas-Zloczower**, Fractionation of Mixed Particulate Solids According to Compressibility Using Ultrasonic Standing Wave Fields, *Chem. Eng. Sci.*, 50, 3275, 1995.
27. **T. Gaida, O. Doblhoff-Dier, K. Strutzenberger, H. Katinger, W. Burger, M. Gröschl, B. Handl, E. Benes**, Selective Retention of Viable Cells in Ultrasonic Resonance Field Devices, *Biotechnol. Prog.*, 12, 73, 1996.
28. **S. T. Woodside, J. M. Piret, M. Grösschl, E. Benes, B. D. Bowen**, Acoustic Force Distribution in Resonators for Ultrasonic Particle Separation, *AIChE Journal*, 44(9), 1998.
29. **H. S. Muralidhara, D. Ensminger, A. Putman**, Acoustic Dewatering and Drying (Low and High Frequency): State of the Art Review, *Drying Technology*, 3(4), (529-566), 1985.
30. **W. Bongert**, U.S. Patent 3, 970,552, 1976.
31. **P. Furedi**, U.S. Patent 4,055,491, 1977.
32. **E. Kowalska, K. Chmura, J. Bien, J.**, *Ultrasonic*, 16, (183-185), 1978.
33. **S. T. Woodside, B. D. Bowen, J. M. Piret**, Measurement of Ultrasonic Forces for Particle-Liquid separations, *AIChE Journal*, 43(7), 1997.
34. **S. P. Chauhan, H. S. Muralidhara, N. S. Senapati**, A Technical Note on Electroacoustic Dewatering (EAD), Battelle-Columbus Division, Columbus, OH, USA, 1986.

35. **N. Senapati**, Ultrasonic Interactions during Sludge Dewatering, Solid/Liquid Separation: Waste Management and Productivity Enhancement (Edited by H. S. Muralidhara), Battelle Press, Columbus, USA, 1989.
36. **H. S. Muralidhara, S. P. Chauhan, N. Senapati, R. Beard, B. Jirjis, B. C. Kim**, Electro-Acoustic Dewatering (EAD) A Novel Approach for Food Processing, and Recovery, Separation Science and Technology, 23, 12&13, 2143-2158, 1988.
37. **H. Yukawa, H. Yoshida, K. Kobayashi, M. Hakoda**, Fundamental Study on Electroosmotic Dewatering of Sludge at Constant Electric Current, Journal of Chemical Engineering of Japan, 9(5), 402-407, 1976.
38. **S. P. Chauhan, H. W. Johnson**, Scale-Up of Electroacoustic Dewatering of Sewage Sludges, Solid/Liquid Separation, Waste Management and Productivity Enhancement, (Edited H.S. Muralidhara), Battelle Press, Columbus 1989.
39. **H. Yukawa, H. Yoshida, K. Kabayashi, M. Hakoda**, Electro-osmotic Dewatering of Sludge under Conditions of Constant Voltage, J. Chem. Eng. Japan, 11(6), 475-480, 1978.
40. **D. J. Shaw**, Introduction to Colloid and Surface Chemistry, 3rd ed., Butterworths, 1989.
41. **E. S. Tarleton, R. J. Wakeman**, Electro-Acoustic Crossflow Microfiltration, Filtration & Separation, 29(5), 425-432, 1992.
42. **P. W. Atkins**, Physical Chemistry, 2nd ed., Oxford University Press, Butler & Tanner Ltd, UK, 1982.
43. **P. J. Antikainen**, Yleinen ja Epäorgaaninen kemia, Werner Söderström Osakeyhtiö, Porvoo, 1980.
44. **P. McFadyen**, Electrophoretic mobility and zeta potential of colloidal particles, Reprinted from International Laboratory, England, 1986.
45. **E. S. Tarleton, R. J. Wakeman**, Microfiltration Enhancement by Electrical and Ultrasonic Force Fields, Filtration & Separation, 27(3), 192-194, 1990.
46. **T. Tuori, P. Martikainen, E. Järvelä**, Enhancement of Bio/Fiber Sludge Filtration by Electro-Acoustic Method, Proc. 6th World Filtration Congress, Nagoya Japan, 206-210, 1993.

47. **A. Shoh**, Industrial Applications of Ultrasound, Ultrasound, Its Chemical, Physical and Biological Effects, (Edited K.S. Suslick), VHC Publishers Inc., New York, 97-122, 1988.
48. **D. J. Bell, P. Dunnill**, Mechanisms for the Acoustic Conditioning of Protein Precipitates to Improve their Separation by Centrifugation, *Biotech. Bioeng.*, 26(7), 691-698, 1984.
49. **E. A. Hiedemann**, Basic Principles of the Application of Sonic and Ultrasonic Energy, *Ultrasonics*, Symposium Series No. 1, 47, 51-56,
50. **C. A. Stokes, J. E. Vivian**, Applications of Sonic Energy in the Process Industries, *Ultrasonics*, Symposium Series No. 1, 47, 11-21,
51. **H. W. St. Clair, M. C. Spendlove, E. V. Potter**, U.S. Bur. Mines Repts. Invest., 4218, 1948.
52. **S. Limin**, Modeling of Acoustic Agglomeration of Fine Aerosol Particles, Ph.D. Thesis, The Pennsylvania State University, 1990.
53. **H. C. Miao**, Aerosol Coagulation in an Acoustic Field, M. Sc. Thesis, The Pennsylvania State University, 1981.
54. **R. Tiwary**, Acoustic Agglomeration of Micron and Submicron Fly-ash Aerosols, Ph.D. Dissertation, The Pennsylvania State University, 1985.
55. **W. C. Hinds**, Aerosol Technology, Properties, Behavior, and Measurements of Airborne Particles, Wiley Inter-Science, 1982.
56. **E. P. Mednikov**, Acoustic Coagulation and Precipitation of Aerosols, Consultants Bureau, New York, 1965.
57. **G. B. Davies**, The Use of Ultrasonics in Beer Clarification, Proc. The 1994 ICHIME Research Event, London U.K., 541-543, 1994.
58. **D. T. Shaw, K. W. Tu**, Acoustic Particle Agglomeration Due to Hydrodynamic Interaction Between Monodisperse Aerosols, *J. Aerosol Sci.*, 10(3), 317-328, 1979.
59. **C. A. Bjerknes**, Hydrodynamische Frenkrafte, Leipzig, 1915.
60. **D. T. Shaw**, Acoustic Agglomeration of Aerosols, Recent Developments in Aerosol Science, Wiley Inter-Science, 279-319, 1978.

61. **S. D. Danolov, M. A. Mironov**, Radiation Pressure Force Acting on a Small Particle in a Sound Field, *Sov. Phys. Acoust.*, 30(4), 1984.
62. **N. L. Shirokova**, Aerosol Coagulation, *Physical Principles of Ultrasonic Technology*, Plenum, New York, 2, 477-541, 1973.
63. **S. V. Pshenai-Severin**, On the Convergence of Aerosol Particles In a Sound Under the Action of the Oseen Hydrodynamic Forces, *Dokl. Akad., Nauk SSSR*, 125(4), 775, 1959.
64. **V. I. Timoshenko**, Investigation of Interaction of Aerosol Particles in a Sound Field, *Sov. Phys. Acous.*, 11(2), 183, 1965.
65. **T. Tuori, P. Martikainen, E. Järvelä**, Suodatustekniikan Tehostaminen Elektroakustisin Menetelmin (Ultrasähkö), Valtion teknillisen tutkimuskeskuksen raportti, 1993.
66. **S. Temkin**, *Elements of Acoustics*, John Wiley & Sons, New York, 1981.
67. **A. Weissler**, *Physico-Chemical Effects of Ultrasonics*, *Ultrasonics*, Symposium Series No. 1, 47,
68. **A. A. Atchley, L. A. Crum**, *Acoustic Cavitation and Bubble Dynamics* (Edited K.S. Suslick), VHC Publishers Inc., New York, 1988.
69. **K. S. Suslick**, The Chemical Effects of Ultrasound, *Scientific American* Feb., 62-68, 1989.
70. **R. J. Wakeman & E. S. Tarleton**, An Experimental Study of Electro-acoustic Crossflow Microfiltration, *Trans IChemE*, 69, Part A, 386-397, 1991.
71. **T. Tuori, J. Heikkinen, R. J. Wakeman, J. A. Gallego-Juarez, E. R. F. de Sarabia, B. Ekberg, A. James**, Development of Deliquoring Method Enhanced by Electric and Acoustic Force Fields, *Brite-EuRam III 12 Months Periodic Progress Report*, 1997.
72. **O. B. Wilson**, *Introduction to Theory and Design of Sonar Transducers*, Peninsula Publishing, Los Altos, USA, 1988.
73. **C. P. Bowden, P. N. Whittington**, The Application of Novel Technologies to Biotechnological Primary Separation, *Bioseparation, State of the Art Report*, (SAR 6), 1985.

74. **B. Brown, J. E. Goodman**, Magnetostrictive and Piezo-electric Transducers in High Intensity Ultrasonics, Iliffe Books Ltd, 75, London, 1965.
75. **R. W. Samsel**, Physical and Economic Limitations in the Application of Sonic and Ultrasonic Energy to Industrial Processing, Ultrasonics, Symposium Series NO. 1, 47, 77-81,
76. **H. Sekki**, Ultraäänilähettimien Ominaisuuksien Kartoitus Neste/Kiintoainerotusta Varten (Ultrasähkö), Valtion teknillisen tutkimuskeskuksen raportti, 1992.
77. **P. N. T. Wells**, Physical Principles of Ultrasonic Diagnosis, Academic Press, London, 53-55, 1969.
78. **L. E. Kinsler, P. Frey**, Fundamentals of Acoustics, J. Wiley, New York, 166-177, 1962.
79. **G. L. Goberman**, Ultrasonics Theory and Application, English Universities Press, 29-34, 1968.
80. **N. E. Sherman**, Ultrasound Propagation in Colloidal Dispersions, Ph.D. Thesis, University of Cambridge, 1989.
81. Malvern 2600 Series Laser Diffraction Particle Sizer, Users Manual, Malvern Instruments, England, 1985.
82. Image Craft, Operators Manual, Princeton Gamma-Tech, USA, 1989.
83. Coulter® Delsa 440, Product Reference Manual, Coulter Electronics Inc., USA, 1988.
84. Haake Viscometers, Instruction Manual, Software VT500, Version 1.3, Germany, 1990.
85. **L. E. Kinsler, A. R. Frey, A. B. Coppens, J. V. Sanders**, Fundamentals of Acoustics, 3rd ed. John Wiley & Sons, New York, 1982.

8 NOMENCLATURE

A	- area, m^2
a	- radius of sphere, m
B	- $\sqrt{(\pi f \rho / \eta)}$, m^{-1}
B'	- permeability, m^2
C	- concentration of electrolytical solution, kg/m^3
C_v	- volume concentration of particles in fluid, kg/m^3
c	- sound velocity, m/s
d	- distance, m
d_n	- collision number, -
d_p	- diameter of particle, m
E	- strength of electric field, V/m
E_m	- elasticity coefficient of medium, -
e	- charge of electron = $1.60219 \cdot 10^{-19} C$
F	- force, N
f	- frequency, s^{-1}
h	- $2\pi/\lambda$, m^{-1}
I	- current, A
$I(0)$	- acoustic intensity at point $x=0$, W/m^2
$I(x)$	- acoustic intensity at a distance x , W/m^2
K	- compressibility of liquid, m^2/N
K_f	- bulk modulus of fluid, kg/ms^2
K_s	- bulk modulus of solid, kg/ms^2
K_{sys}	- system bulk modulus, kg/ms^2
K'	- compressibility of solid, m^2/kg
k	- Boltzmann's constant = $1.38066 \cdot 10^{-23} JK^{-1}$
k_s	- shape factor, -
k_0	- conductivity of electrolytical solution, $1/ohm m^3$
k_w	- wave number in the fluid, m^{-1}
L	- inertia coefficient, m

m_p	- mass of particle, kg
N_A	- Avogadro's constant = $6.022 \cdot 10^{23} \text{ mol}^{-1}$
n	- particle concentration number, -
n_v	- particle concentration number in the agglomeration volume, -
n_0	- ionic concentration, m^{-3}
p	- pressure, N/m^2
q	- charge, As
r	- radius of particle, m
r_p	- radius of piston, m
S	- $9[1 + 1(1/\text{Br})] 4\text{Br}$, -
T	- temperature, K
t	- time, s
U_f	- fluid velocity amplitude, m/s
u_E	- mobility of electrophoresis, m^2/sV
u_f	- velocity of fluid, m/s
u_o	- amplitude of instantaneous velocity of particle, m/s
u_p	- particle velocity, m/s
Δu	- velocity difference, m/s
V	- volume, m^3
V_p	- perturbation velocity of fluid, m/s
v	- volume fraction of suspended particle, kg/m^3
v'	- velocity of center of particle, m/s
v_o	- amplitude of perturbation velocity of fluid particles, m/s
X	- $1/2 + (9/4\text{Br})$, -
x	- distance from surface, m
Z	- acoustic impedance, $\text{kg}/\text{m}^2\text{s}$
z	- charge of ion, C
α	- adsorption coefficient or attenuation, m^{-1}
β	- agglomeration coefficient, -
δ	- depth of penetration, m
ϵ	- permittivity, C^2/Nm^2

ϵ_c	- collision efficiency, -
ϵ_f	- fill-up efficiency, -
ϵ_0	- permittivity of vacuum, C^2/Nm^2
ϵ_r	- dielectric constant of material, -
ζ	- zetapotential, V
η	- kinematic viscosity of fluid, m^2/s
η_p	- particle entrainment factor, -
κ	- $(2e^2n_0z^2/\epsilon kT)^{1/2} = (2e^2N_{Ac}z^2/\epsilon kT)^{1/2}$, m^{-1}
λ	- wavelength, m
μ	- dynamic viscosity of fluid, Ns/m^2
ρ	- density of medium, kg/m^3
ρ_f	- density of fluid, kg/m^3
ρ_p	- density of particle, kg/m^3
ρ_r	- ratio of particle density to fluid density, -
T_p	- particle relaxation time, s
v_E	- rate of electrophoresis, m/s
Φ	- phase factor, -
\emptyset	- porosity
ϕ_v	- volume fraction of particles, kg/m^3
Ψ	- electric potential, V
Ψ_0	- potential of surface, V
ω	- angular frequency, rad/s

